NASA Contractor Report 4586

Analysis of Selected Materials Flown on Interior Locations of the Long Duration Exposure Facility

H. A. Smith, K. M. Nelson, D. Eash, and H. G. Pippin

Contracts NAS1-18224 and NAS1-19247
Prepared for Langley Research Center

April 1994

NASA Contractor Report 4586

Analysis of Selected Materials Flown on Interior Locations of the Long Duration Exposure Facility

H. A. Smith, K. M. Nelson, D. Eash, and H. G. Pippin
Boeing Defense & Space Group • Seattle, Washington

National Aeronautics and Space Administration
Langley Research Center • Hampton, Virginia 23681-0001

Prepared for Langley Research Center
under Contracts NAS1-18224 and NAS1-19247

April 1994

FOREWORD

This report describes the results from the testing and analysis of selected materials flown on the interior of the Long Duration Exposure Facility (LDEF). This work was carried out by Boeing Defense and Space Group under two Contracts, NAS1-18224, Task 12 (October 1989 through May 1991), and NAS1-19247, Tasks 1 and 8 (initiated May 1991). Sponsorship for these two programs was provided by the National Aeronautics and Space Administration, Langley Research Center (LaRC), Hampton, Virginia, and The Strategic Defense Initiative Organization, Key Technologies Office, Washington, D.C.

Mr. Lou Teichman, NASA LaRC, was the NASA Task Technical Monitor. Mr. Teichman was replaced by Ms Joan Funk, NASA LaRC, following his retirement. Mr. Bland Stein, NASA LaRC, was the Materials Special Investigation Group Chairman, and was replaced by Ms. Joan Funk and Dr. Ann Whitaker, NASA Marshall Space Flight Center, following Mr. Stein's retirement. The Materials & Processes Technology organization of the Boeing Defense & Space Group was responsible for providing the support to both contracts. The following Boeing personnel provided critical support throughout the program.

Bill Fedor	Program Manager
Sylvester Hill	Task Manager
Dr. Gary Pippin	Technical Leader
Dalton Eash	Testing and Analysis
Hal Smith	Testing and Analysis
Dr. Karl Nelson	Testing and Analysis

List of Figures

List of Figures (continued)

List of Tables

1.0 INTRODUCTION

This report summarizes the examination and testing by Boeing Defense & Space Group of selected materials flown for 69 months in low Earth orbit on interior locations of the Long Duration Exposure Facility (LDEF). The primary purpose of the LDEF was to provide a platform for experiments requiring exposure to space environments. Interest in examining support hardware and structure increased as the flight duration was extended. This report includes results of specific observations and measurements on heat shrink tubing, fiberglass shims, nylon wire harness clamps, and silver-coated hex nuts. A section discussing general observations on materials in relatively protected areas of the spacecraft is also included. Materials discussed in this report were generally subjected to the vacuum of space, some degree of thermal cycling, localized contamination, and potentially, intermittent exposures to external environmental factors at certain locations.

2.0 LDEF MISSION PROFILE

The LDEF is a large (about 9 meters in length, 4.3 meters in diameter), reusable, unmanned spacecraft to accommodate technology, science, and applications experiments which require long-term exposure to the space environment. LDEF was designed to be transported into space in the payload bay of a Space Shuttle, free-fly in low Earth orbit (LEO) for an extended time period, and then be retrieved by a Shuttle during a later flight. The LDEF was passively stabilized, and each surface maintained a constant orientation with respect to the direction of motion.

The LDEF was deployed by the Shuttle Challenger into a 482 km. nearly circular orbit with a 28.4 degree inclination on April 7, 1984. The planned 10-month to 1-year mission carried 57 experiments. A schematic diagram of the location(s) of each experiment on the LDEF is shown in figure 1. Due to schedule changes and the loss of the Space Shuttle Challenger, the duration of this flight was extended well beyond the original planned exposure period. The levels of exposure to atomic oxygen and solar radiation as functions of position on the LDEF are shown in figures 2 and 3, respectively.

The LDEF was retrieved by the Space Shuttle Columbia on January 12, 1990 after spending 69 months in orbit. A photo of the LDEF during retrieval operations is shown in figure 4. During these 69 months, LDEF completed 32,422 orbits of Earth and decreased in altitude to 340 km., where it was grappled, photographed extensively from the Shuttle crew cabin, and then placed in the Shuttle payload bay for return to Earth. The LDEF remained in the payload bay of the Space Shuttle Columbia for the landing at Edwards Air Force Base and during the ferry flight to Kennedy Space Center (KSC). The LDEF was removed from Columbia at KSC and brought to the Spacecraft Assembly and Encapsulation Building (SAEF-2) where the LDEF and its experiments were examined visually and photographed, radiation measurements were conducted, and the experiments removed from the structure tray by tray. Each tray was photographed individually subsequent to removal. System level tests were carried out for particular experiments and support hardware. External surfaces were examined for evidence of impacts, contamination, and other exposure induced materials changes.

BAY / ROW	A	B	C	
1	A0175	S0001	GRAPPLE	
2	A0178	S0001	A0015, A0187, M0006	
3	A0187	A0138	A0023, A0034, A0114, A0201	TRAILING EDGE
4	A0178	A0054	S0001	
5	S0001	A0178	A0178	P0005 P0003
6	S0001	S0001	A0178	
7	A0175	A0178	S0001	
8	A0171	S0001, A0056, A0147	A0178	
9	S0069	S0010, A0134	A0023, A0034 A0114, A0201	LEADING EDGE
10	A0178	S1005	GRAPPLE	
11	A0187	S0001	A0178	
12	S0001	A0201	S0109	

BAY / ROW	D	E	F
1	A0178	S0001	S0001
2	A0189, A0172 S0001	A0178	P0004, P0006
3	MOOC8, M0002	A0187, S1002	S0001
4	M0003	S0001	A0178
5	A0178	S0050, A0044, A0135	S0001
6	A0201, S0001	A0023, S1006 S1003, M0002	A0038
7	A0178	S0001	S0001
8	M0003	A0187	M0004
9	M0003, M0002	S0014	A0076
10	A0054	A0178	S0001
11	A0178	S0001	S0001
12	A0023, A0019, A0180	A0038	S1001

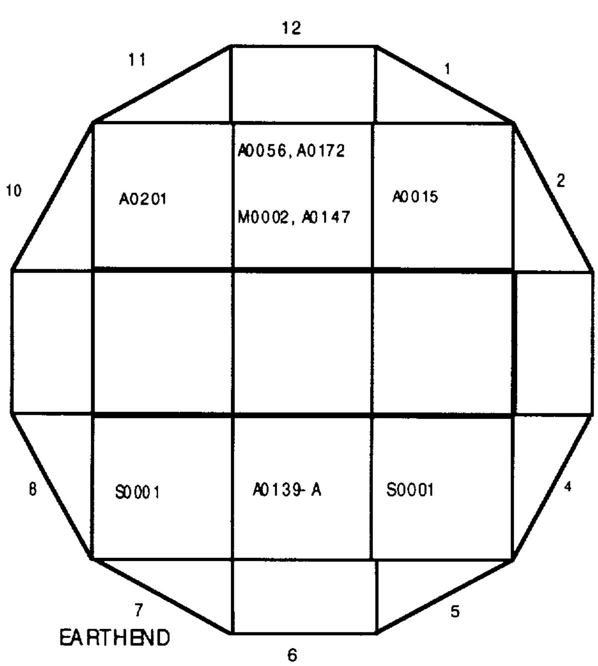

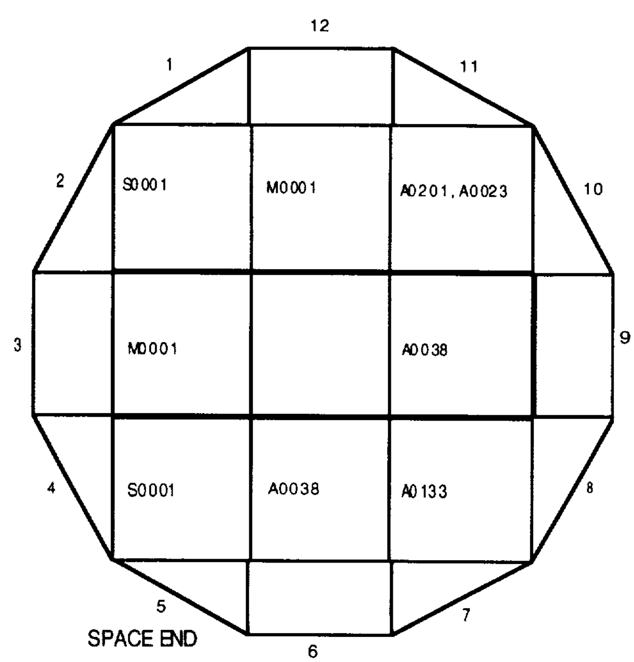

Figure 1. Diagram showing the locations of experiments on LDEF.

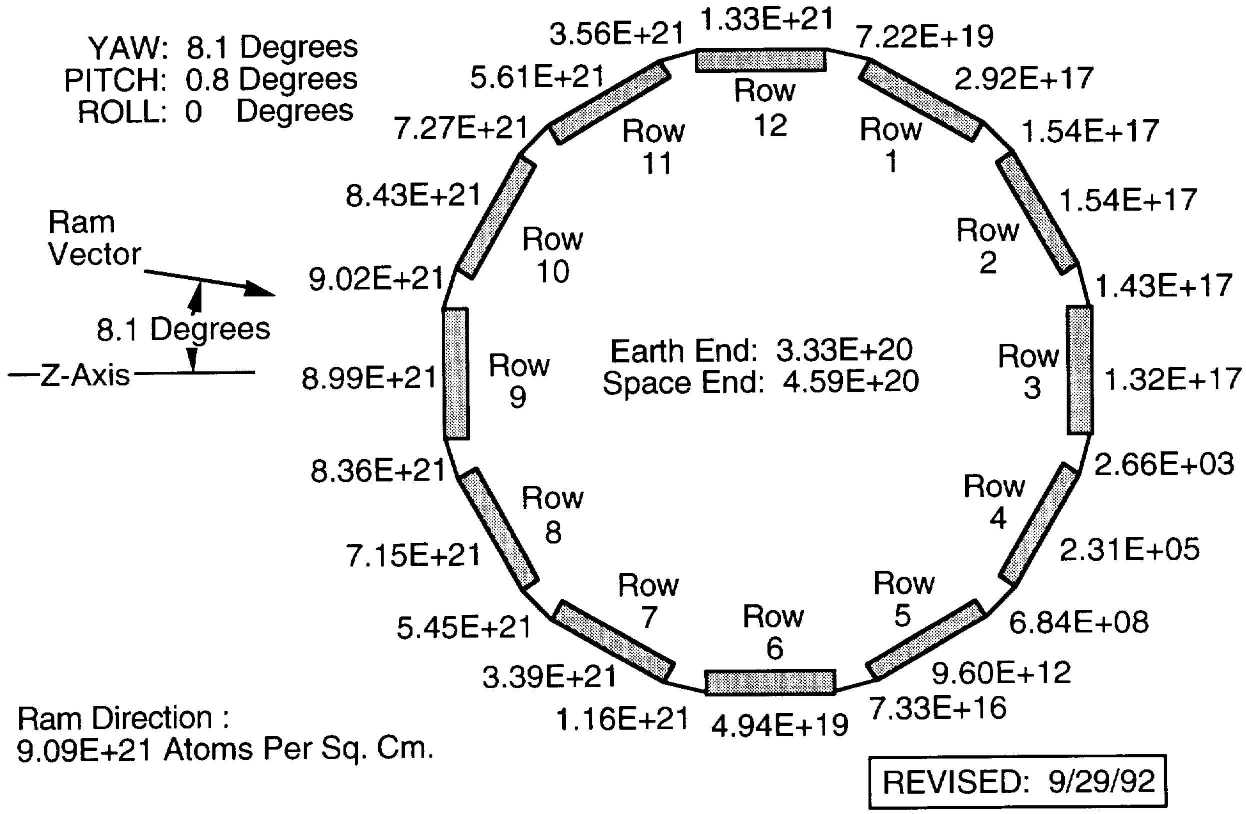

Figure 2. Atomic oxygen fluences at end of mission for all row, longeron, and end-bay locations including the fluence received during the retrieval attitude excursion.

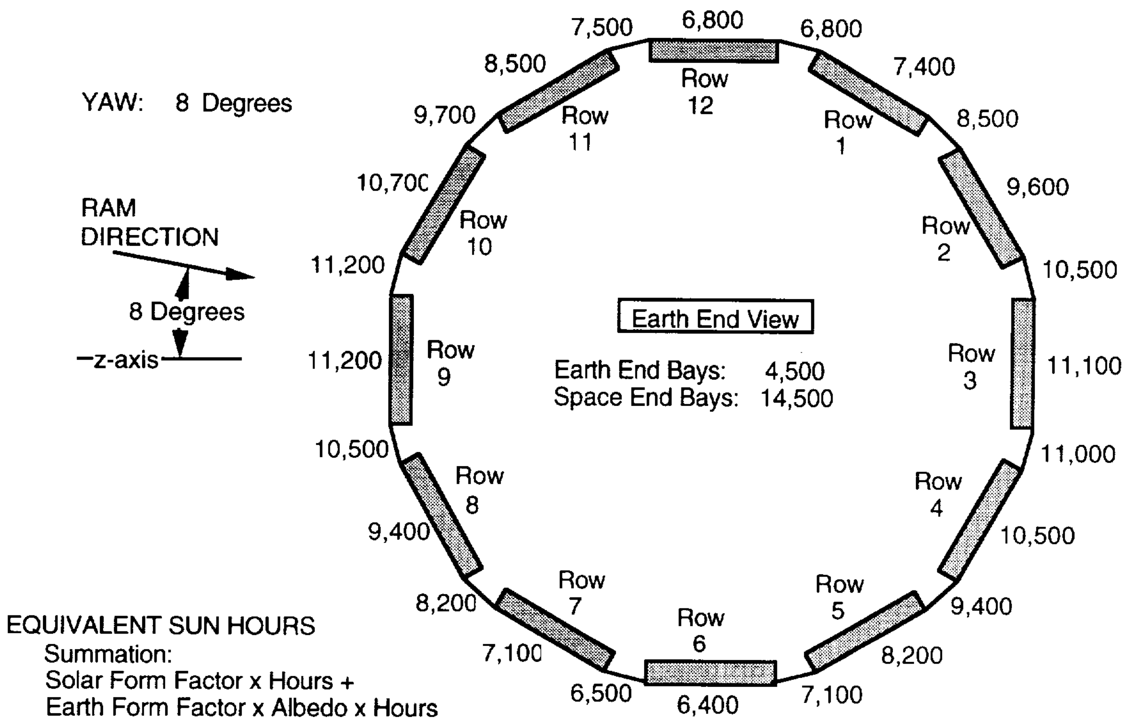

Figure 3. Cumulative equivalent sun hours of solar exposure for all row, longeron, and end-bay locations at end of mission.

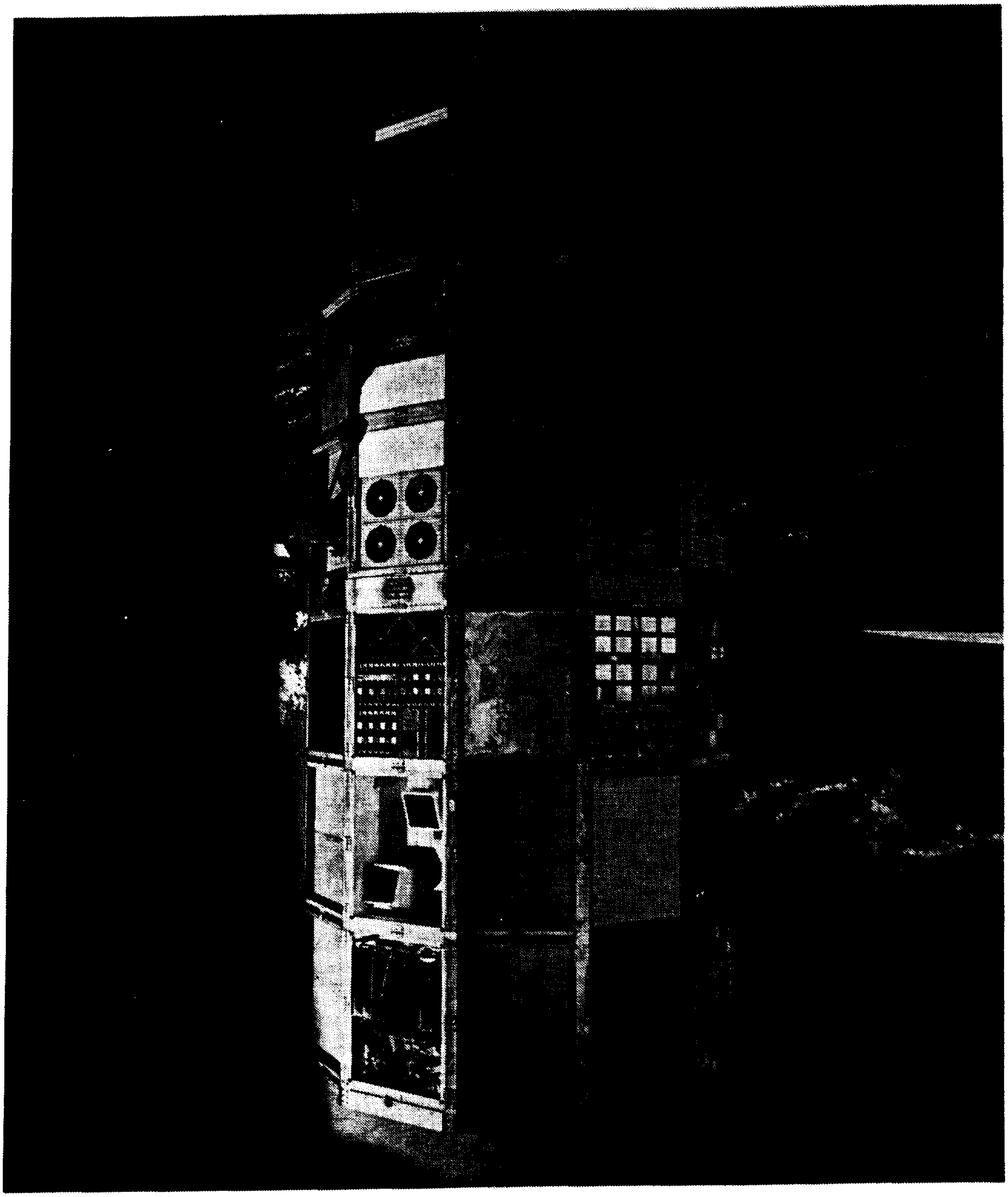

Figure 4. NASA photograph of the LDEF during retrieval operations in January 1990.

3.0 HARDWARE LOCATIONS

Figures 5 through 8 are schematic representations of the LDEF structure showing the locations of the aluminum wire harness clamps and the location identifiers for the specific clamps retained by the LDEF Materials Special Investigation Group (MSIG) for subsequent examination. Tests were carried out on twenty-one specimens from the group labeled in the figures. The locations of the wire harness clamps along the longerons and intercostals were labeled alphabetically looking from the Earth end, starting at the longeron between rows 12 and 1 (A) and continuing clockwise around the spacecraft. The clamps selected for potential analysis along a given longeron were numbered sequentially from the Earth end. The remaining clamps were removed from the LDEF and saved, but were not labeled by location. Nylon clamps were chosen for testing from the same locations as ten of the heat shrink tubing specimens. Figures 5-8 also identify the location of each nylon clamp specimen tested in terms of the intercostals and longerons positions. The silver-coated hex nuts examined were used to fasten titanium clamps at both the space end and Earth ends of LDEF.

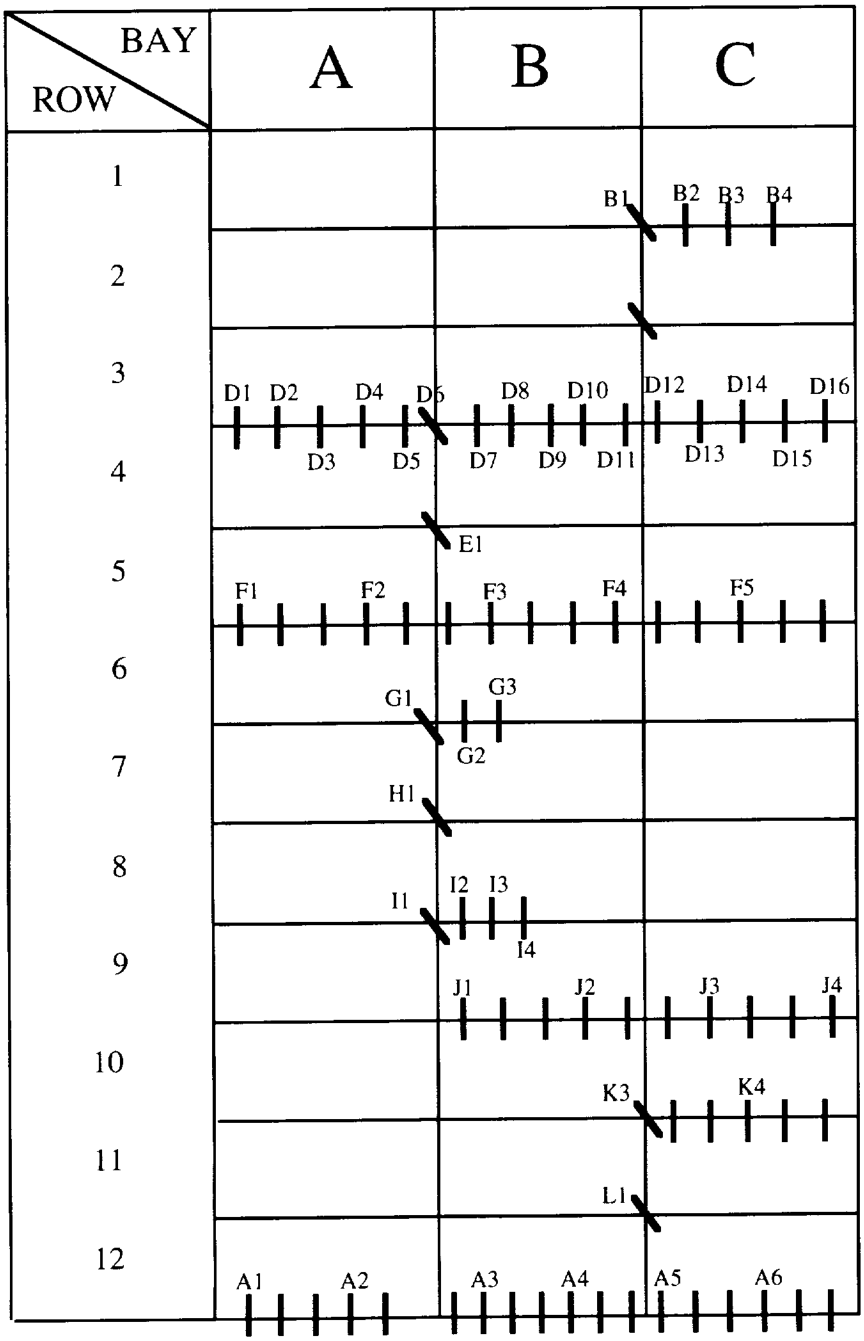

Figure 5. Locations of aluminum wire harness clamps with heat shrink tubing for all rows and bays A, B, and C.

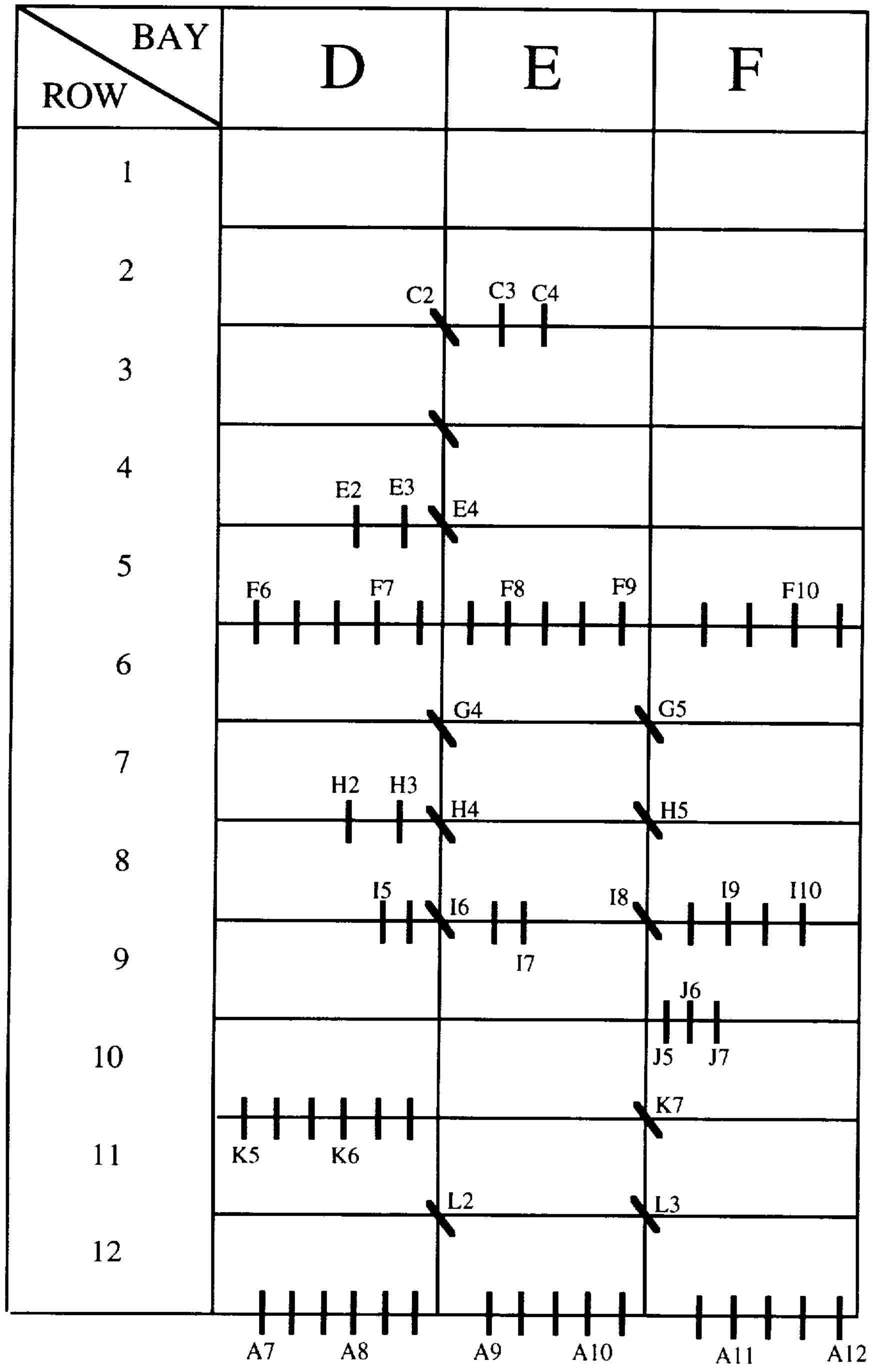

Figure 6. Locations of aluminum wire harness clamps with heat shrink tubing for all rows and bays D, E, and F.

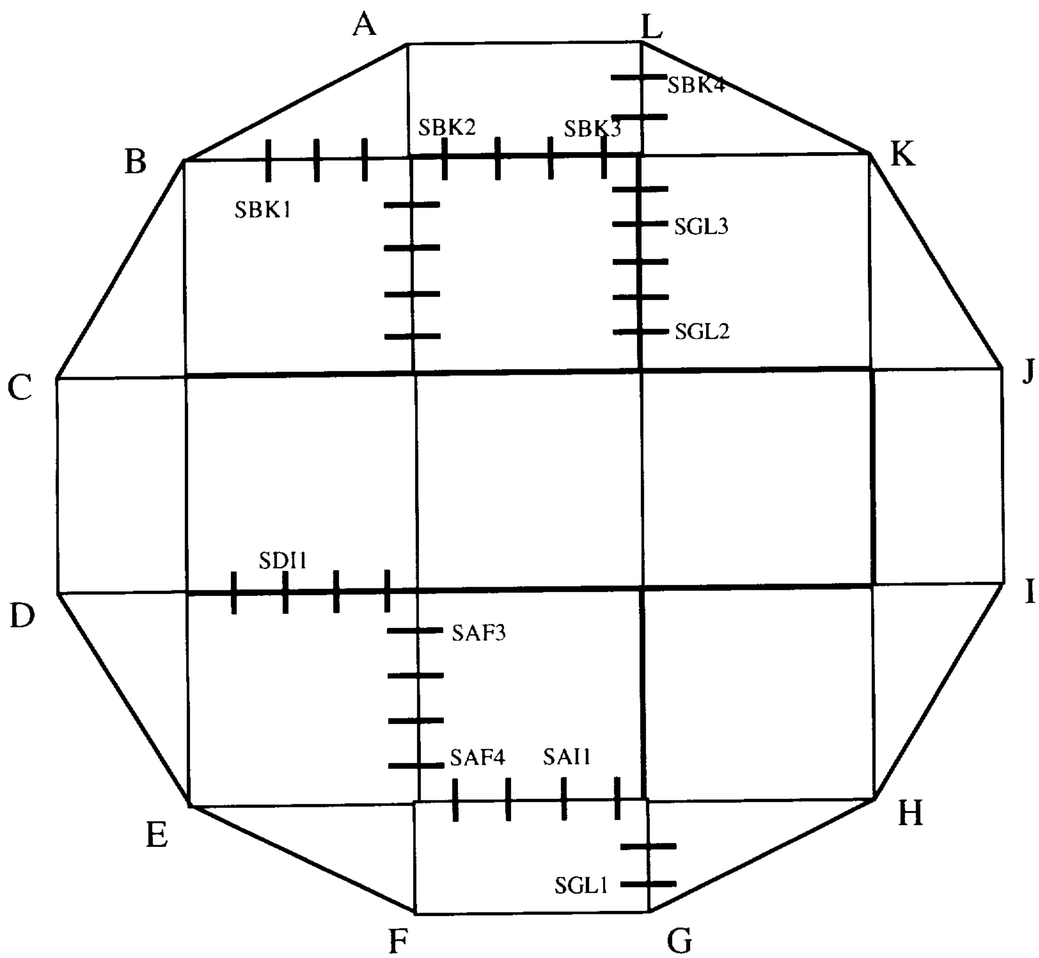

Figure 7. All space-end locations of aluminum wire harness clamps with heat shrink tubing.

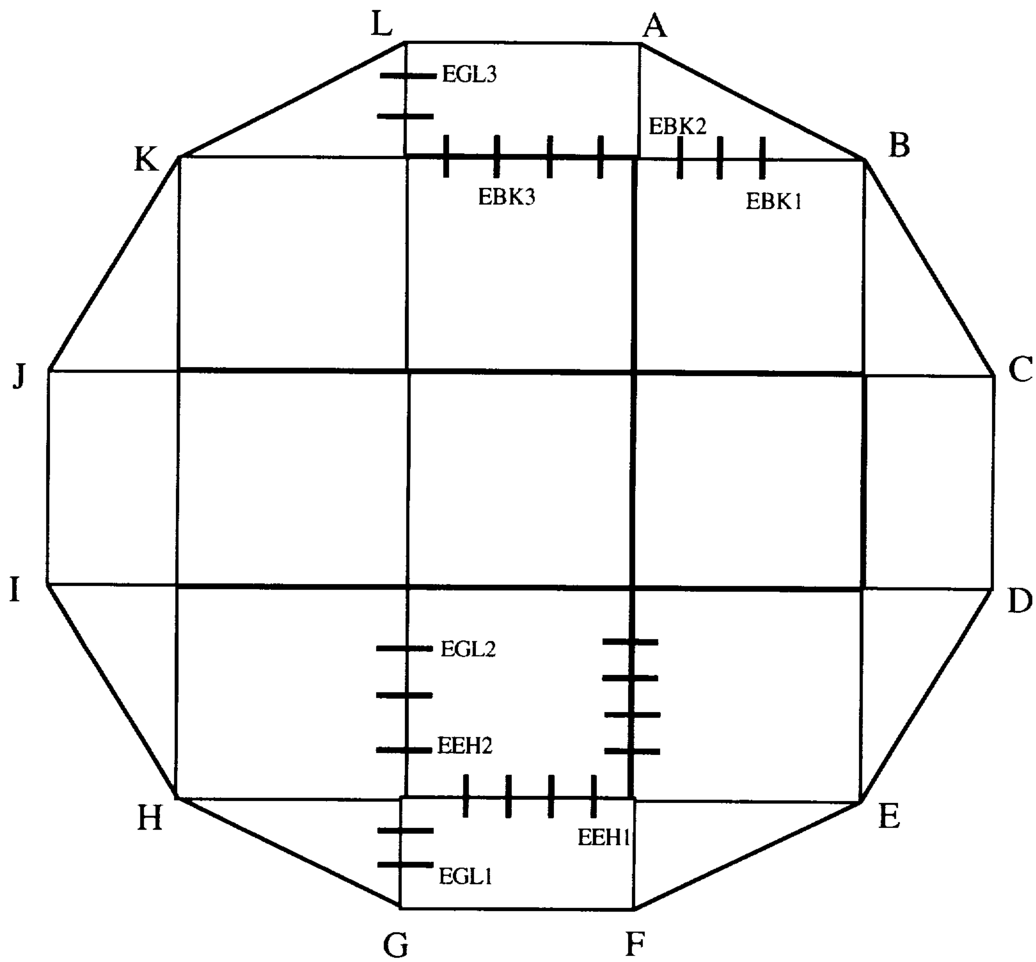

Figure 8. All Earth-end locations of aluminum wire harness clamps with heat shrink tubing.

4.0 GENERAL OBSERVATIONS

The only visible evidence of change in the condition of materials located on the interior of LDEF was at locations which received an outgassed film deposit. The visual observations of individual tray interiors also showed the generally good condition of materials not directly exposed to atomic oxygen and/or solar exposure. Visible changes were observed at locations near vent paths where molecular contamination accumulated.

Kapton™ thermal control blankets used on the interior facing sides of experiment trays appeared in excellent condition subsequent to the flight. Figure 9 shows a representative tray containing this material. The viscous damper shroud included a dome of spun aluminum. This half-sphere was mounted at the space end interior and maintained its mirrored surface. One area of the shroud dome had a thin molecular film deposit with a distinct diffraction pattern. The shape and color pattern of the deposit showed that one specific contamination source created this film. The remainder of the damper shroud was adhesive backed tape attached to a fiberglass shell. This material appeared in excellent condition. The Teflon™ coating on the interior wiring also appeared to be in excellent condition after the flight. The areas of the LDEF structure painted with Z-306(Chemglaze, now Lord Chemical) black paint appeared unchanged except for areas with contamination deposits. An example of the deposition patterns from venting through holes for fastening tray lids appearing on the longeron is shown in figure 10. Figure 11 shows contaminant film shadow patterns on the Z-306 painted interior side of tray B4. The pattern was caused by interference from a nearby structural support beam.

Selected materials were subjected to more quantitative tests. The interior materials investigated in more detail were chosen because visible changes were associated with particular specimens of the materials, and because specimens of the materials were available from several well-specified locations.

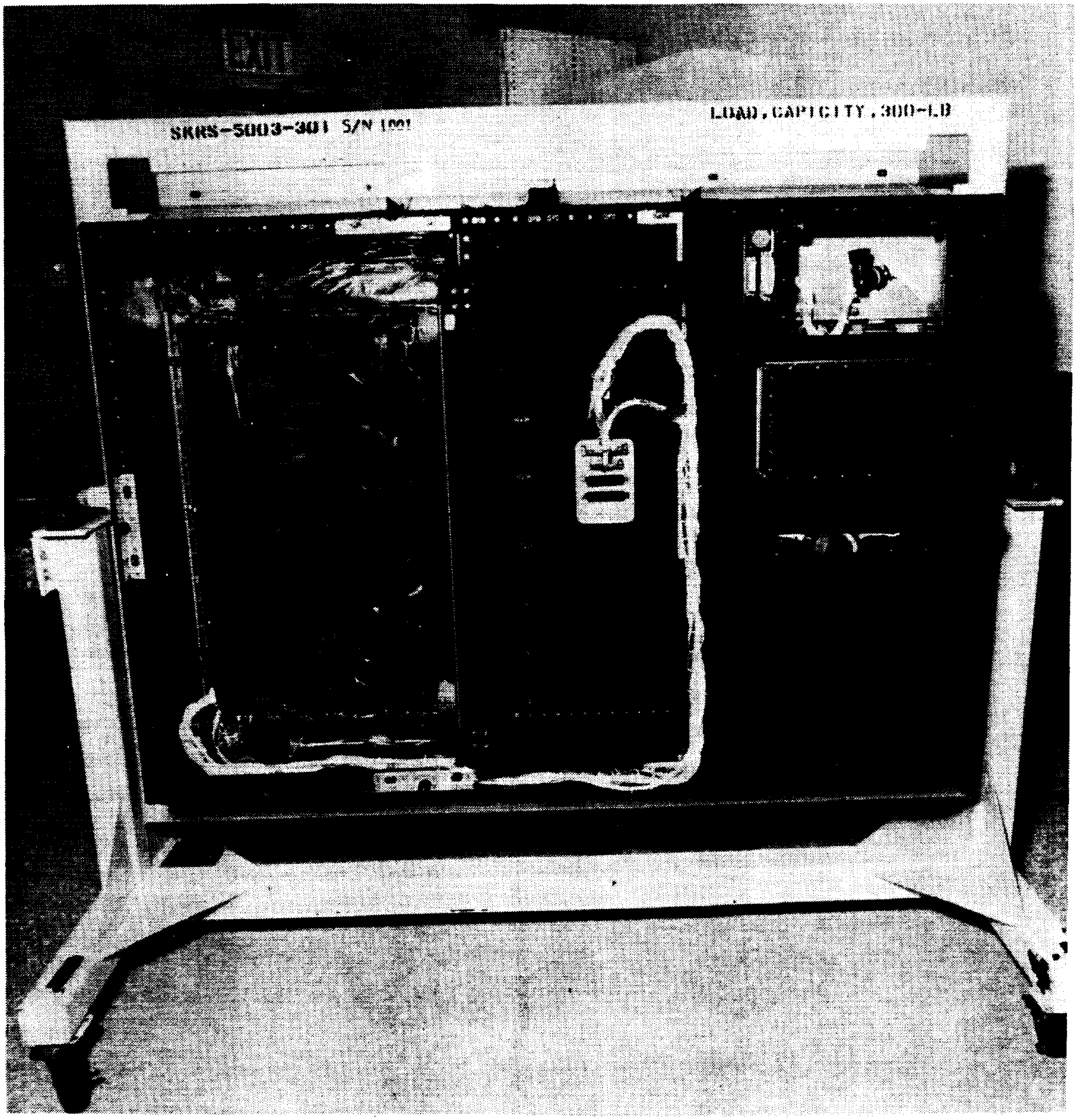

Figure 9. NASA post-flight photo of interior facing side of tray F12. Kapton thermal blanket on left appears specular. Wire bundles, paint, other hardware appear in good physical condition with little evidence of aging.

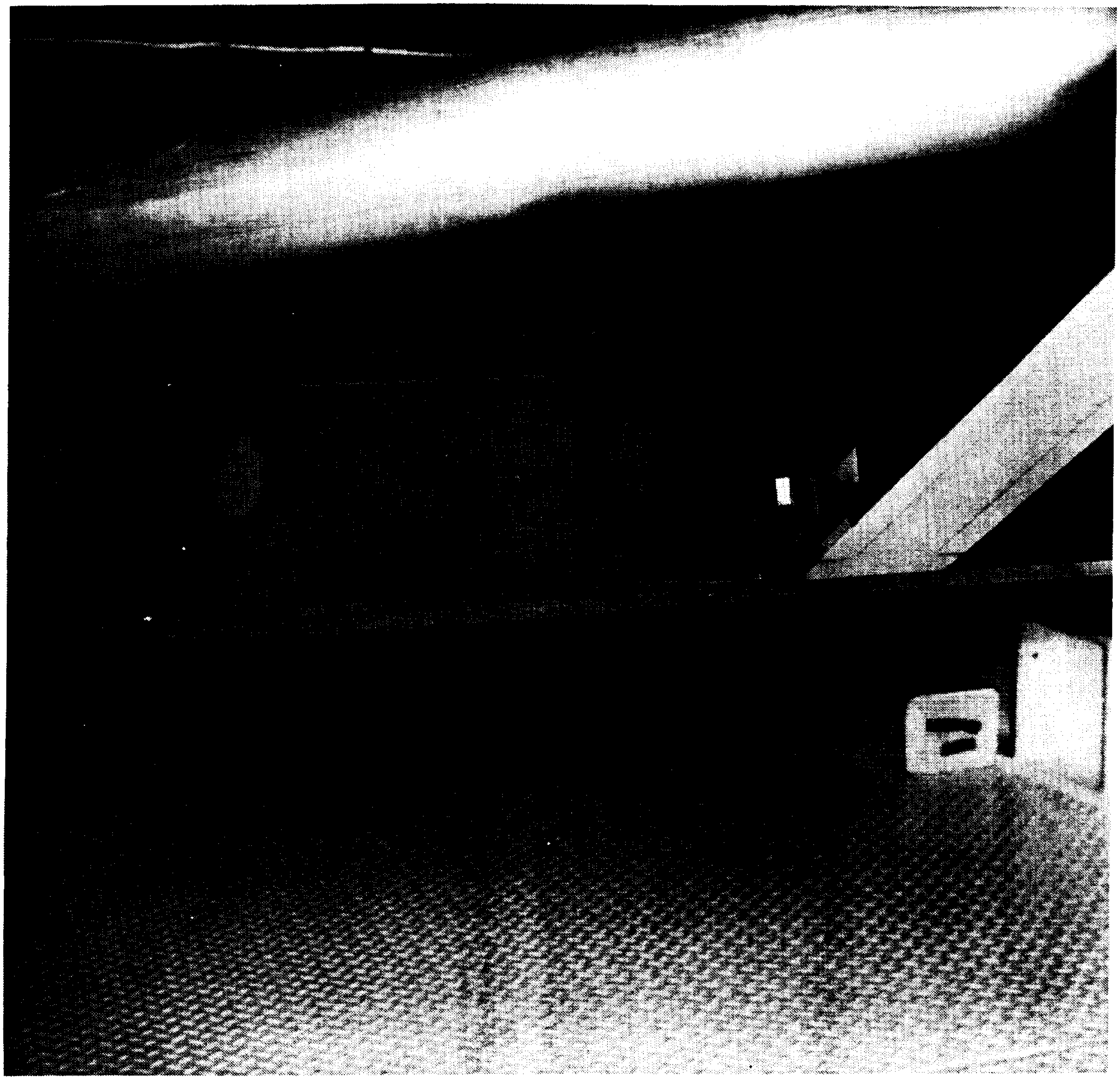

Figure 10. NASA photo of longeron K, between rows 10 and 11, bay A, Earth end to the left, showing patterns induced by outgassing of contaminants and/or environmental exposures through bolt holes in tray lip where tray covers were fastened to trays pre-flight and post-flight. The side of the longeron facing row 10 is in view.

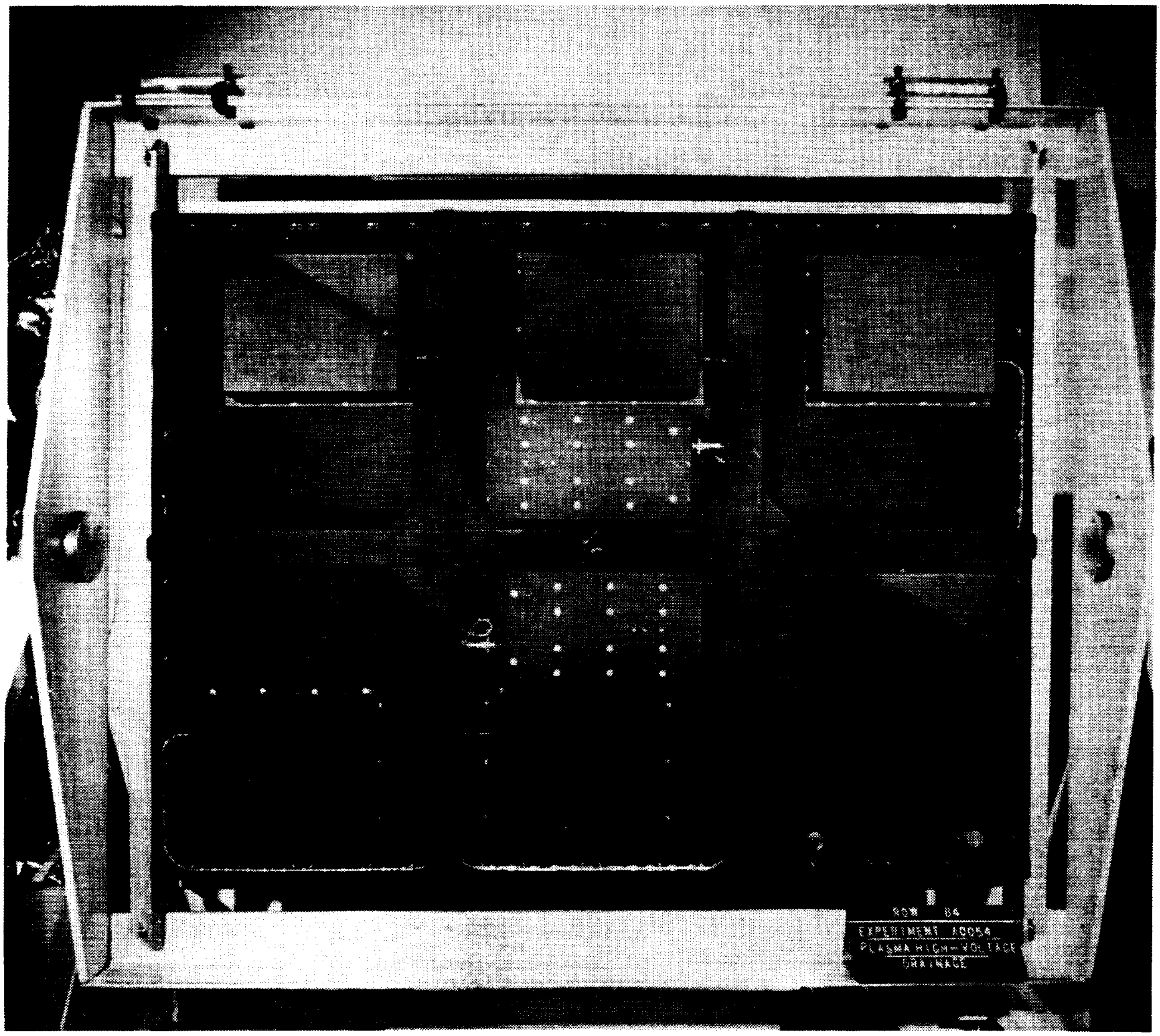

Figure 11. NASA photo of interior facing side of tray B4.

5.0 EXPOSURE CONDITIONS

The LDEF flew during the entire range of solar conditions, from solar minimum to solar maximum. Exposed surfaces received between 4000 and 14000 Equivalent Sun Hours of solar radiation including both direct solar and Earth-reflected components. Thermal data taken on-orbit at several locations on LDEF demonstrated that the bulk thermal cycling was relatively mild. Interior temperatures were typically 15-to-30°C, and verified the pre-flight thermal model predictions. The actual recorded temperatures from the seven thermocouples on the interior of the LDEF ranged from 2°F to 57°C. Specific external surfaces experienced different ranges of temperatures. Certain black, highly absorbing surfaces reached temperatures in excess of 100°C. Trays coated with white thermal control paints or silverized Teflon^{TM} were much colder; the Experiment S1001 radiator coated with MS-74 white paint reached about -83°C.

Atomic oxygen exposure of external surfaces varied from $9 \times 10^{+21}$ atoms/cm^2 for the ram direction to essentially zero toward the trailing edge. The mission dose of protons was less than a kilorad. The total electron dose (all energies) was about 30 kilorads at the surface. These exposures levels to particulate radiation barely reached the threshold (~2.5-25 kilorads) for observable effects for most materials. Exceptions are the plastic track detectors used for the cosmic ray experiments and possibly solar cells and quartz crystal oscillators. The meteoroid and debris impact distribution is also a strong function of location with leading edge locations receiving the majority of the strikes. More detailed descriptions of the LDEF environment can be found in a series of reports defining the atomic oxygen, solar ultraviolet, thermal, solar particulate radiation, and meteoroid and debris contributions (refs. 1-5).

Contaminant films created by thermal vacuum induced outgassing were observed on many external and interior surfaces of LDEF. These films were generally one of two distinct types; those films formed by outgassing of silicone based material and those films formed by outgassing of organic based materials.

6.0 SPECIFIC MATERIALS AND EXPOSURES

Visual inspection of the interior of LDEF in the SAEF-2 Building at KSC revealed distinct differences in the condition of areas on longerons between rows 3 and 4 near the wire harness clamps relative to areas around any other wire harness clamps. Teflon^{TM} (PTFE) coated wire bundles, multi-layer insulation blankets, Z-306 painted surfaces, and a spun aluminum surface occupied large surface areas on the interior of the LDEF and except for contamination at specific locations, appeared visually to be unchanged as a result of the flight. The nylon wire harness clamps appeared to be slightly embrittled due to their space exposure. The heat shrink tubing flown outgassed less than the ground control specimens. The extent of bake-out varied from location to location. The glass transition temperature of the heat shrink tubing material flown was virtually unchanged relative to the ground controls.

6.1 WIRE HARNESS MATERIALS

Aluminum wire harness clamps, partially clad with heat shrink tubing, were mounted on longerons and intercostals on the interior of LDEF to hold electrical wire bundles in place. Observation of brown films in close proximity to aluminum wire harness bundle clamps mounted to the interior of longerons between rows 3 and 4 was the basis for the examination of the aluminum wire harness clamps, the heat shrink tubing on each clamp, and the fiberglass shims placed between the tubing and the aluminum clamp. No discolored films were observed around wire harness bundles at any other locations on the longerons and intercostals. Figures 12-14 are photographs of specific locations within the interior of LDEF showing examples of the wire harness clamps.

The heat shrink tubing and/or fiberglass composite shims on the trailing edge longeron may have outgassed more than similar hardware at other locations. Damage to heat shrink tubing on clamps mounted on the interior of longerons between rows 3 and 4 may have been caused by periodic exposure to solar radiation and/or atomic oxygen through gaps at the corners of trays on the leading edge. Certain interior trailing edge locations were line of sight to the gaps. Solar exposure would have been sweeping and oxygen exposure continual. Outgassed material from the heat shrink tubing and fiberglass shims also may have darkened due to ultraviolet radiation exposure after condensing on the surface. However, no similar darkened outgassed material was visible around heat shrink tubing located between rows 8 and 9, even though these locations should have received similar amounts of heating from solar UV through gaps in the trailing edge hardware. It is also possible that differences in observed outgassing from heat shrink tubing specimens from different locations is because of subtle differences in the thermal histories of each clamp in orbit. Thermogravimetric analysis of selected tubing specimens showed essentially no difference between flight specimens and ground control specimens. The areas on the trailing edge longeron were darker than corresponding areas in other locations. Thermal data from the M0003 experiment (ref. 6) shows a temperature range about 5-10°C higher for tray D8 than for tray D4. This could have effected the long term residual curing of specific heat shrink tubing specimens and changed their outgassing characteristics. However, the specifics of each location; thermal mass differences, optical properties of the surfaces, and shadowing by nearby structure, leave large uncertainties in the actual thermal histories at each location. Essentially, the heat shrink tubing specimens each performed their task. All specimens were in-place and intact at the end of mission.

Specimens from the set of wire harness clamps from the trailing edge longerons of LDEF exhibited greater amounts of blue-tinged metal than those from other areas. The locations of the samples are

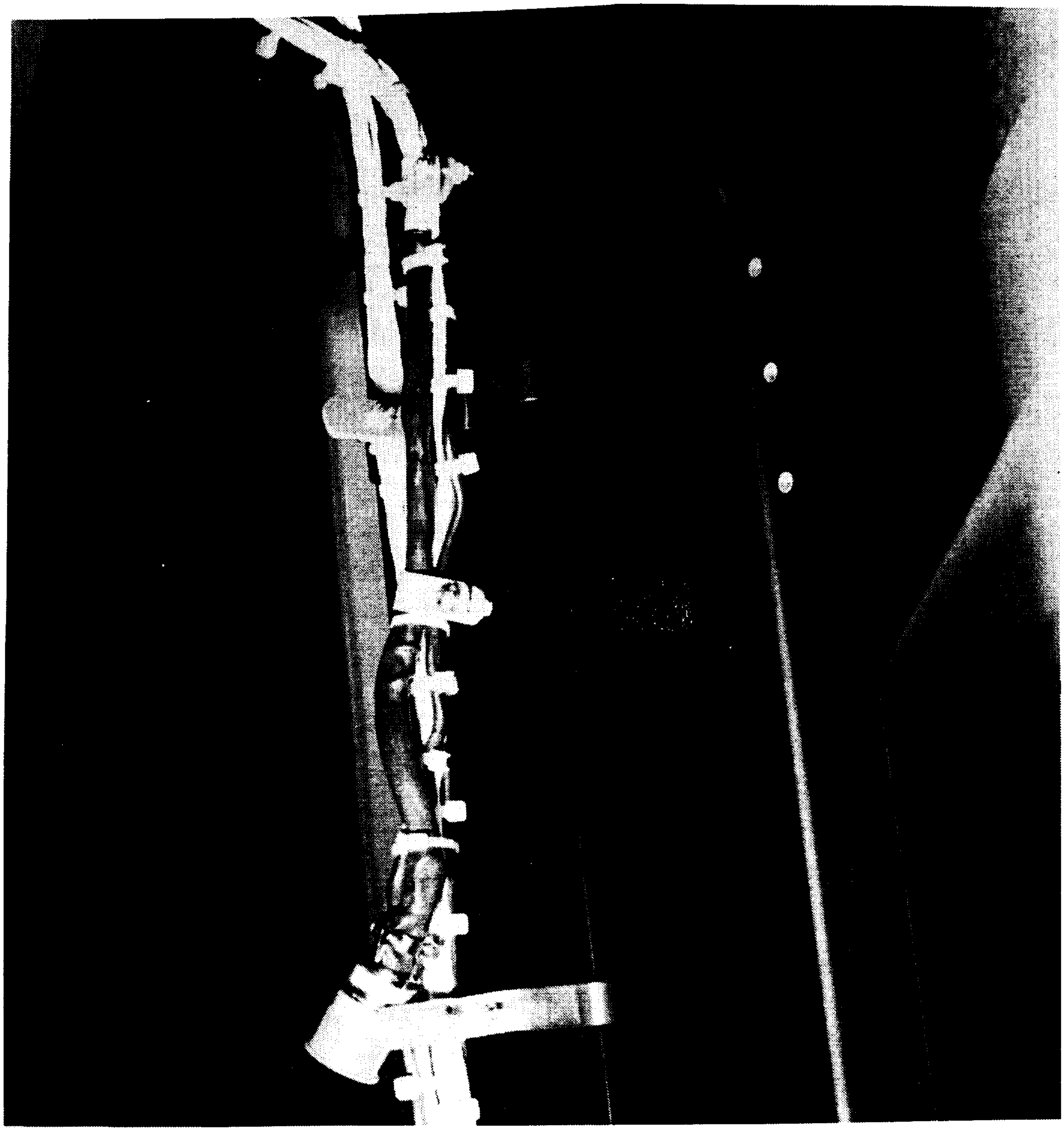

Figure 12. NASA photo of wire harness clamps with heat shrink tubing mounted on the longeron between rows 3 and 4, Bay C. The covered receptacle is pointed toward the Earth end of LDEF.

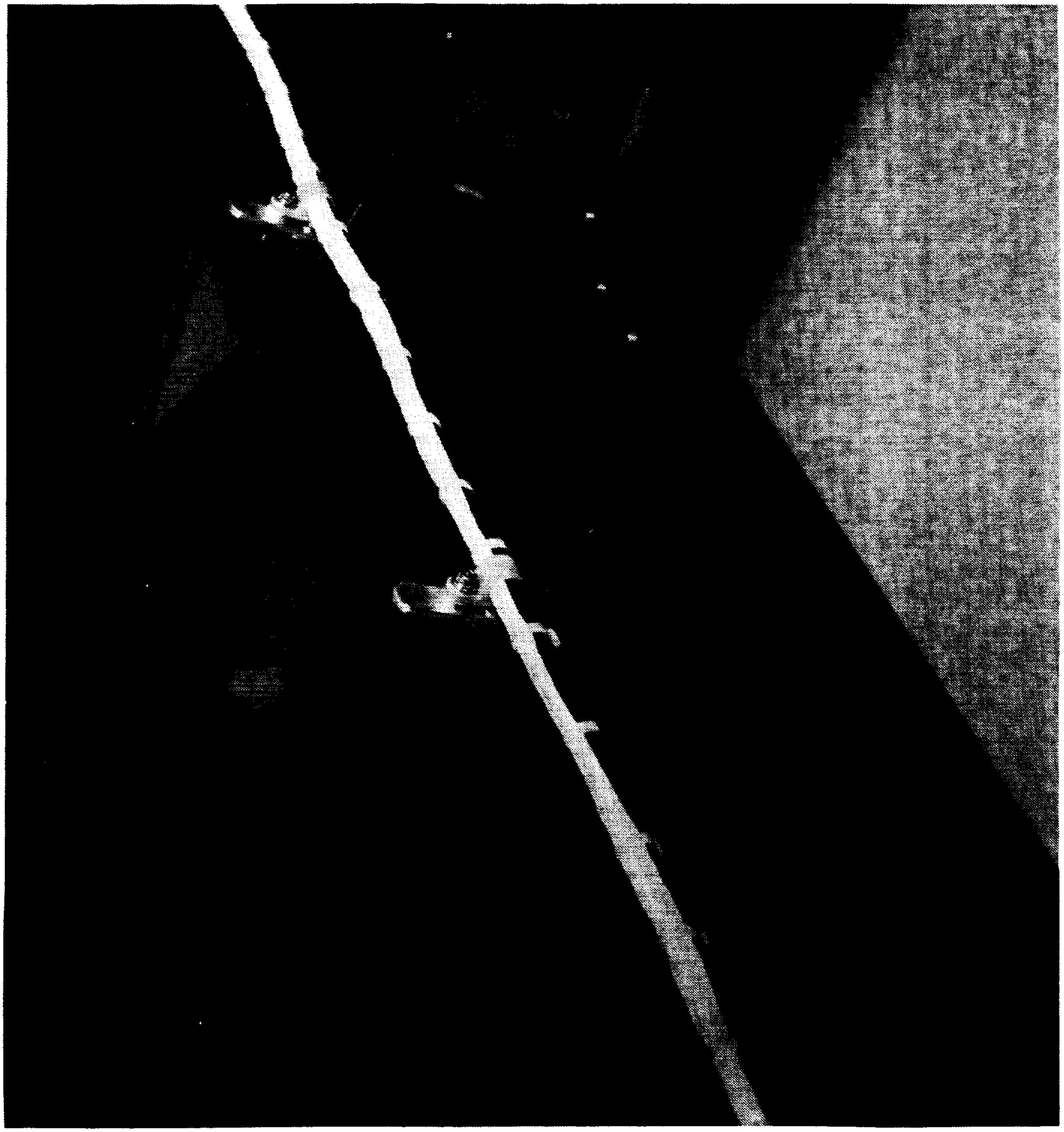

Figure 13. NASA photo of wiring and associated wire harness clamps along the longeron between row 1 and row 12, Bay A. Earth end of LDEF is toward the bottom of the page.

ORIGINAL PAGE
BLACK AND WHITE PHOTOGRAPH

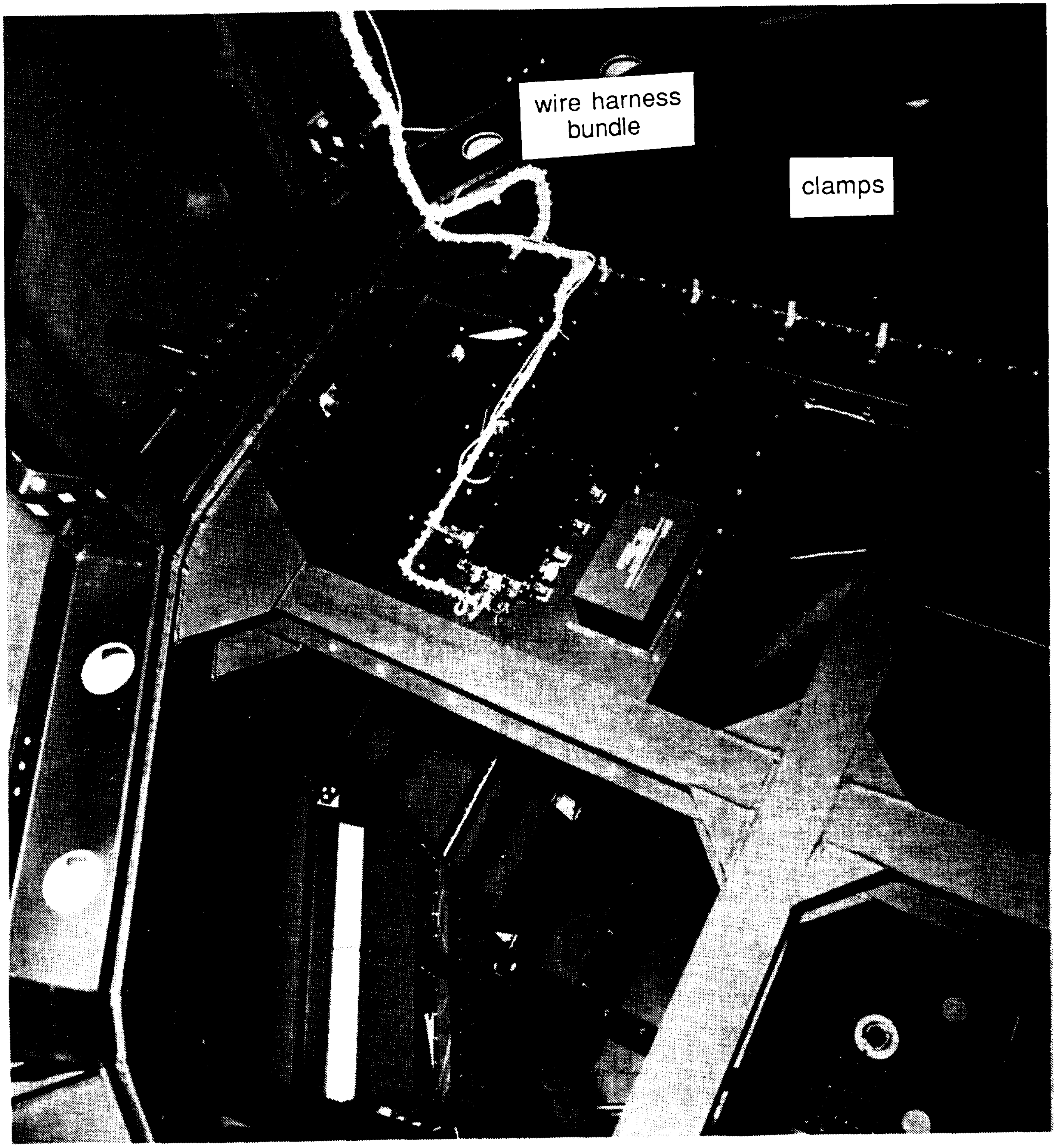

Figure 14. NASA photo of center ring viewed from space end of LDEF. Row 6 keel pin is at upper left. Center ring clamps and wire harness bundles are clearly visible.

shown in figures 5-8 (note that the labels on these clamps do not refer directly to row or bay numbers). One ground clamp and twenty-one flight clamps were used for testing. The test methods used were Total Mass Loss (TML) and Collectible Volatile Condensable Matter (CVCM) measurements, Thermo-Gravimetric Analysis (TGA), and Infrared Spectrophotometry (IR). All twenty-one flight samples were tested for TML and CVCM as were three composite backing shims (one from the longeron between rows 3 and 4, one from the longeron between rows 9 and 10, and one ground control specimen). Selected flight samples were also examined using TGA and IR techniques. The results of the testing were analyzed statistically ('leading/trailing' vs. 'sides/ends' and flight vs. ground) to determine if the means of the TML and CVCM values for the selected groupings were significantly different, thus asserting that the chosen sets were from different populations. Differences in the average of the means would indicate that the groups of samples experienced different exposure histories.

For the TML, CVCM, and TGA analyses of the heat shrink tubing from each location chosen for examination, four specimens from each clamp were taken from the portion of the tubing between the clamp and the structure. These specimens are labeled 'structure facing' and directly contacted a longeron or intercostal. Four specimens were also taken from selected clamps chosen for examination from the 'interior facing' surface exposed to the interior environment of the LDEF. Figure 15 is a diagram showing the details of the clamps. The TML and CVCM tests were run according to the NASA SP-R-0022A Outgassing Test with the sample bar at 125 $\pm$ 1°C, the collection plate at 25 $\pm$ 1°C, the vacuum at 10^{-6} torr for 24 hours, and equilibrium of the samples at 50% RH for 24 hours prior to weighing. Table 1 contains the raw data from the outgassing measurements on the heat shrink tubing.

Results of comparisons of fiberglass shims from individual clamps are shown in table 2. The TML of the flight composite shims were significantly different (level of confidence [LOC] >0.95) in comparison with the ground specimens. The flight samples appear to have undergone some bakeout as shown by the lower TML's and CVCM's in comparison with the ground control specimen. This result is as expected. The small cross-sectional area of the composite shim exposed to space allowed some outgassing to occur, but probably at a low rate since volatile species would have to diffuse to the one exposed surface.

The outgassing measurements reported in table 1 were used for comparison of the TML and CVCM values for sets of heat shrink tubing samples. Groups of leading and trailing edge samples were compared with groups of samples from side and end locations. Flight specimens were compared with ground specimens. Specimens from structure-facing sides were compared with interior-facing sides for each individual piece of heat shrink tubing. The results were compared using two-tailed t-tests and two-tailed Z-tests. To determine if the chosen groupings belonged to the same or different populations the averages of the means of the TML and CVCM measurements of the two groupings were examined. The hypothesis that the chosen groupings are from the same population was compared against the alternative hypothesis that the two groupings are from different populations. For specific tubing pieces, the means for TML and CVCM measurements of interior-facing specimens and structure-facing specimens were compared using the t-test. For the grouping of the tubing pieces both the t test (normal population, standard deviation unknown) and the Z test (large sample, standard deviation of groups known) were used to indicate the level of confidence that the groupings are from different populations. Results of group comparisons using the t statistic are shown in table 3. Table 4 provides a summary of the averages of TML and CVCM measurements from each clamp. Table 5 contains the results of the statistical tests used to determine if specific groupings of clamps belonged to the same population or to different populations, based on their average outgassing levels. Tables 6 and 7 give the LOC's for both the t and Z test statistics for the comparisons between results of the TML and CVCM measurements of the tubing samples.

LDEF CABLE CLAMPS
IDENTIFICATION OF SAMPLING LOCATIONS

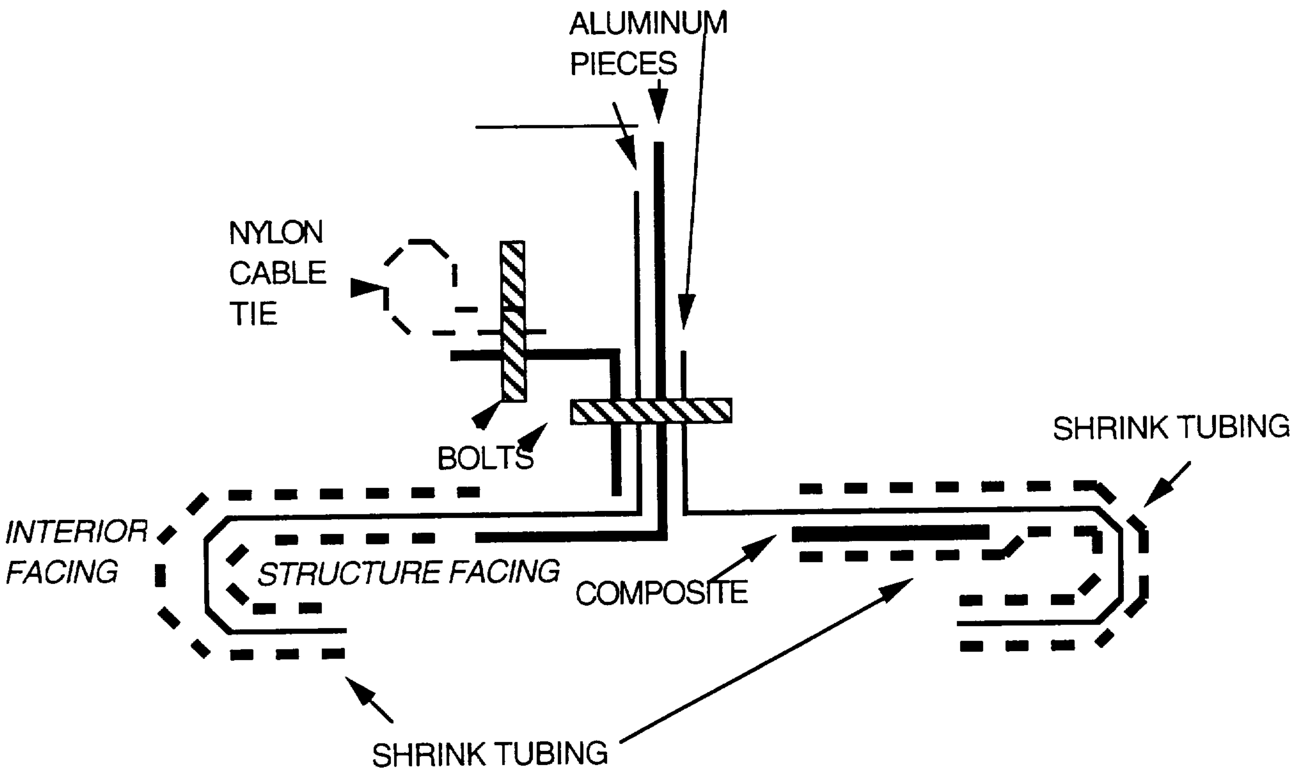

Figure 15 Location of components on wire harness clamps.

SAMPLE	POSITION	SAMPLE WEIGHT(g)	SAMPLE WT LOSS(g)	TML (%)	COLLECTOR WT GAIN(g)	CVCM (%)
D3	STRUCTURE	0.254957	0.000288	0.113	0.000112	0.044
	FACING	0.176103	0.00022	0.125	0.000083	0.047
Longeron		0.279965	0.000328	0.117	0.000179	0.064
3 - 4		0.294275	0.000332	0.113	0.000145	0.049
Bay A						
	INTERIOR	0.253891	0.000295	0.116	0.000156	0.061
	FACING	0.241947	0.000259	0.107	0.000126	0.052
		0.350837	0.000386	0.110	0.000126	0.036
		0.342926	0.000357	0.104	0.00016	0.047
	AVG			**0.113**		**0.050**
D9	STRUCTURE	0.245548	0.000318	0.130	0.000126	0.051
	FACING	0.201347	0.000234	0.116	0.000169	0.084
Longeron		0.323617	0.000374	0.116	0.000189	0.058
3 - 4		0.3181	0.000386	0.121	0.000191	0.060
Bay B						
	INTERIOR	0.277212	0.000402	0.145	0.000138	0.050
	FACING	0.307017	0.000439	0.143	0.000157	0.051
		0.301755	0.000407	0.135	0.000171	0.057
		0.279156	0.000382	0.137	0.00018	0.064
	AVG			**0.130**		**0.059**
D10	STRUCTURE	0.326303	0.00044	0.135	0.000187	0.057
	FACING	0.276454	0.000409	0.148	0.000155	0.056
Longeron		0.293009	0.000403	0.138	0.000153	0.052
3 - 4		0.311401	0.000428	0.137	0.000153	0.049
Bay B	**AVG**			**0.139**		**0.054**
D15	STRUCTURE	0.268414	0.000303	0.113	0.000165	0.061
	FACING	0.217116	0.000286	0.132	0.00014	0.064
Longeron		0.338335	0.000383	0.113	0.000184	0.054
3 - 4		0.317834	0.000399	0.126	0.000223	0.070
Bay C						
	INTERIOR	0.349071	0.000394	0.113	0.000202	0.058
	FACING	0.351178	0.000415	0.118	0.00018	0.051
		0.319797	0.0004	0.125	0.00017	0.053
		0.299487	0.000397	0.133	0.000199	0.066
	AVG			**0.122**		**0.060**

Table 1. Results of TML and CVCM measurements on heat shrink tubing specimens from the LDEF.

SAMPLE	POSITION	SAMPLE WEIGHT(g)	SAMPLE WT LOSS(g)	TML (%)	COLLECTOR WT GAIN(g)	CVCM (%)
A 9	STRUCTURE	0.363068	0.000391	0.108	0.000167	0.046
Longeron	FACING	0.33407	0.000359	0.107	0.000143	0.043
12-1		0.273358	0.000322	0.118	0.000127	0.046
Bay E		0.270833	0.000331	0.122	0.000125	0.046
	AVG			**0.114**		**0.045**
A 6	STRUCTURE	0.31044	0.000309	0.100	0.000123	0.040
Longeron	FACING	0.283245	0.000307	0.108	0.000116	0.041
12-1						
Bay C	INTERIOR	0.284712	0.000309	0.109	0.000138	0.048
	FACING	0.241465	0.000308	0.128	0.000148	0.061
	AVG			**0.111**		**0.048**
C 2	STRUCTURE	0.347066	0.000326	0.094	0.000182	0.052
Longeron	FACING	0.39418	0.000439	0.111	0.000208	0.053
2-3						
Bays D-E	INTERIOR	0.287559	0.000311	0.108	0.000155	0.054
	FACING	0.340398	0.000387	0.114	0.000159	0.047
	AVG			**0.107**		**0.051**
C 4 *	STRUCTURE	0.23813	0.000348	0.146	0.000148	0.062
Longeron	FACING	0.26322	0.000397	0.151	0.000179	0.068
2-3						
Bay E		0.326367	0.00039	0.119	0.000185	0.057
		0.294437	0.000381	0.129	0.000169	0.057
	AVG			**0.136**		**0.061**
F 3	STRUCTURE	0.239521	0.00021	0.088	0.000102	0.043
	FACING	0.199744	0.000185	0.093	0.000095	0.048
Longeron		0.253031	0.00028	0.111	0.00014	0.055
5-6		0.28727	0.000278	0.097	0.000143	0.050
Bay B						
	INTERIOR	0.328686	0.000333	0.101	0.000161	0.049
	FACING	0.310199	0.000294	0.095	0.000121	0.039
		0.248336	0.000264	0.106	0.000141	0.057
		0.209228	0.000236	0.113	0.000111	0.053
	AVG			**0.100**		**0.049**

Table 1. Results of TML and CVCM measurements on heat shrink tubing specimens from the LDEF (continued).

***Specimens from location C4 were outgassed for 2-3 hours longer than the specification calls for.**

SAMPLE	POSITION	SAMPLE WEIGHT(g)	SAMPLE WT LOSS(g)	TML (%)	COLLECTOR WT GAIN(g)	CVCM (%)
H 4	STRUCTURE	0.000279	0.000132	0.106	0.000132	0.050
	FACING	0.260807	0.000274	0.105	0.00013	0.050
Longeron		0.32831	0.000346	0.105	0.000164	0.050
7 - 8		0.290735	0.000308	0.106	0.000145	0.050
Bay E						
	INTERIOR	0.398302	0.000383	0.096	0.000236	0.059
	FACING	0.392861	0.000404	0.103	0.000196	0.050
		0.308991	0.000289	0.094	0.000124	0.040
		0.36474	0.000403	0.110	0.000182	0.050
	AVG			**0.103**		**0.050**
I 2	STRUCTURE	0.205194	0.000281	0.137	0.000115	0.056
	FACING	0.251767	0.000343	0.136	0.000128	0.051
Longeron		0.270564	0.000392	0.145	0.000132	0.049
8 - 9		0.25648	0.00034	0.133	0.000137	0.053
Bay B						
	INTERIOR	0.295162	0.000403	0.137	0.000142	0.048
	FACING	0.341671	0.00043	0.126	0.000132	0.039
		0.289133	0.000423	0.146	0.000153	0.053
		0.282546	0.00039	0.138	0.000165	0.058
	AVG			**0.137**		**0.051**
I 4	STRUCTURE	0.27856	0.000409	0.147	0.000166	0.060
	FACING	0.290007	0.000364	0.126	0.000132	0.046
Longeron		0.302676	0.000333	0.110	0.000121	0.040
8 - 9		0.325222	0.000325	0.100	0.000163	0.050
Bay B						
	INTERIOR	0.294298	0.000418	0.142	0.000175	0.059
	FACING	0.271385	0.00036	0.133	0.000165	0.061
		0.251303	0.000285	0.113	0.000101	0.040
		0.232509	0.00026	0.112	0.000163	0.070
	AVG			**0.123**		**0.053**
I 9	STRUCTURE	0.294428	0.000363	0.123	0.000157	0.053
	FACING	0.235384	0.000326	0.138	0.000141	0.060
Longeron		0.293198	0.000363	0.124	0.000174	0.059
8 - 9		0.315922	0.000373	0.118	0.000166	0.053
Bay F						
	AVG			**0.126**		**0.056**

Table 1. Results of TML and CVCM measurements on heat shrink tubing specimens from the LDEF (continued).

SAMPLE	POSITION	SAMPLE WEIGHT(g)	SAMPLE WT LOSS(g)	TML (%)	COLLECTOR WT GAIN(g)	CVCM (%)
J 1	STRUCTURE	0.23459	0.000336	0.143	0.000153	0.065
Longeron	FACING	0.216536	0.000283	0.131	0.000158	0.073
9-10		0.314443	0.000403	0.128	0.00017	0.054
Bay B		0.343043	0.000429	0.125	0.000182	0.053
	AVG			**0.132**		**0.061**
J 6	STRUCTURE	0.210489	0.000214	0.102	0.000124	0.059
	FACING	0.290804	0.000333	0.115	0.000144	0.050
Longeron		0.291849	0.000347	0.119	0.000132	0.045
9-10		0.277908	0.000367	0.132	0.000113	0.041
BAY F						
	INTERIOR	0.277953	0.000318	0.114	0.000107	0.038
	FACING	0.321232	0.000343	0.107	0.000129	0.040
		0.23575	0.000238	0.101	0.000122	0.052
		0.235723	0.000265	0.112	0.000116	0.049
	AVG			**0.113**		**0.047**
K 4	STRUCTURE	0.226027	0.000308	0.136	0.000129	0.057
	FACING	0.19599	0.000256	0.131	0.000139	0.071
Longeron		0.213199	0.00019	0.089	0.000131	0.061
9-10		0.211832	0.000235	0.111	0.000097	0.046
BAY C						
	INTERIOR	0.316816	0.000319	0.101	0.000131	0.041
	FACING	0.277694	0.000288	0.104	0.000168	0.060
		0.24157	0.000309	0.128	0.000141	0.058
		0.252033	0.000314	0.125	0.000162	0.064
	AVG			**0.115**		**0.057**
K 6	STRUCTURE	0.296109	0.00035	0.118	0.000157	0.053
	FACING	0.336972	0.000385	0.114	0.000174	0.052
Longeron						
10-11	INTERIOR	0.351957	0.000306	0.087	0.000186	0.053
Bay D	FACING	0.300966	0.000371	0.123	0.000181	0.060
	AVG			**0.111**		**0.054**

Table 1. Results of TML and CVCM measurements on heat shrink tubing specimens from the LDEF (continued).

SAMPLE	POSITION	SAMPLE WEIGHT(g)	SAMPLE WT LOSS(g)	TML (%)	COLLECTOR WT GAIN(g)	CVCM (%)
EGL2	STRUCTURE	0.364999	0.000646	0.177	0.000247	0.068
	FACING	0.404837	0.000738	0.182	0.000282	0.070
EARTH END		0.251381	0.00051	0.203	0.000162	0.064
		0.24434	0.000576	0.236	0.000176	0.072
	INTERIOR	0.260929	0.000544	0.208	0.000208	0.080
	FACING	0.418267	0.000706	0.169	0.000318	0.076
		0.285014	0.000464	0.163	0.00016	0.056
		0.2347	0.000487	0.207	0.000129	0.055
	AVG			**0.193**		**0.068**
EBK1	STRUCTURE	0.376133	0.00038	0.101	0.000152	0.040
	FACING	0.315151	0.000346	0.110	0.000136	0.043
EARTH END		0.316607	0.00032	0.101	0.000136	0.043
		0.32448	0.000311	0.096	0.00013	0.040
	AVG			**0.102**		**0.042**
SGL3	STRUCTURE	0.363418	0.000387	0.106	0.0002	0.055
	FACING	0.405405	0.000413	0.102	0.000202	0.050
SPACE END						
	INTERIOR	0.437773	0.000408	0.093	0.000189	0.043
	FACING	0.343517	0.000342	0.100	0.000177	0.052
	AVG			**0.100**		**0.050**

Table 1. Results of TML and CVCM measurements on heat shrink tubing specimens from the LDEF (continued).

SAMPLE	POSITION	SAMPLE WEIGHT(g)	SAMPLE WT LOSS(g)	TML (%)	COLLECTOR WT GAIN(g)	CVCM (%)
SKB2	STRUCTURE	0.291361	0.000293	0.101	0.00014	0.048
	FACING	0.290318	0.000289	0.100	0.000125	0.043
SPACE END		0.38359	0.000445	0.116	0.00019	0.050
		0.400314	0.000482	0.120	0.000168	0.042
	INTERIOR	0.370268	0.00038	0.103	0.000142	0.038
	FACING	0.440497	0.000418	0.095	0.000136	0.031
		0.323413	0.000372	0.115	0.000167	0.052
		0.342612	0.000478	0.140	0.000174	0.051
	AVG			**0.111**		**0.044**
GROUND	STRUCTURE	0.157607	0.000289	0.183	0.000117	0.074
	FACING	0.171503	0.000265	0.155	0.000107	0.062
		0.276069	0.000462	0.167	0.000156	0.057
		0.276681	0.000437	0.158	0.000154	0.056
	INTERIOR	0.303261	0.000582	0.192	0.000167	0.055
	FACING	0.276592	0.000465	0.168	0.00012	0.043
		0.188418	0.000329	0.175	0.000162	0.086
		0.2810195	0.000447	0.159	0.000157	0.056
	AVG			**0.170**		**0.061**

Table 1. Results of TML and CVCM measurements on heat shrink tubing specimens from the LDEF (continued).

SAMPLE	POSITION	SAMPLE WEIGHT(g)	SAMPLE WT LOSS(g)	TML (%)	COLLECTOR WT GAIN(g)	CVCM (%)
D3	STRUCTURE	0.163342	0.000567	0.347	0.000034	0.021
Longeron	FACING	0.136918	0.000451	0.329	0.000025	0.018
3-4						
Bay A	**AVG**			**0.338**		**0.020**
J 6	LARGER	0.140068	0.000545	0.389	0.000009	0.006
Longeron		0.136628	0.000454	0.332	0.000028	0.020
9-10						
Bay F	SMALLER	0.084222	0.000326	0.387	0.000005	0.006
		0.076025	0.000286	0.376	0.000012	0.016
	AVG			**0.371**		**0.012**
Flight Specimens	**AVG.**			**0.360**		**0.015**
GROUND		0.118392	0.000462	0.390	0.000048	0.041
		0.114911	0.000454	0.395	0.000029	0.025
	AVG			**0.393**		**0.033**

Table 2. Results of TML and CVCM measurements on composite shim specimens from the LDEF.

CLAMP	NUMBER OF SAMPLES	TML t Test	CVCM t Test
D3	8	0.146	0.029
D9	8	0.362	0.109
D15	8	0.02	0.094
A6	4	0.142	0.206
C2	4	0.092	0.045
F3	8	0.104	0.011
H4	8	0.108	0.004
I2	8	0.168	0.051
I4	8	0.047	0.122
J6	8	0.119	0.061
K4	8	0.027	0.037
K6	4	0.093	0.075
EGL2	8	0.111	0.027
SGL3	4	0.125	0.073
SKB2	8	0.045	0.047
GROUND	8	0.093	0.026

Table 3. Results of statistical analyses on TML and CVCM measurements comparing interior-facing and structure-facing specimens on individual wire harness clamps.

CLAMP LOCATION	TML Wt %	CVCM Wt %
D3	0.113	0.050
D9	0.130	0.059
D10	0.139	0.054
D15	0.122	0.060
I2	0.137	0.051
I4	0.123	0.053
I9	0.126	0.056
J1	0.132	0.061
J6	0.113	0.047
H4	0.103	0.050
K4	0.115	0.057
K6	0.111	0.054
EGL2	0.193	0.068
EBK1	0.102	0.042
SGL3	0.100	0.050
SKB2	0.111	0.044
F3	0.100	0.049
C2	0.107	0.051
A6	0.111	0.048
A9	0.114	0.045
GROUND	0.170	0.061

Table 4. Summary of results of TML and CVCM measurements on LDEF heat shrink tubing samples.

'Leading/Trailing' clamps vs. 'sides/ends' clamps

TEST STATISTIC	TML(%)	CVCM(%)
Z	7.83	3.33
t	7.76	3.29

Flight Specimens vs. Ground Control Specimens

TEST STATISTIC	TML(%)	CVCM(%)
Z	9.32	1.71
t	3.81	1.72

Table 5. Results of statistical analyses on average TML and CVCM values comparing 'leading/trailing' locations vs. 'sides/ends' locations and flight vs. ground control specimen groupings.

Interior Facing vs. Structure Facing Specimens

SAMPLE COMPARISON	LOC TML	LOC CVCM
D3		
D9		
D15		
A6		
C2		
F3		
H4	ALL >0.99	ALL > 0.99
I2		
I4		
J6		
K4		
K6		
EGL2		
SGL3		
SKB2		
GROUND		

Table 6. Level of confidence (LOC) in hypothesis that compared sets of heat shrink tubing samples from a specific piece of heat shrink tubing belong to the same population.

'Leading/Trailing' clamps vs. 'sides/ends' clamps

Test Statistic	LOC for TML	LOC for CVCM
Z	>0.99	>0.99
t	>0.99	>0.99

Flight Specimens vs. Ground Control Specimens

Test Statistic	LOC for TML	LOC for CVCM
Z	>0.99	>0.90
t	>0.99	>0.90

Table 7. Level of confidence in hypothesis that compared sets of heat shrink tubing samples belong to different populations.

Each test statistic shows to a high level of confidence that the groups are from different populations; that is, the differences in the means are not due to chance. The statistical analysis of the outgassing measurements, listed in Table 6, shows that sample groups from the structure facing side of the heat shrink tubing on a particular clamp and from the interior facing side of the same clamp belong to the same population to a level of confidence (LOC) >0.99, for each heat shrink tubing tested. The statistical analysis of the outgassing measurements, listed in table 7, show that the averages of the outgassing measurements for leading/trailing and side/end locations (TML and CVCM, LOC>0.99) and flight ground (TML only, LOC >0.99) populations are significantly different. The lower LOC (>0.90) for differences between the flight and ground CVCM measurement averages may be due to the LDEF flight sample absorbing moisture after retrieval, bringing the CVCM values in line with those of the ground sample, which was exposed to 6 years of ambient humidity.

The reasons behind the differences are not completely understood. The leading and trailing edge surfaces did receive more solar UV than other locations. The discoloration around the trailing edge specimens, not observed on the leading edge, could have been due to a combination of oxygen atoms fixing deposits in place and subsequent exposure discoloring the surface. The leading edge interior surface would have seen UV, causing degradation of the heat shrink tubing polymer, but no atomic oxygen would be available. The detailed temperature history of each location was likely rather complex and could also be a significant factor.

The greater average TML values for the leading/trailing edge set in comparison with the set of specimens from all other locations was not expected. The expectation was that the more solar ultraviolet on the exterior of a surface, the greater the extent of bake out of the material on the interior. However, the data did not completely correlate with this hypothesis, the space end being the exception. Variations in mass, optical properties of external surfaces, and proximity of other structure or hardware on the interior all contribute to the uncertainty in the thermal history of each piece of heat shrink tubing. Specimens from location C4 were inadvertently outgassed for 2-3 hours beyond the standard outgassing period. Initial measurements on the tubing from the clamp at location EGL2 (Earth end) show anomalously high TML and CVCM values relative to other flight specimens. A second set of outgassing measurements on this tubing confirmed the initial results. The reason for these high values is not known. These measurements, and the measurements on tubing from C4, were not used in the averaging and statistical analysis, but are reported for completeness.

The raw data for the TML and CVCM measurements on selected composite samples is presented in table 2. There are significant differences between the average TML values of the leading/trailing set in comparison with the set of specimens from all other locations, and between the flight and ground samples. The flight samples appear to have undergone some bakeout in comparison with the ground samples. The CVCM measurements indicated differences but the LOC was minimal (LOC >0.80) for an indication of strong differences. The low LOC for differences between the mean values of CVCM for the two sets may have been due to the absorption of water vapor previously mentioned.

Results of the statistical analyses of outgassing measurements of the heat shrink tubing and composite shims indicate significant differences in the exposure conditions of these materials depending on location. The TGA analyses of selected heat shrink tubing and composite shim specimens are presented in table 8. There is a high LOC (>0.98) between the leading/trailing set and the sides/end set weight loss values and a minimum LOC (>0.80) for the flight vs. ground weight losses. Comparison of the averages of the onset temperatures shows no significant differences between different groups of samples. This data is shown on the actual TGA curves in appendix A. The ground control curves were obtained using individual pieces cut from different locations of the same specimen; the curves are essentially identical.

Sample	Location	X1 (°C)	X2 (°C)	Delta WT %	X1''' (°C)	X2''' (°C)	Onset (°C)
D3							
	Structure facing	29.83	905.5	-97.68	268.87	496.73	480.63
	Structure facing	29.87	903.13	-97.59	319.63	501.3	490.78
	Interior facing	28.62	903.1	-97.55	349.92	499.38	488.73
	Interior facing	29.53	903.77	-96.88	295.78	497.12	480.88
	Average	29.46	903.9	-97.43	308.55	498.63	485.26
	Standard deviation			0.367			5.26
J6							
	Structure facing	27.63	902.35	-96.6	384.85	494.9	476.1
	Interior facing	31.1	902.98	-96.53	377.33	497.22	483.01
	Interior facing	30.07	902.57	-96.69	296.4	502.43	489.35
	Average	29.6	902.63	-96.61	340.86	498.18	482.82
	Standard Deviation			0.080			6.63
Flight Specimens							
	Average	29.52	903.45	-97.07	311.91	499.19	484.21
	Standard Deviation			0.511			5.49
Ground Control Specimen							
	Structure facing	29.65	903.58	-97.04	302.12	500.02	482.78
	Structure facing	30.2	905.18	-97.47	338.35	501.98	485.68
	Interior facing	30.32	903.85	-98.39	350.6	496.7	480.39
	Interior facing	29.4	902.37	-97.47	302.53	501.98	485.68
	Average	29.89	903.75	-97.59	323.4	498.96	482.90
	Standard Deviation			0.569			2.17

Table 8. TGA Analysis of LDEF Heat Shrink Tubing from Wire Harness Clamps.

6.2 NYLON WIRE BUNDLE CLAMPS

A summary of the data obtained from analyses on ten nylon clamps flown on LDEF and a sample of Zytel™, a nylon 6/6 used for comparison, is presented in table 9. During preparation of the test specimens from the clamps a noticeable difference in brittleness compared to the non-flown nylon material was observed. Flight specimens from wire harness clamp locations D15, F3, I2, I4, J6, and K4 cracked. The observed cracking did not correlate with other test results. Hardness, melting point and heat of fusion measured by a DuPont Thermal Analyzer Model 2100, crystallinity measured by X-ray Diffraction, and crystallinity index obtained from infrared (IR) absorption measurements with a Digilab Model FTS-60, are reported for all samples and the control. Table 9 includes qualitative estimates of the crystallinity determined by X-ray diffraction. The qualitative level of degradation by-products detected by pyrolysis GC and extent of amide breakage by IR measurements are recorded by numerical indices. The indices range from 0 to 4, with higher values indicating greater effects. Crystallinity is indicated by ND (not detected), VSC (very slight crystallinity), and SC (slight crystallinity). Very few apparent changes in the nylon properties were observed after 69 months exposure in low Earth orbit. Slight chemical changes due to rupture of the amide link were detected by IR absorption. Lower molecular weight degradation products were detected by pyrolysis gas chromatography (GC) using a Perkin-Elmer Model Sigma 1B. The heat of fusion of the non-flown piece of nylon 6/6 was lower than for each space flown nylon grommet. The maximum change detected for any property of these components had no real effect on their performance. The observed changes are within the random variation of the measured properties. The cause of the slight surface oxidation on one specimen cannot be unambiguously determined. On-orbit oxidation would require a coincidental alignment of the nylon grommet with a gap at the corner of a tray, allowing slight oxygen exposure. Figures 1 through 44 in appendix B show the results of these measurements.

Sample	Shore D Hardness	T_m (°C)	Heat of Fusion (J/gm)	Degradation Byproducts Py-GC	X-ray Diffraction	surface oxidation	crystallinity index by IR	amide linkage breakage
D3	83	254.8	62.17	2	ND[1]	N4	1.7	4
D9	83	251.9	61.9	2	ND[1]	N4	1.7	3
D15	83	249.6	58.35	3	ND[1]	N4	1.5	3
F3	84	248.7	57.41	3	SC[2]	N4	1.7	3
H4	84	255.9	53.52	2	VSC[3]	N4	1.8	4
I2	83	253.7	57.58	3	ND[1]	N4	1.6	2
I4	83	251.7	59.83	3	VSC[3]	N4	1.6	3
J6	84	255.3	52.9	3	VSC[3]	N4	1.4	4
K4	82	252.0	57.11	3	ND[1]	P5	1.7	1
SBK2	83	255.3	57.56	4	ND[1]	N4	1.5	4
Zytel™	85	252.5	51.82	NONE	SC[2]	N4	1.5 to 1.7	0

1) ND not detected
2) SC slight Crystallinity
3) VSC very slight crystallinity
4) N none
5) P Partial

Table 9. Results of characterization of the post-flight condition of selected nylon 6/6 grommets from the interior of the LDEF. A non-flight sample of Zytel™, a Nylon 6/6, was used for comparison.

6.3 Analysis of Silver-Coated Nuts

Silver-plated nuts from the intercostal clips were removed and analyzed (MS21046 Style B -C4 and -C5, "Nut, Self Locking, Hexagon-Regular Height 800°F, 125 ksi ftu"). Twenty-four nuts were made available for this analysis, which included fourier transform infrared spectroscopy (FTIR), X-ray photoelectron spectroscopy, Auger electron spectroscopy and photomicroscopy. The nuts were removed from the intercostal clips on the inside of LDEF from the Earth end (12 each) and from the space end (12 each) locations shown in figure 16. Two sizes of nuts were examined. The smaller, 1/4" nuts examined were from location #1, and the larger, 3/8" nuts examined were from location #5, on the intercostal clip. The breakaway torque of each nut, along with any additional tests conducted, is given in table 10. Each nut was also photographed. Four silvered nuts were sent to SPS Technology, Jenkintown, Pennsylvania, for examination of threads for anomalies such as coldwelding. No such anomalies were observed.

Photographs were taken of all the nuts before any testing. A photograph of a typical hex nut is shown in figure 17. All of the nuts were tarnished or coated. The color and distribution of tarnish varied between nuts and over the surface of each nut. There was no apparent correlation between the location of the nuts and the amount of tarnish. The tarnish was scratched on the edges of the flats where the wrench had loosened them. No other erosion or degradation of the protective silver coating was observed by photomicroscopy of the surfaces and/or cross-sections.

FTIR analysis of tarnish removed from the nuts was performed using a Bio-Rad Digilab FTS 60 FTIR. Some spectra were obtained using a UMA 300A infrared microscope attachment but suffered from optical effects and were difficult to interpret. A protein-like compound, which absorbs 1655 and 1540 wavenumbers, was observed on the surfaces of the nuts. The spectrum shown in figure 18 is from FTIR analysis of the tarnish removed from the nuts. The dark tarnish consists of silicone and silica/silicates from the decomposition of silicone, and of the amide material that may have originated from urethane paint. These results are consistent with the analysis of other LDEF surfaces. The observation of the stronger hydrocarbon bands and the nitrocellulose have not been observed on other surfaces, and are believed to be unique to these samples. The protein-like compound could be from urethane paint. Urethane functional groups absorb strongly at 1730 and less strong at 1540. The amide linkage in peptides and proteins absorb at 1640-1650 and 1540-1550 wavenumbers. The methyl and methylene hydrocarbon groups were observed in the spectra at 2800 and 3000 wavenumbers. Dimethylsiloxane-type silicone was observed on nut 920 FE #5 as a strong absorption at 1020 and 1100 wavenumbers (spectra not shown). Silica or silicate, possibly from the decomposition of silicone was observed on other nuts as absorptions in the 1000 to 1150 wavenumber region. In addition, nitrocellulose of unknown origin (some lacquers are similar), and a cotton fiber was observed on 916 AC #1.

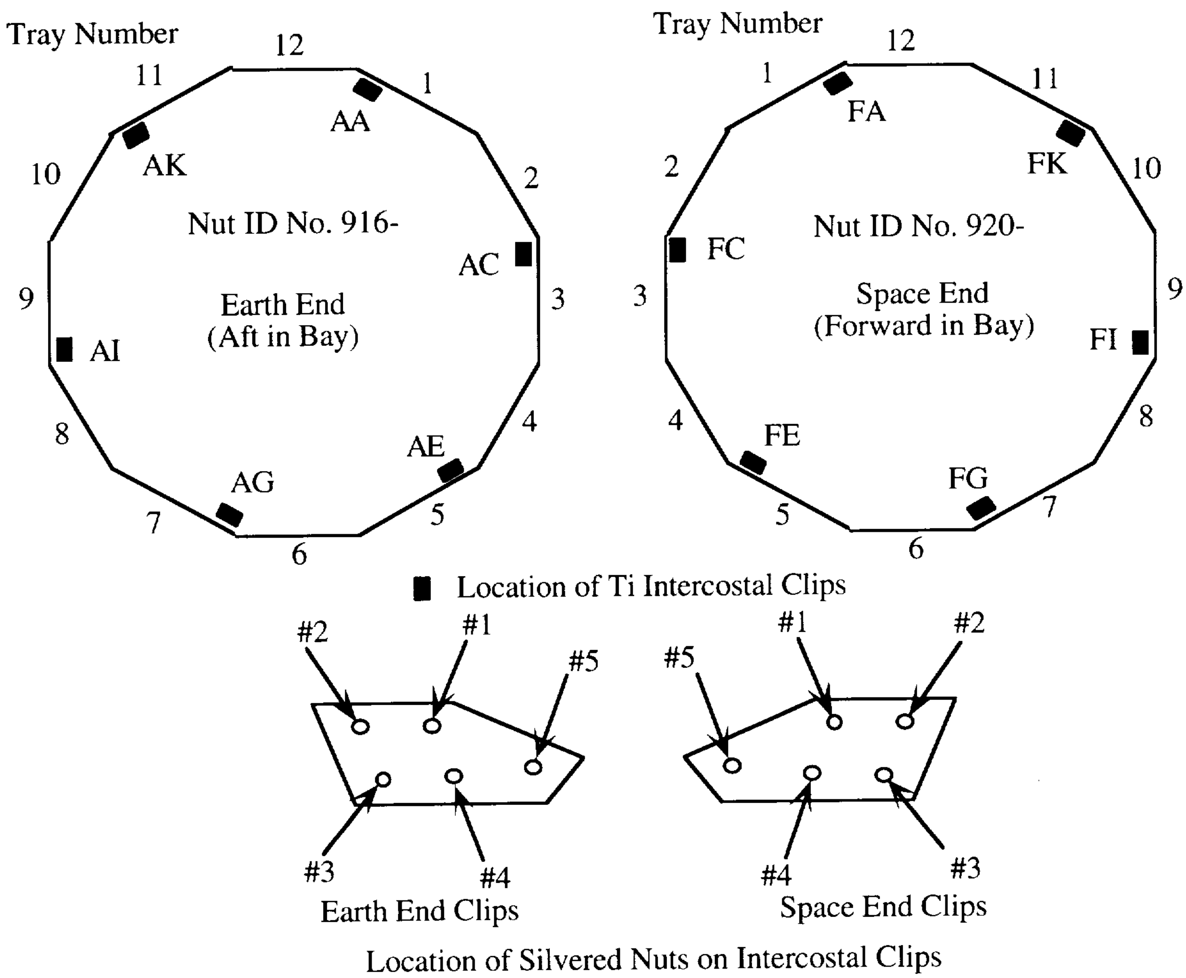

Figure 16. Silver plated nuts removed from LDEF. The nuts were removed from the intercostal clips on the inside of LDEF from the Earth end (12 each) and from the space end (12 each).

Nut ID.	Torque	Analysis Technique	Nut ID.	Torque	Analysis Technique
1/4" Silvered Nuts:					
916 AA #1	11.3 Nt-m	ESCA	920 FA #1	8.4 Nt-m	Cross-section
916 AC #1	11.5	FTIR	920 FC #1	10.7	
916 AE #1	11.8		920 FE #1	9.5	FTIR
916 AG2 #1	7.9		920 FG #1	10.1	
916 AI2 #1	24.1		920 FI #1	14.0	
916 AK #1	10.7		920 FK #1	14.0	ESCA
3/8" Silvered Nuts:					
916 AA #5	19.7 Nt-m	ESCA	920 FA #5	21.6 Nt-m	
916 AC #5	21.9	FTIR	920 FC #5	21.9	
916 AE #5	21.7		920 FE #5	21.3	FTIR
916 AG #5	20.2		920 FG #5	25.3	
916 AI #5	19.5		920 FI #5	23.0	Cross-section
916 AK #5	22.5		920 FK #1	29.0	ESCA

Table 10. Silver-Plated Nuts Analysis.

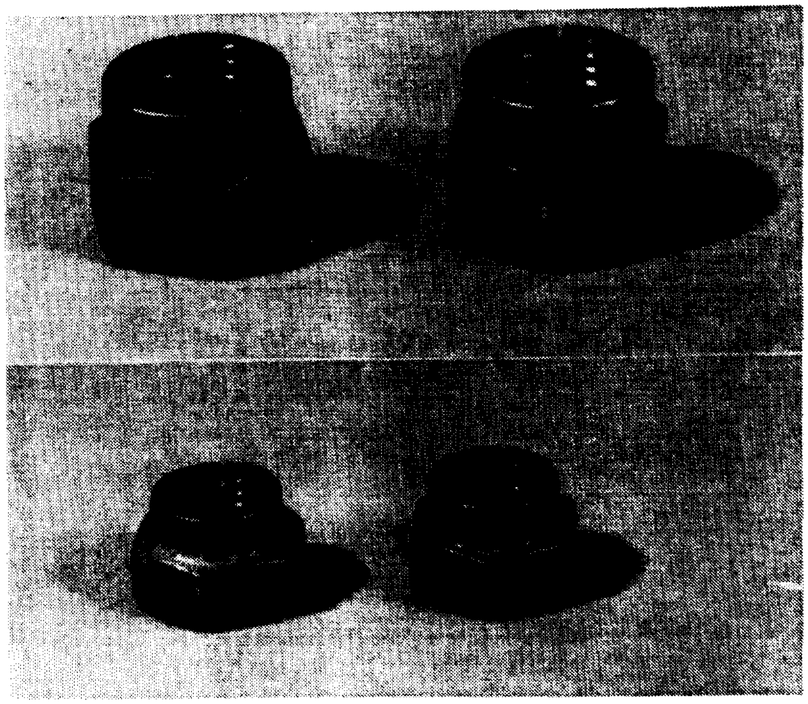

Dash Nos.	Thread MIL-S-8879	A MAX	A MIN	B MAX	B MIN	C MIN	D Dia. ±.020	F MIN	X	Axial Strength Lbs. MIN	Weight LBS/100 Ref	K Dia. MIN
C-4	.2500-28UNJF-3B	.328	.240	.439	.430	.482	.273	.116	.005	4,580	.99	.410
C-6	.3750-24UNJF-3B	.469	.318	.564	.553	.622	.398	.153	.006	11,450	2.15	.533

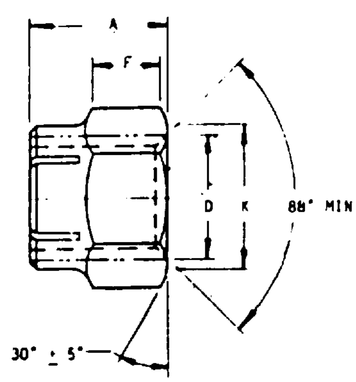

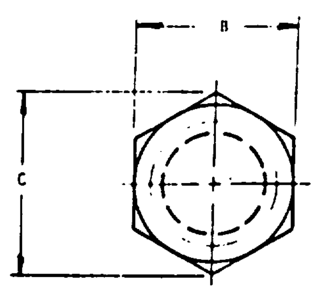

Figure 17. Photograph of silver-plated nuts at 2X magnification and corresponding diagram and data for each nut type.

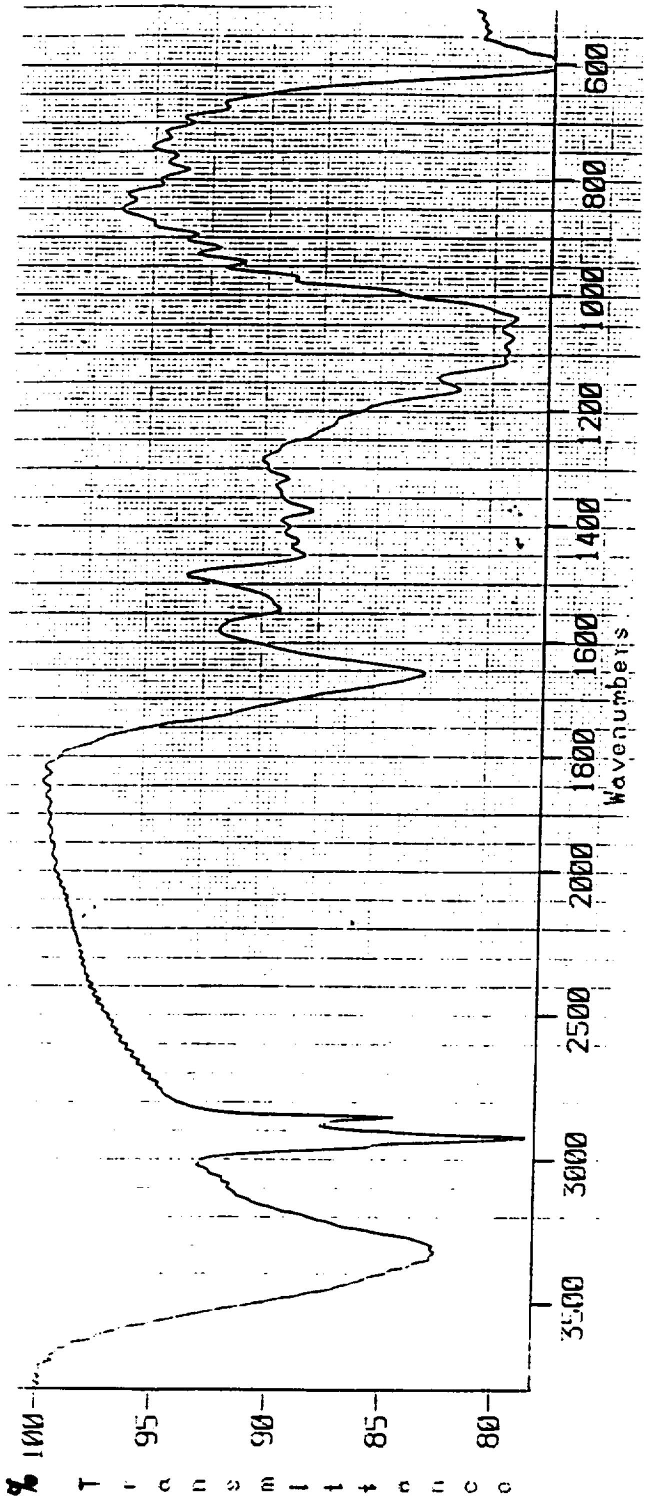

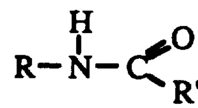

the amide linkage in peptide and proteins absorbs at 1640-1650 and 1540-1550 wavenumbers.

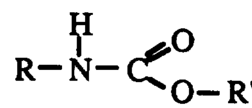

the similar urethane functional group absorbs strongly at 1730, and less strongly at 1540 wavenumbers.

Figure 18. Results of FTIR analysis of tarnish removed from the nuts.

7.0 SUMMARY

In general, the hardware on the interior of LDEF, which was shielded from direct exposure to atomic oxygen, solar protons and electrons, impacts and solar radiation, remained in good condition and performed its engineering functions. Exposure to the vacuum component of the space environment and mild thermal cycling resulted in outgassing of the materials. Contamination which varied by location and degree, was observed on the interior hardware. The following specific conclusions regarding the interior hardware have been reached.

Kapton™ thermal control blankets used on the interior facing sides of the experiment trays appeared in excellent condition subsequent to the flight.

The Z-306 painted structure appeared unchanged except for areas with contamination deposits.

The TML and CVCM measurements of the structure facing and interior facing side of the same heat shrink tubing clamps showed similar results. Based on the TML and CVCM measurements, the heat shrink tubing had different post-flight properties when comparing leading and trailing locations with side and edge locations. The flight versus representative non-flown material had different TML values while the CVCM values had a much lower level of confidence that the data was from different populations. The lower confidence value for the CVCM data may be due to the moisture the flight samples absorbed upon retrieval prior to testing.

The TML data from the composite shims indicates there are significant differences between the leading/trailing edge locations and specimens from other locations, and between the flight and ground samples.

A variety of different tests were conducted on the nylon wire bundle clamps which showed no significant differences in pre- and post-flight properties other than those attributed to random variations in the material. The maximum changes detected had no real effect on the performance of the clamps.

Silver-plated nuts from the intercostal clips showed no erosion or degradation of the protective silver coating. However, the nuts were tarnished, with the amount and color of the tarnish varying over each nut and between nuts. The tarnish consisted of silicone and silica/silicates from the decomposition of silicone and of amide material which may have originated from urethane paints.

A principal lesson from LDEF is that properly selected materials, placed on the interior of a structure, subject to vacuum and mild thermal cycling, may be expected to perform well over extended time periods. The interior facing materials examined did not appear to be close to end of performance life. For satellites under harsher thermal conditions, the performance of some of the types of materials examined here could be significantly effected. While it is unlikely that high energy particles caused any significant damage to the materials examined, electronics on interior surfaces are known to be effected by cosmic rays. These subjects merit further examination on other flights.

8.0 References

1. R.J. Bourassa and J.R. Gillis, NASA CR 189627, Atomic Oxygen Exposure of LDEF Experiment Trays, May 1992.

2. R.J. Bourassa and J.R. Gillis, NASA CR 189554, Solar Exposure of LDEF Experiment Trays, February 1992.

3. W.M. Berrios, "Use of the LDEF's Thermal Measurement System for the Verification of Thermal Models," First LDEF Post-Retrieval Symposium, NASA CP 3134, Part 1, p.69, June 1991.

4. T.W. Armstrong and B.L Colborn, "Scoping Estimates of the LDEF Satellite Induced Radioactivity," Report No. SAIC-90/1462, September 1990.

5. T. See, M. Allbrooks, D. Atkinson, C. Simon, and M. Zolensky, "Meteoroid and Debris Impact Features Documented on the LDEF–A Preliminary Report Compiled by Members of the LDEF Meteoroid and Debris Special Investigation Group," Pub. 84, JSC #24608, August 1990.

6. T.D. Le and G.L. Steckel, "Thermal Expansion Behavior of LDEF Metal Matrix Composites," Second LDEF Post-Retrieval Symposium, NASA CP 3194, Part 3, p.977, June 1992.

APPENDIX A

HEAT SHRINK TUBING AND SHIMS

List of Figures

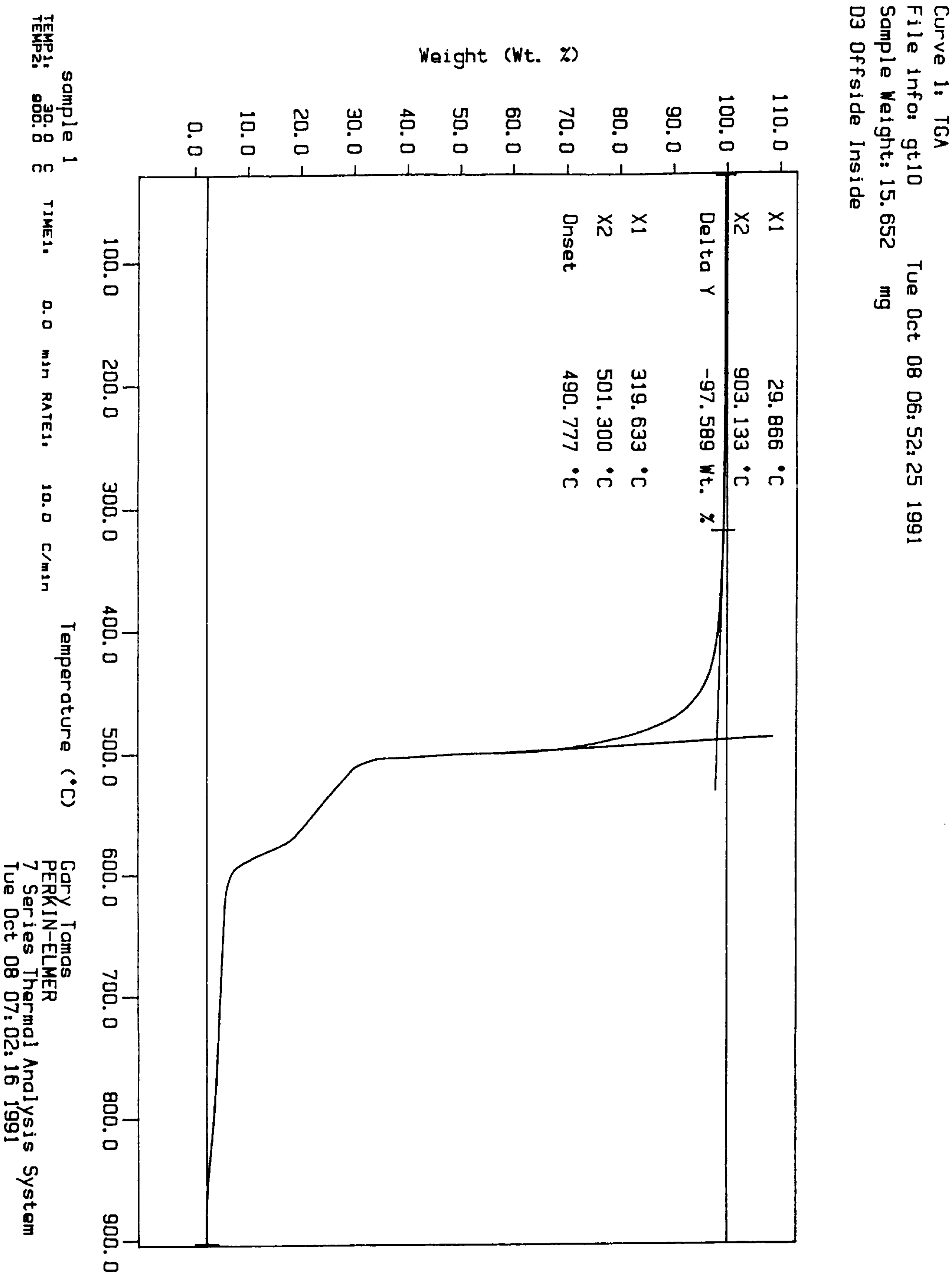

Figure 1. TGA measurement for structure-facing heat shrink tubing specimen D3.

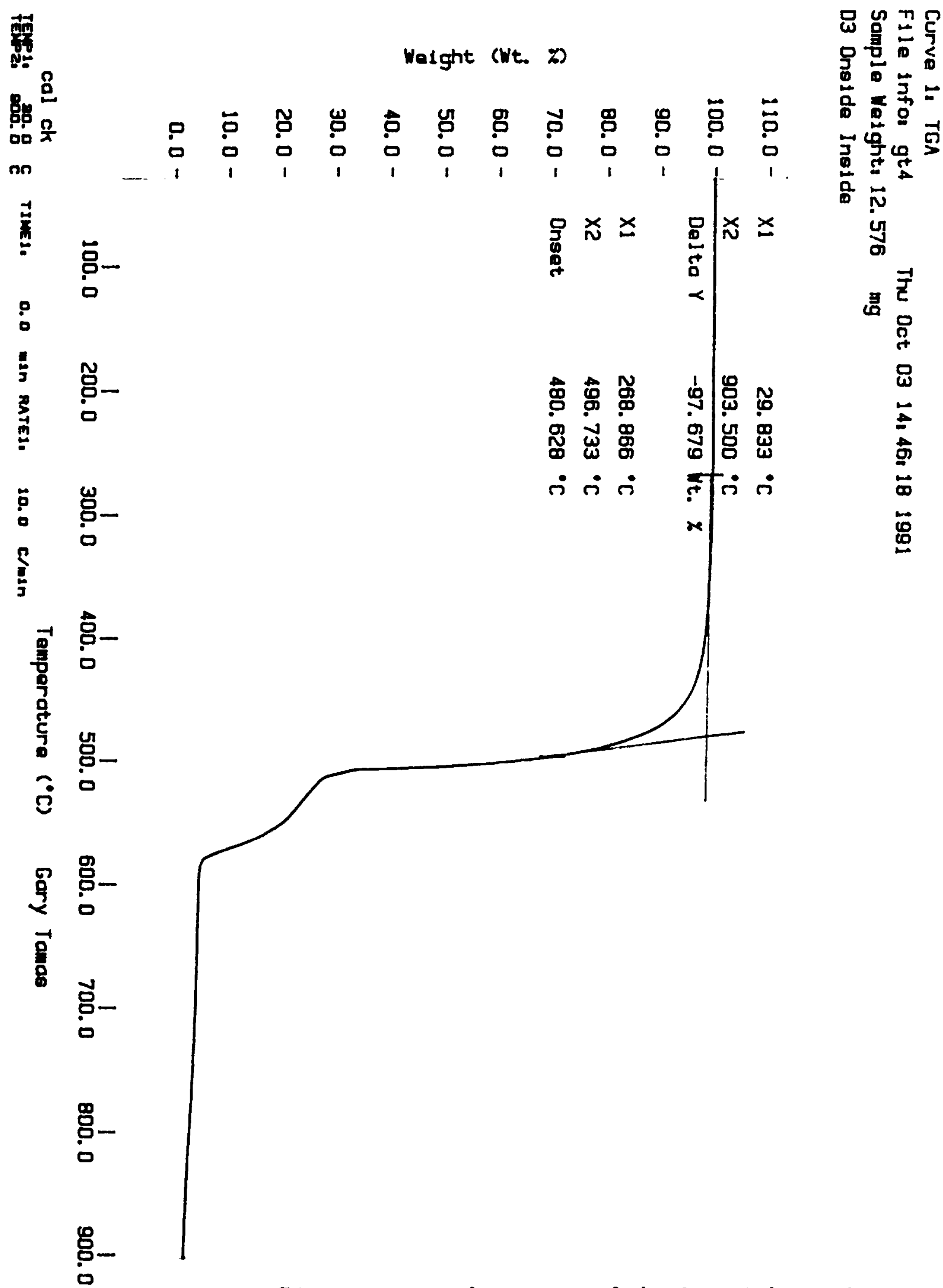

Figure 2. TGA measurement for structure-facing heat shrink tubing specimen D3.

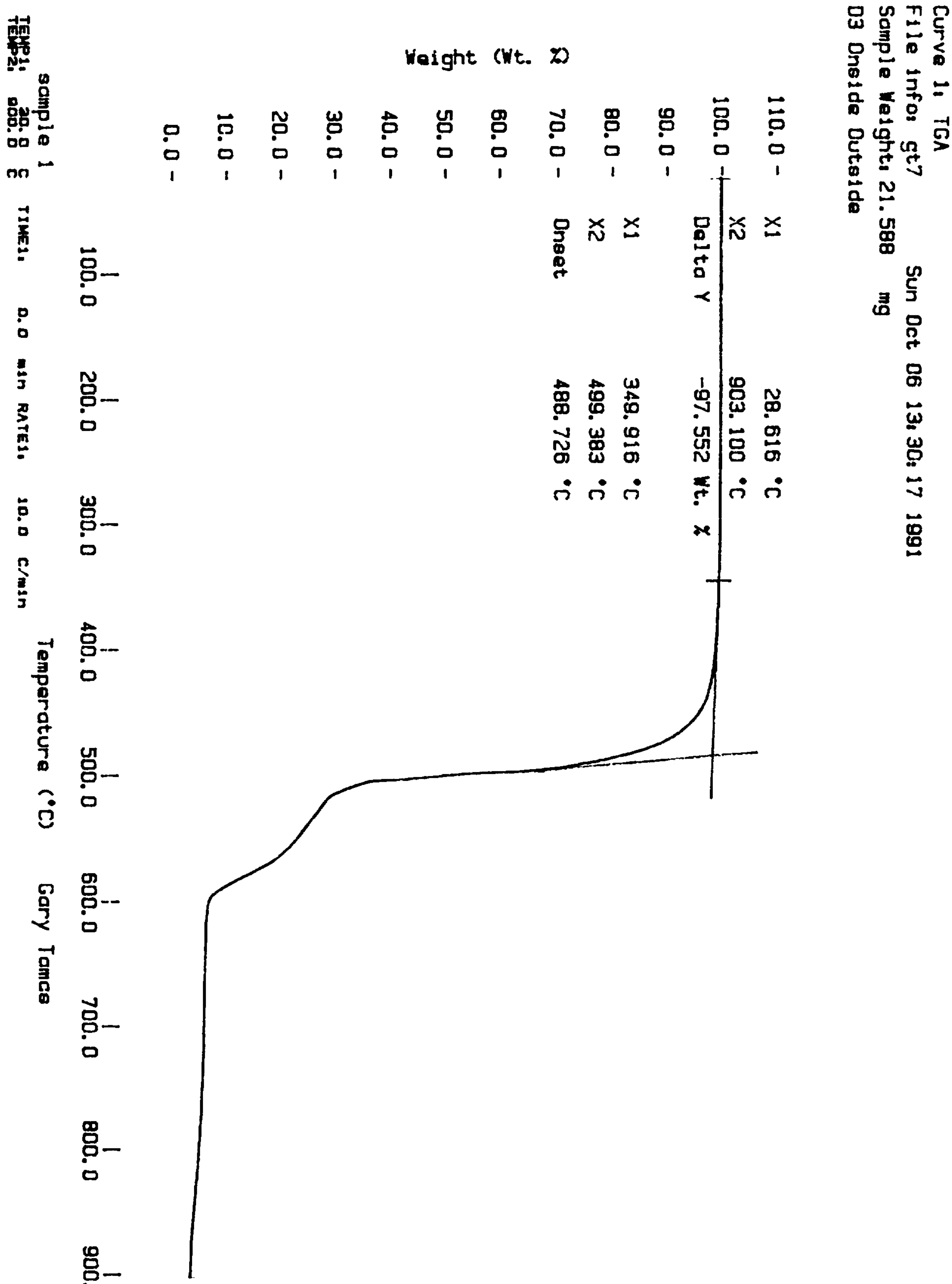

Figure 3. TGA measurement for interior-facing heat shrink tubing specimen D3.

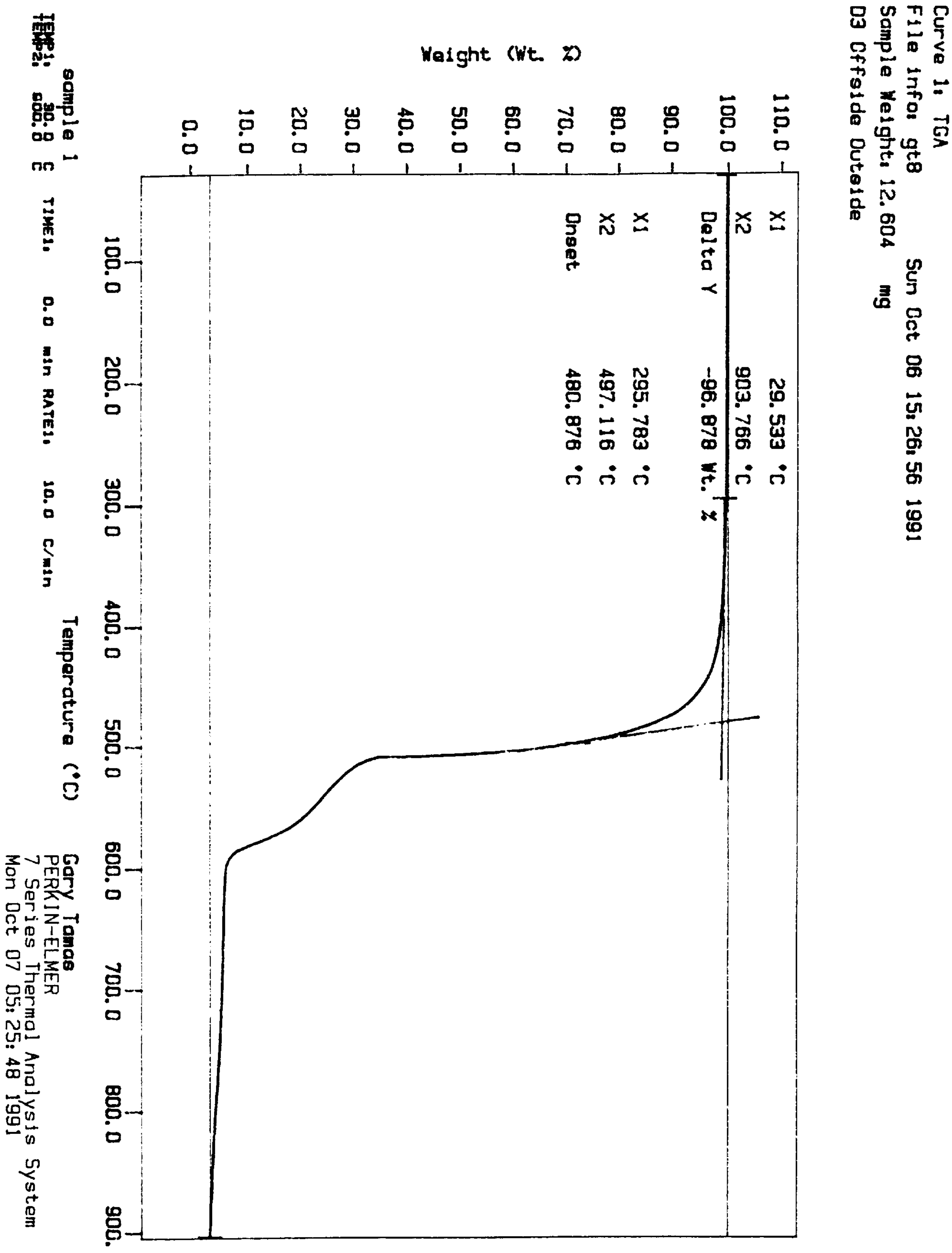

Figure 4. TGA measurement for interior-facing heat shrink tubing specimen D3.

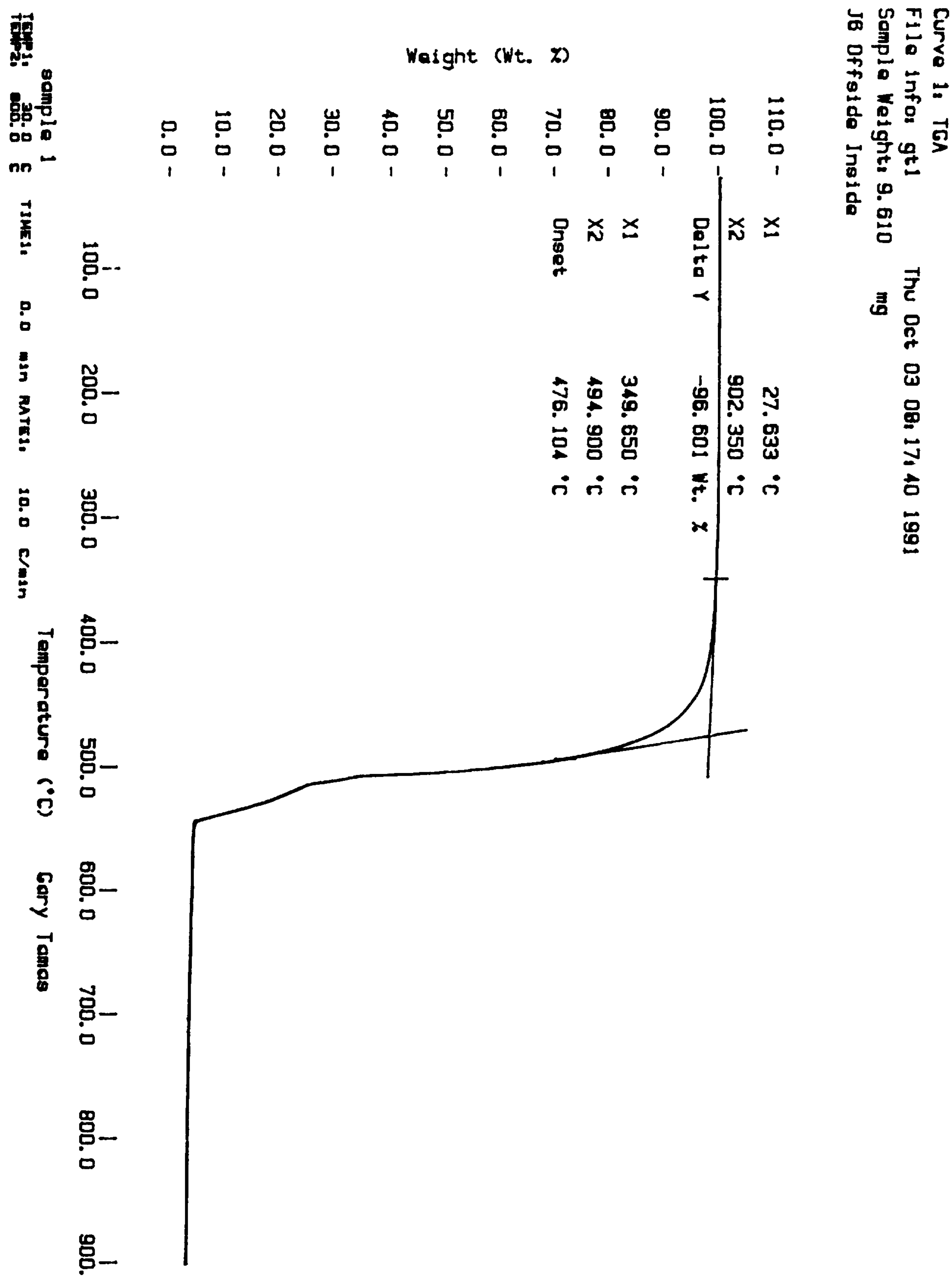

Figure 5. TGA measurement for structure-facing heat shrink tubing specimen J6.

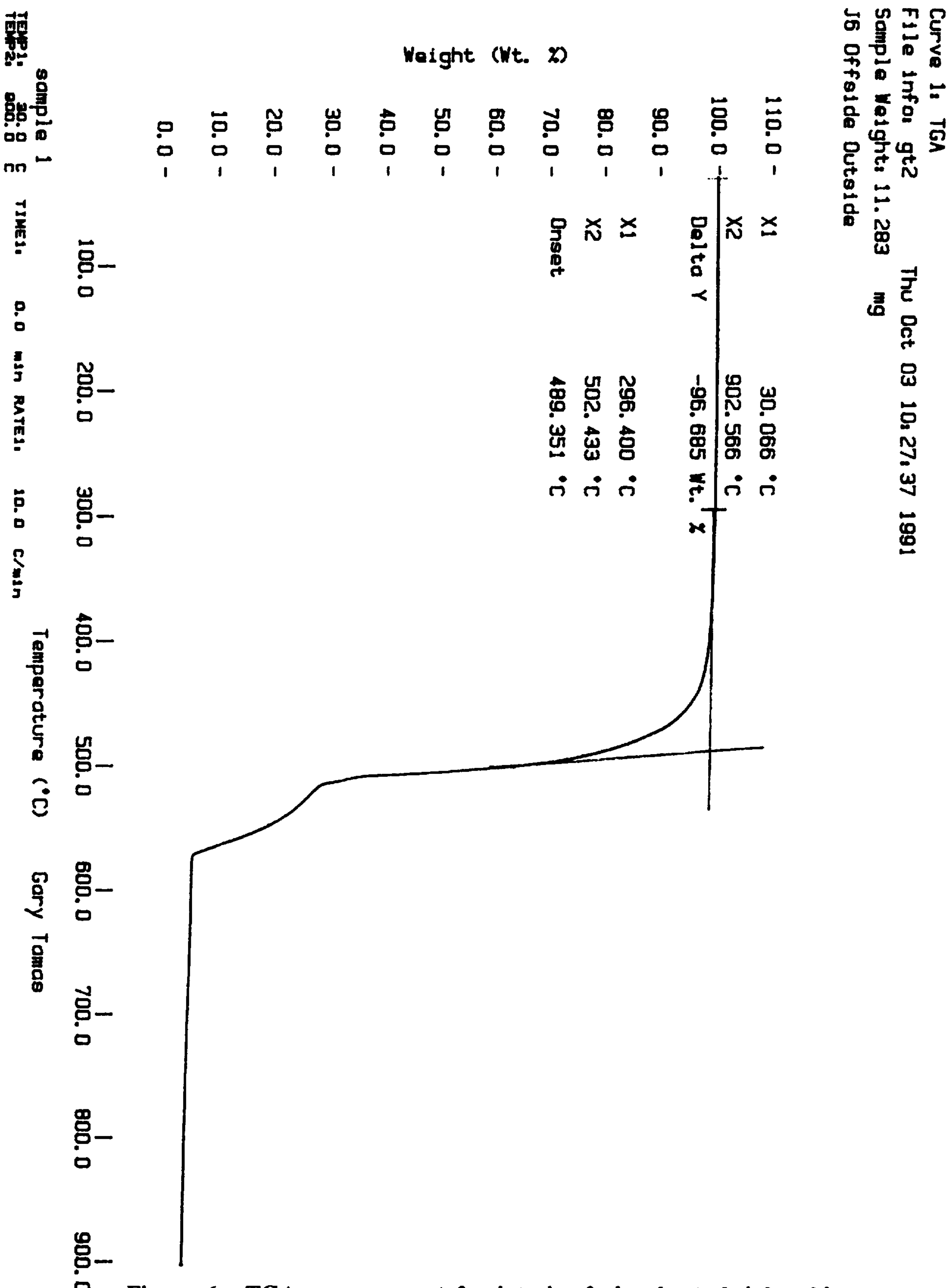

Figure 6. TGA measurement for interior-facing heat shrink tubing specimen J6.

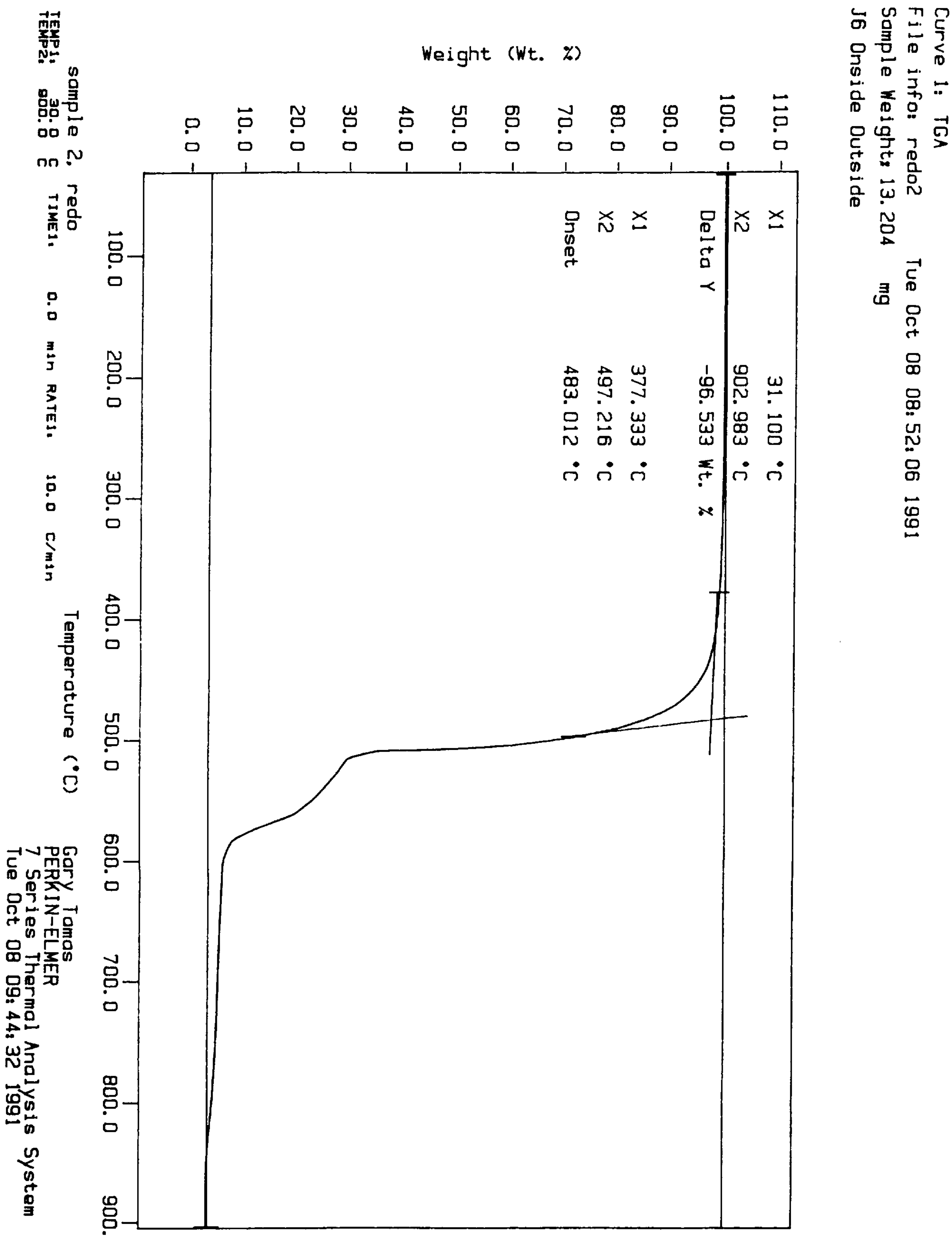

Figure 7. TGA measurement for interior-facing heat shrink tubing specimen J6.

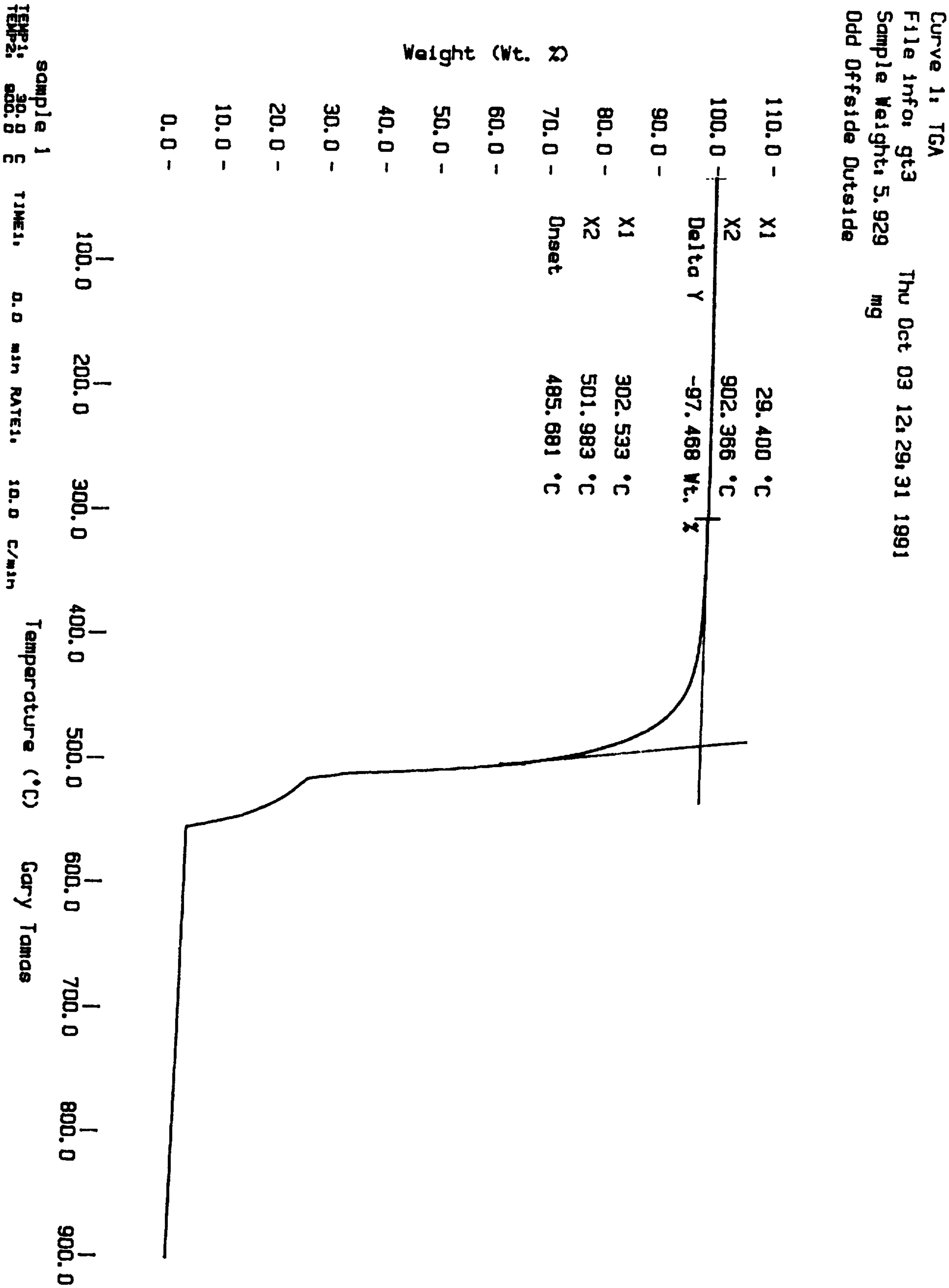

Figure 8. TGA measurement for ground control heat shrink tubing specimen.

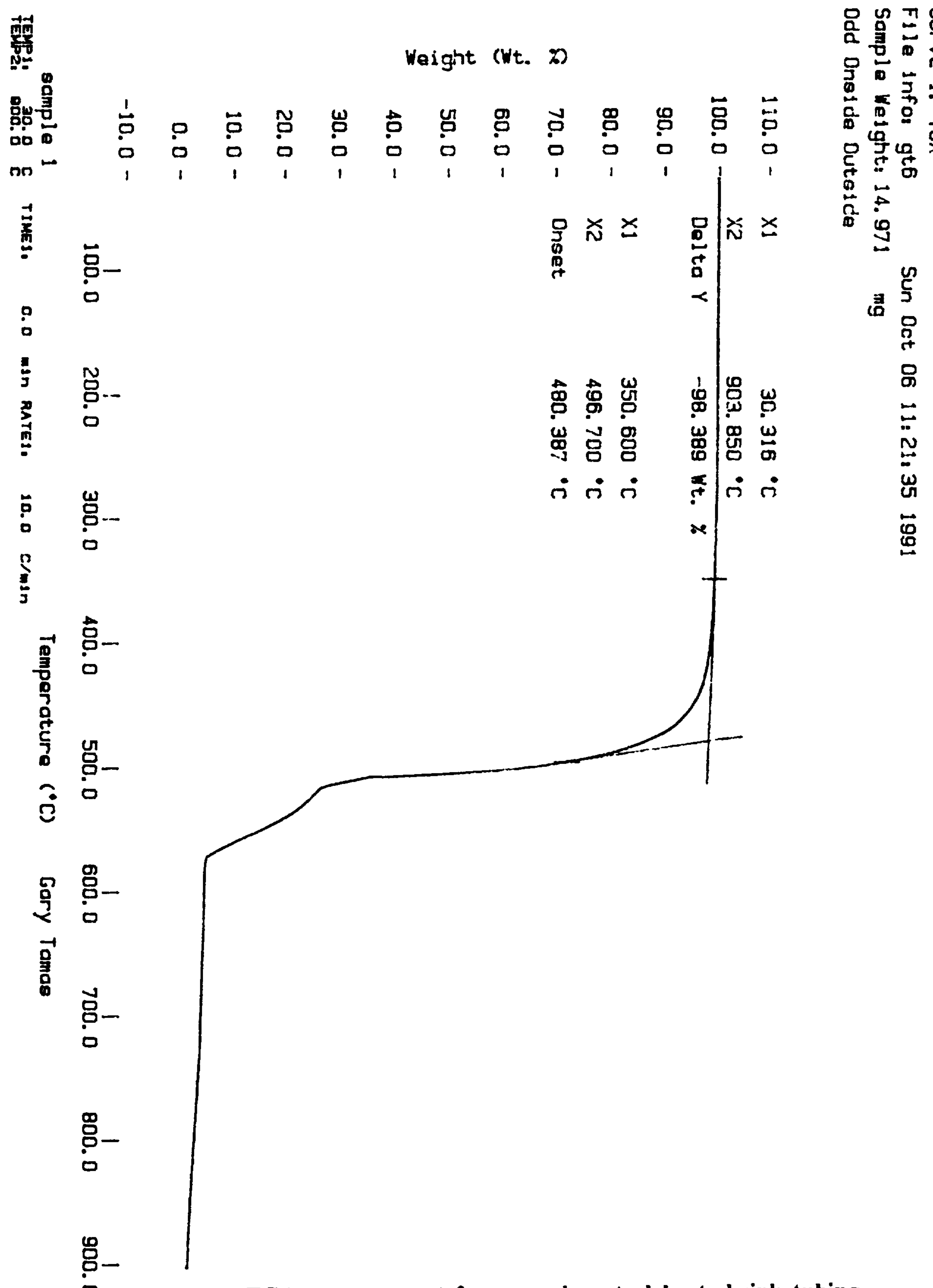

Figure 9. TGA measurement for ground control heat shrink tubing specimen.

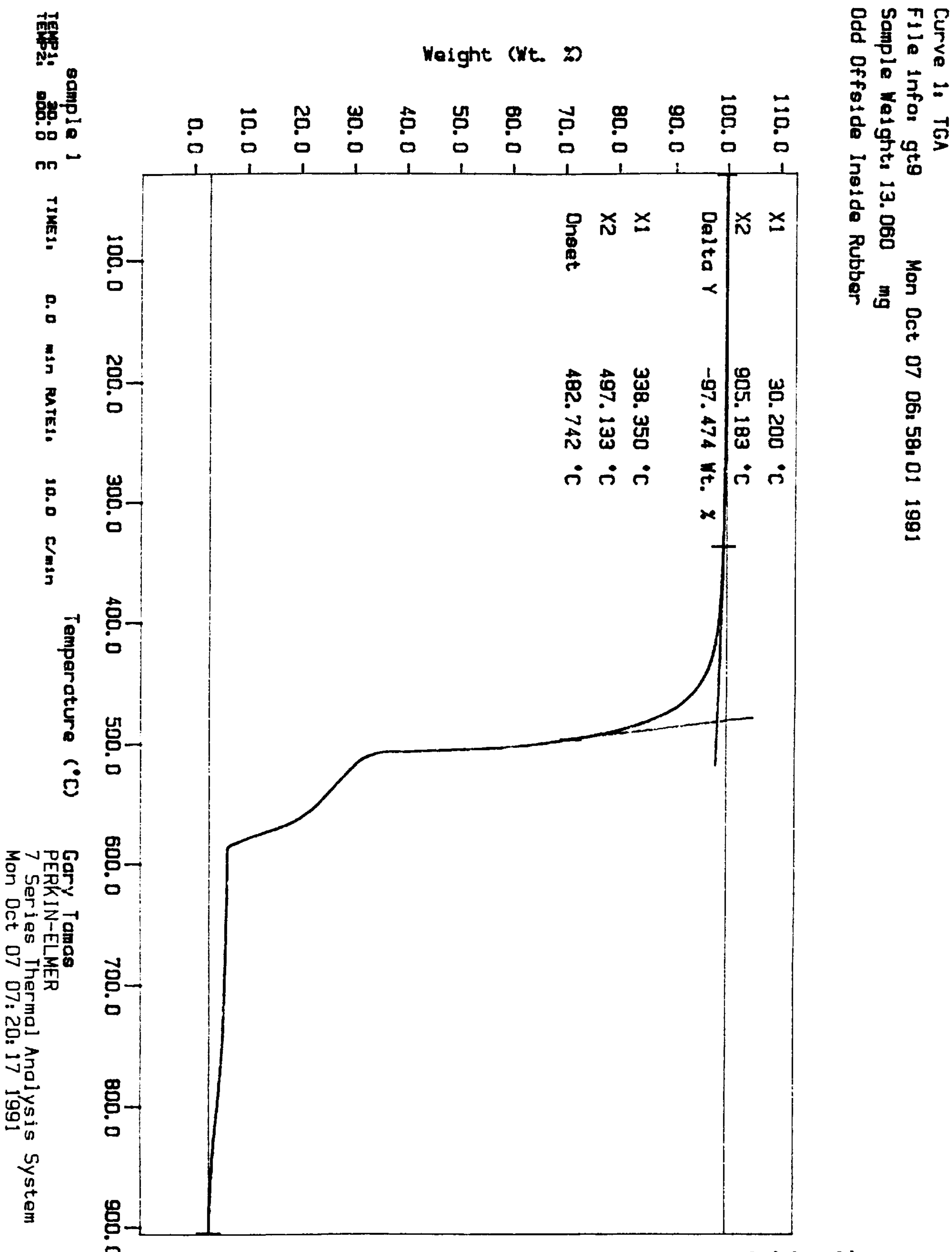

Figure 10. TGA measurement for ground control heat shrink tubing specimen.

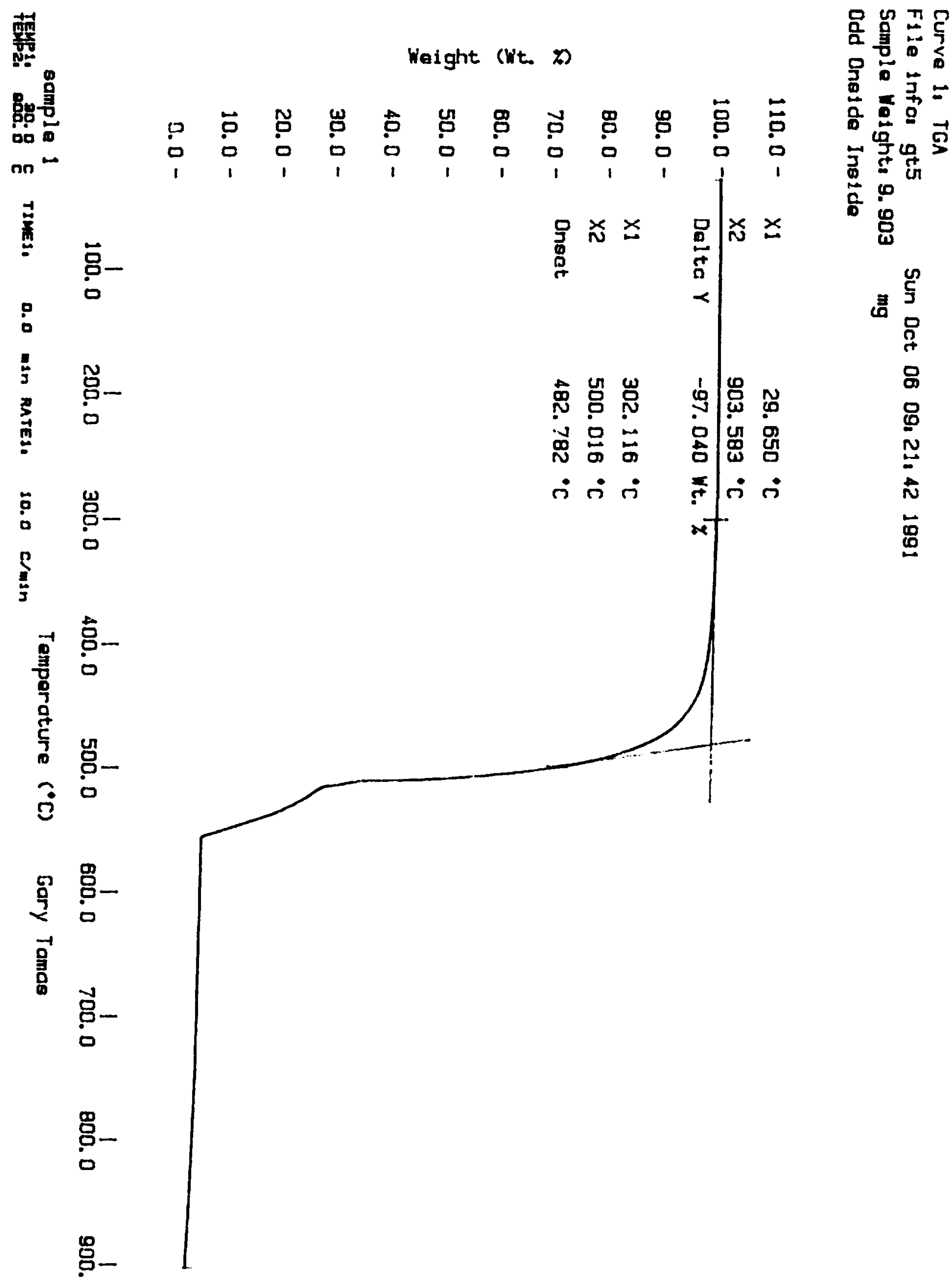

Figure 11. TGA measurement for ground control heat shrink tubing specimen.

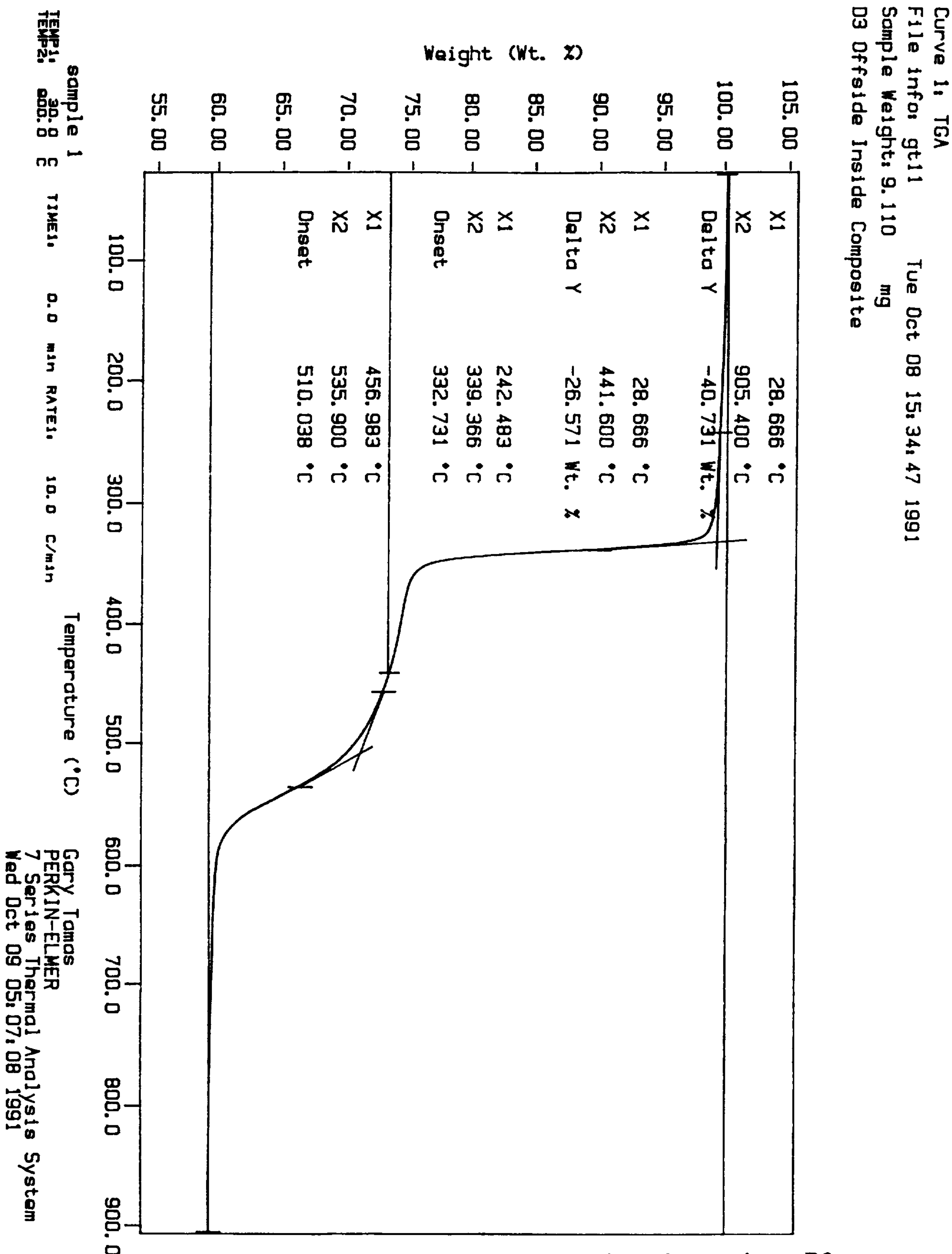

Figure 12. TGA measurement for composite shim specimen D3.

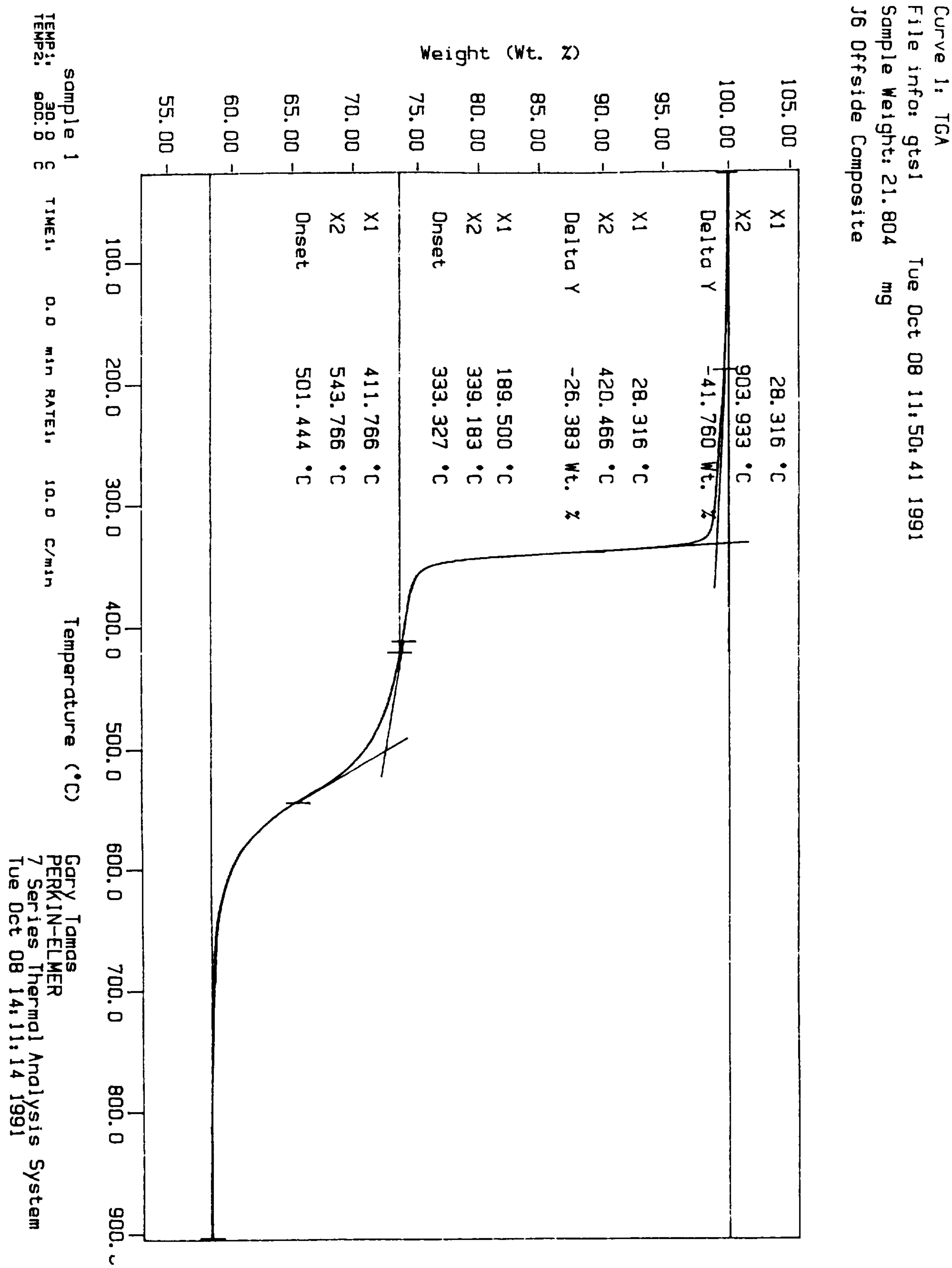

Figure 13. TGA measurement for composite shim specimen J6.

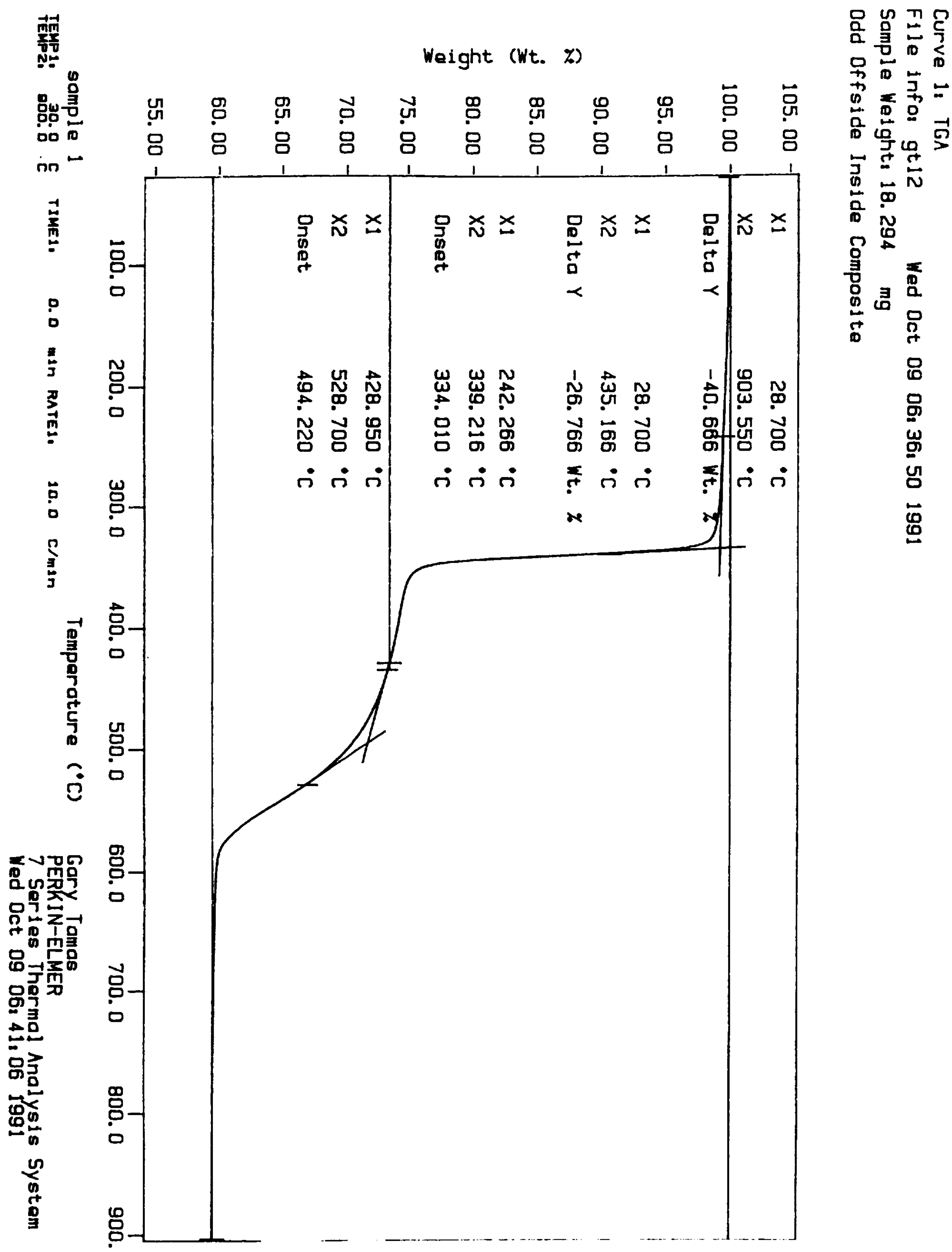

Figure 14. TGA measurement for ground control composite shim specimen.

APPENDIX B

NYLON WIRE BUNDLE CLAMPS

List of Figures

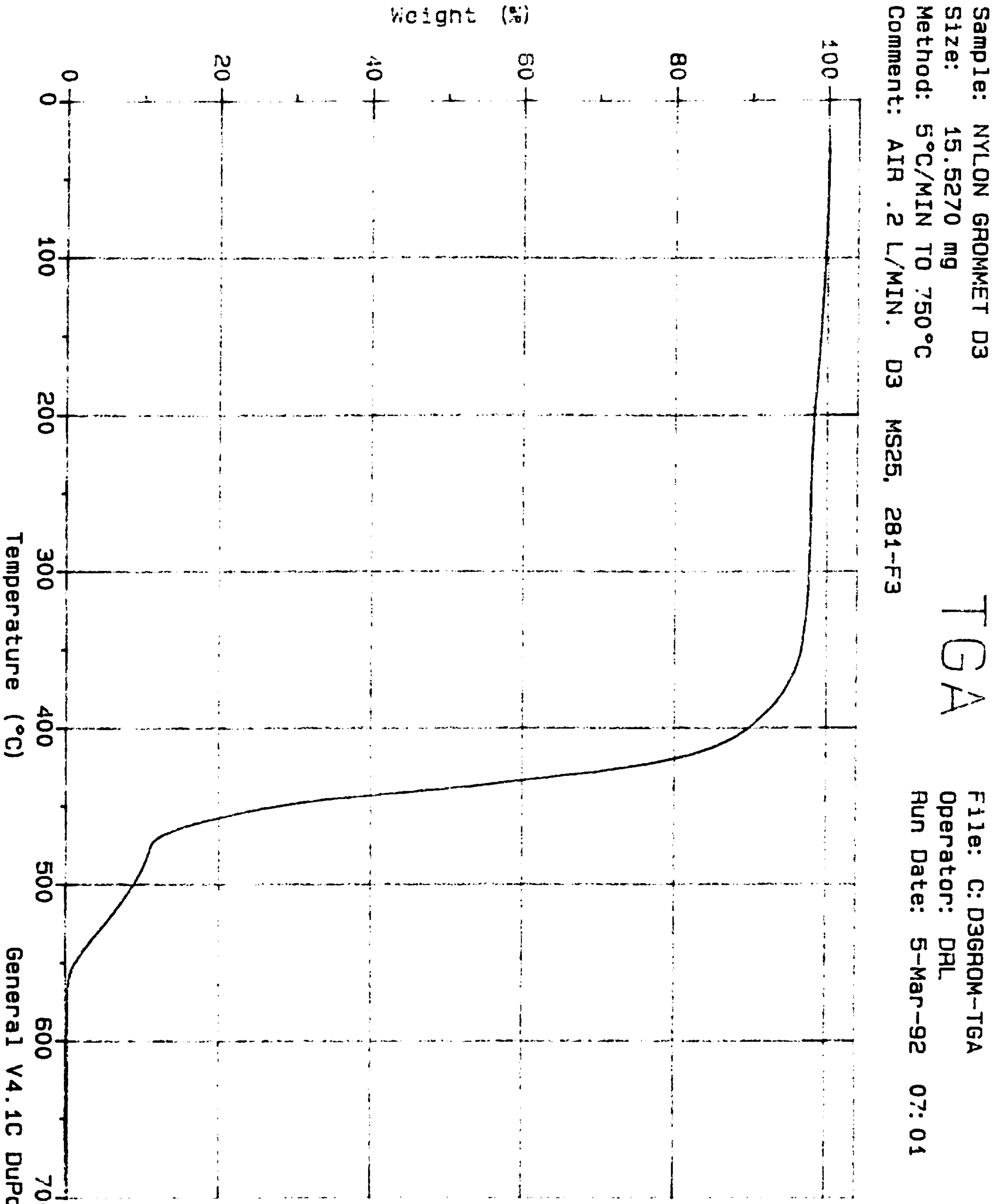

Figure 1. TGA measurement on wire harness bundle nylon grommet D3.

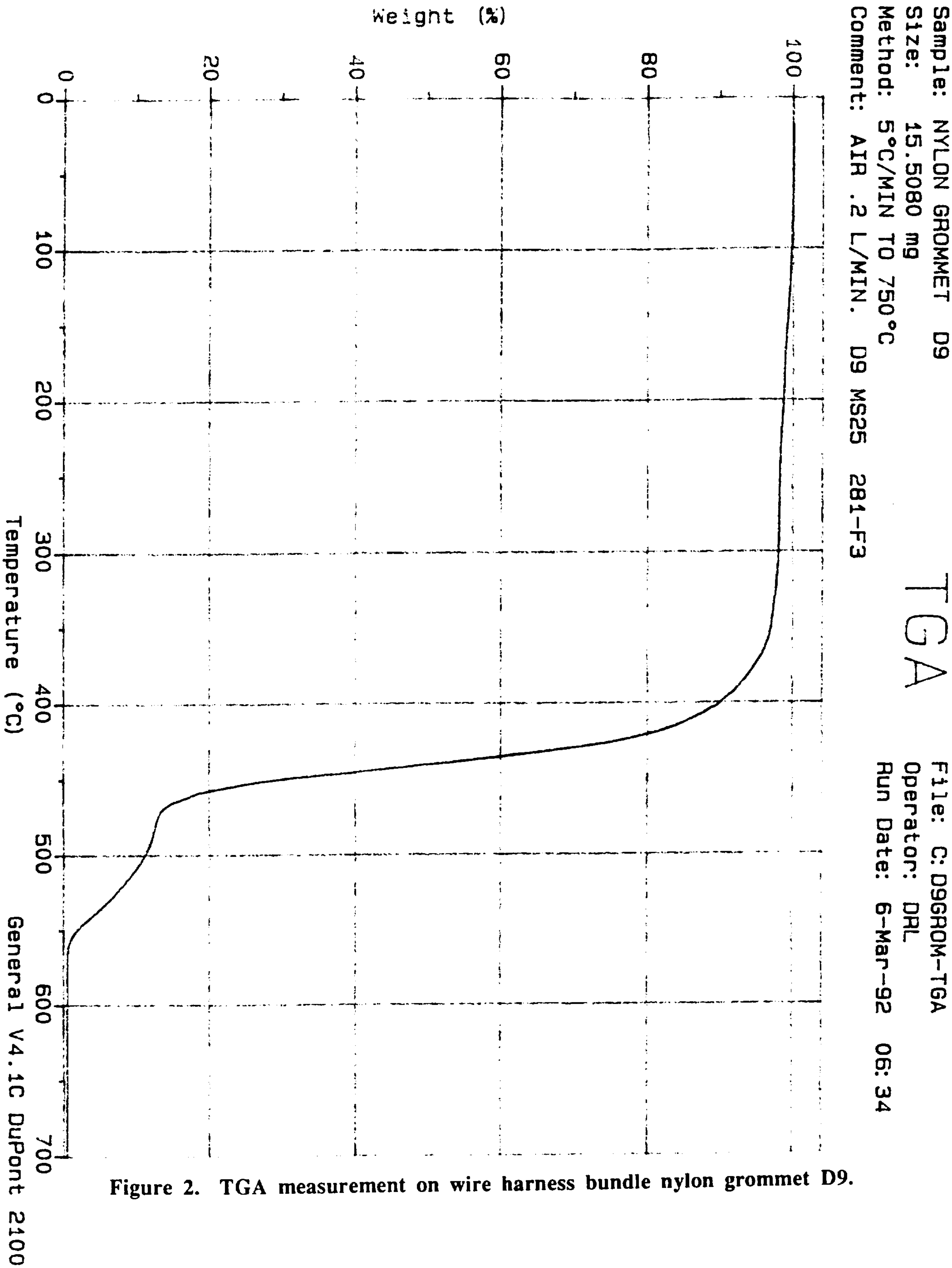

Figure 2. TGA measurement on wire harness bundle nylon grommet D9.

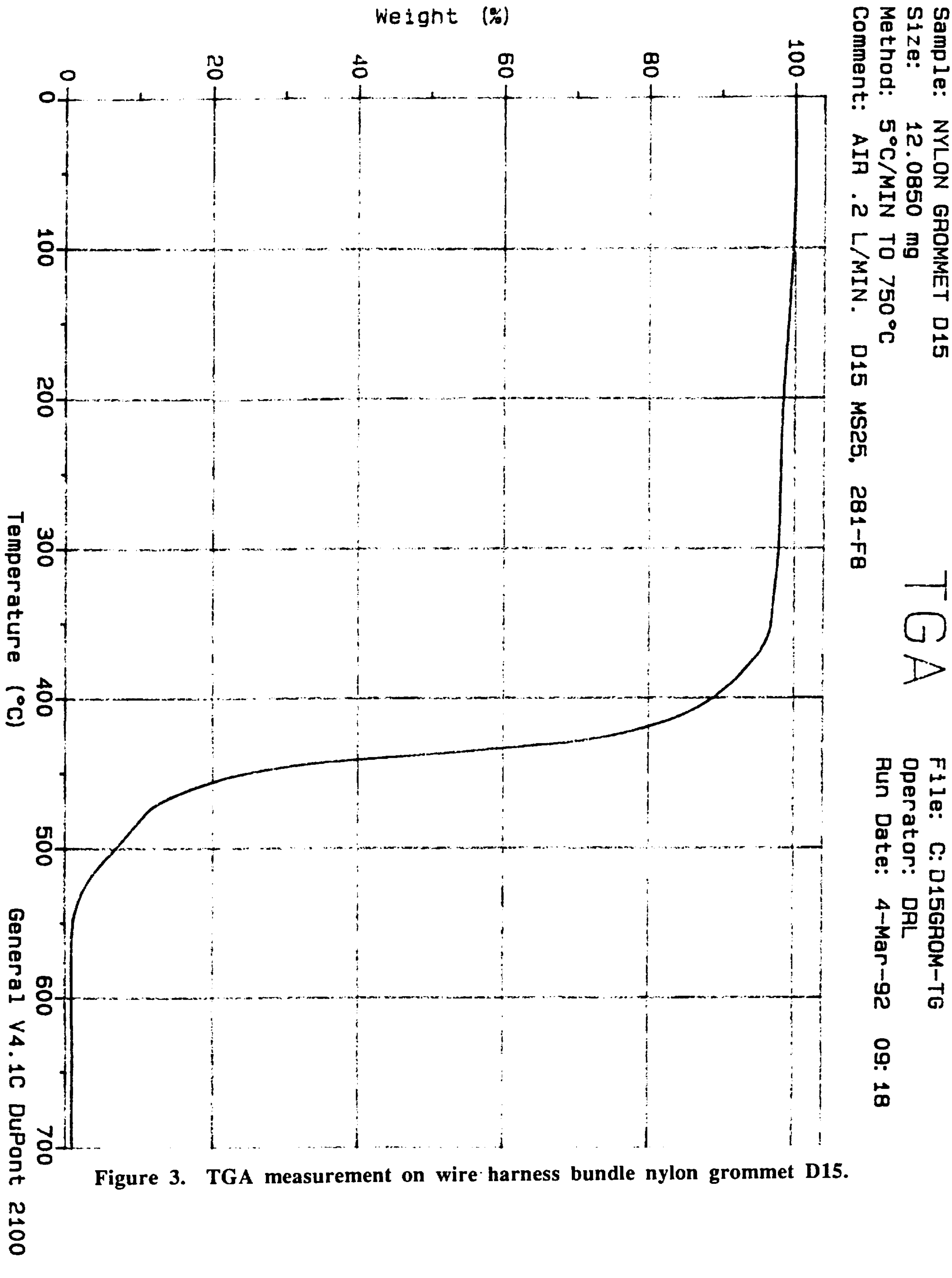

Figure 3. TGA measurement on wire harness bundle nylon grommet D15.

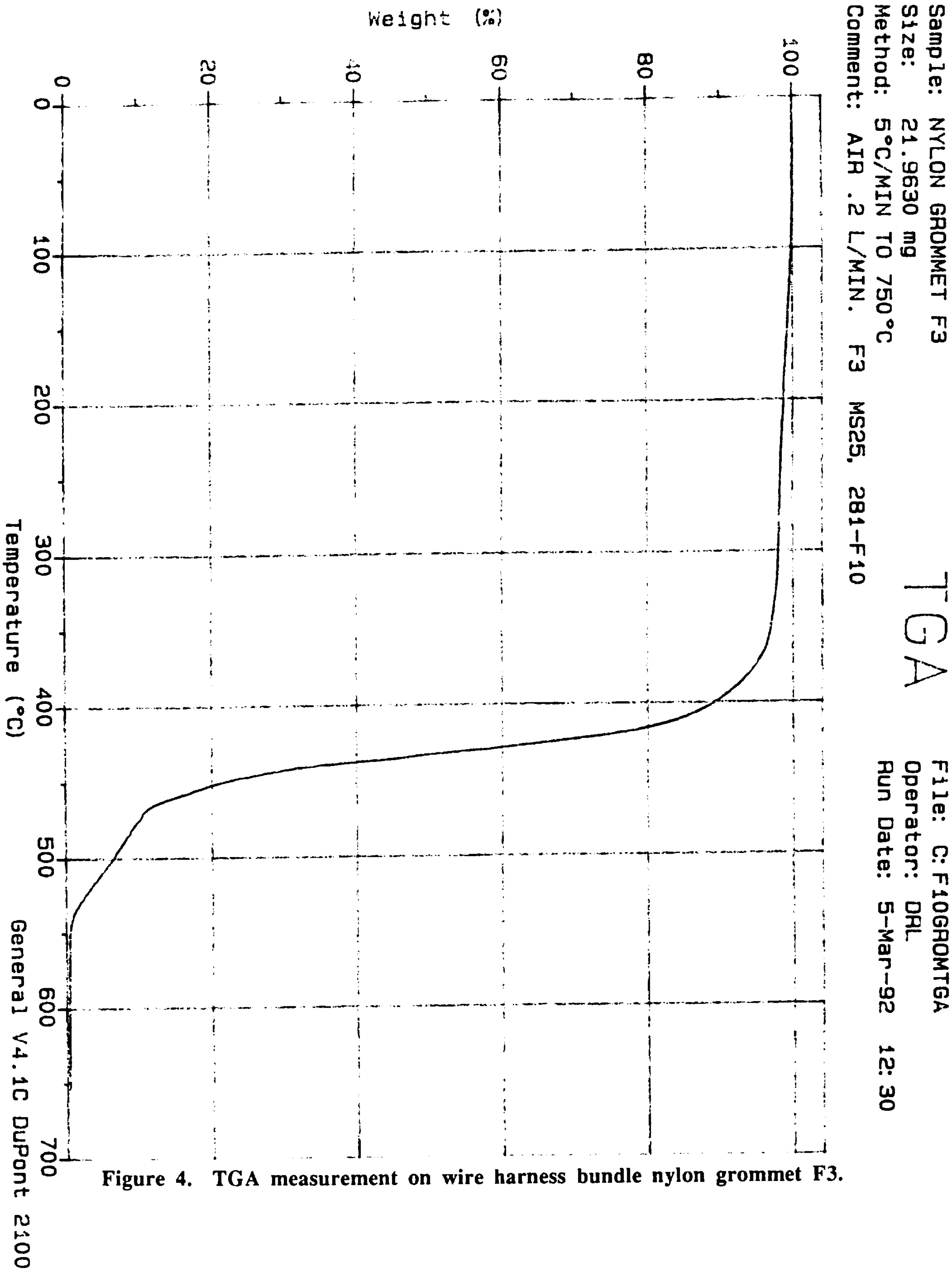

Figure 4. TGA measurement on wire harness bundle nylon grommet F3.

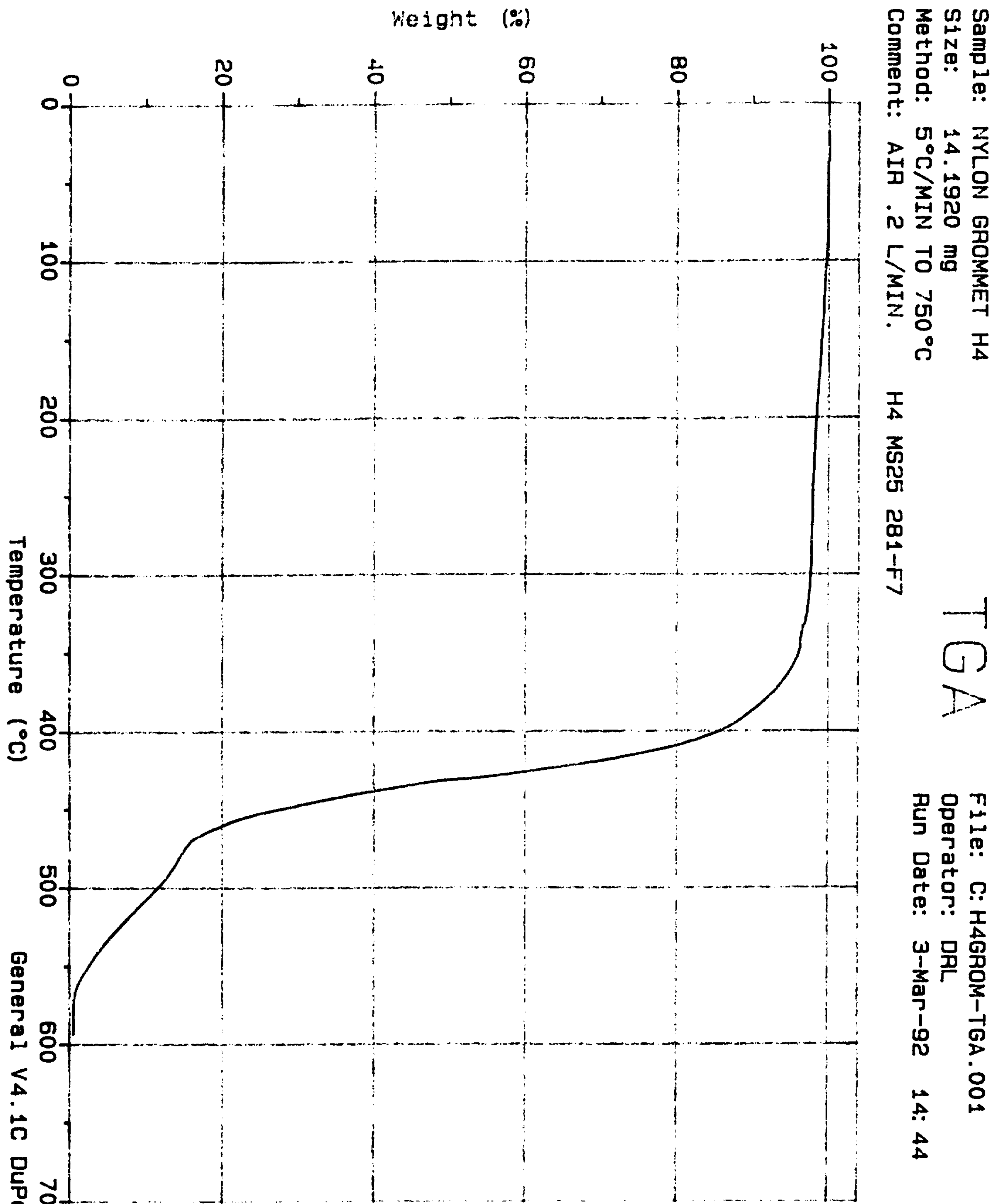

Figure 5. TGA measurement on wire harness bundle nylon grommet H4.

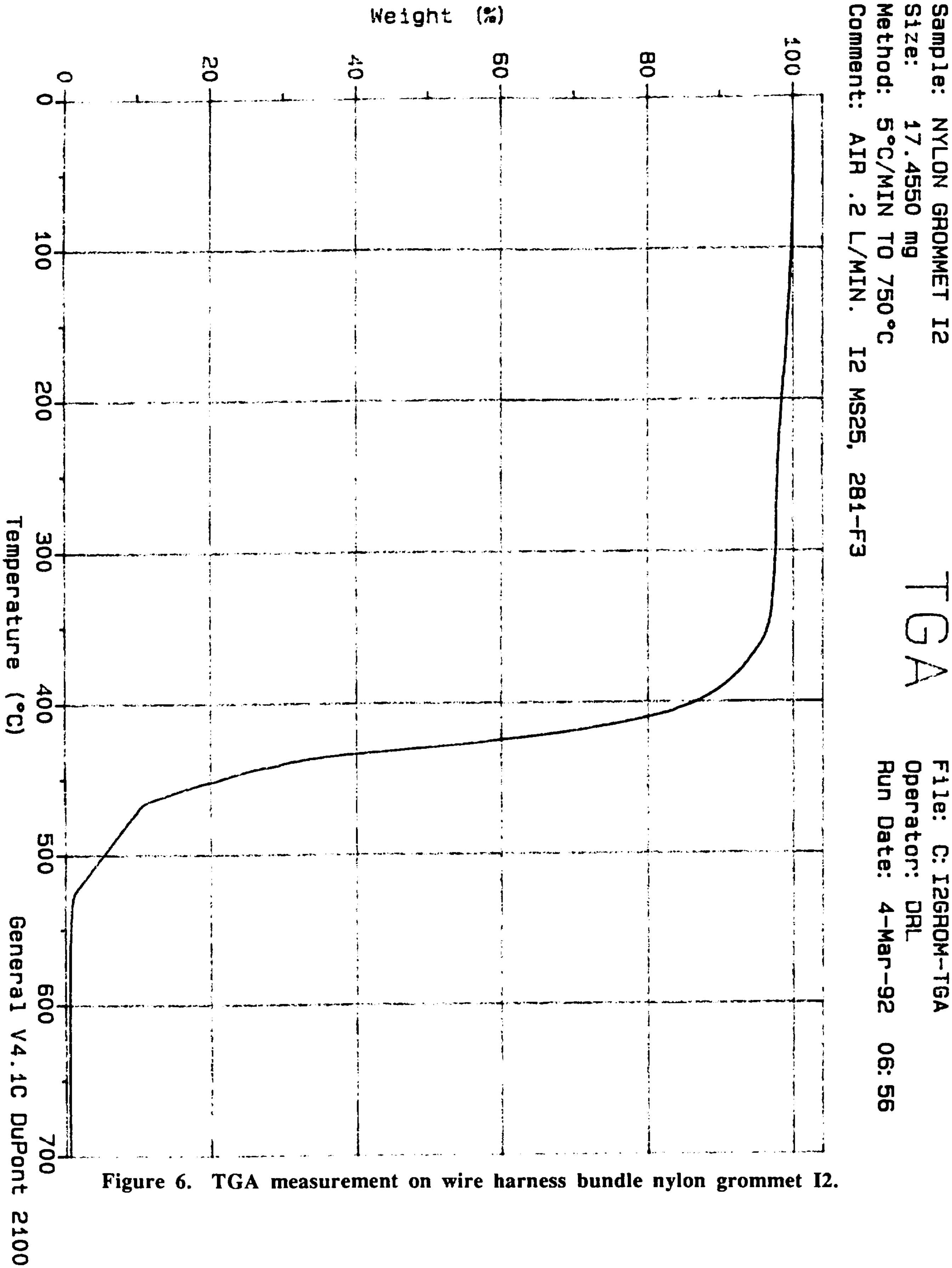

Figure 6. TGA measurement on wire harness bundle nylon grommet I2.

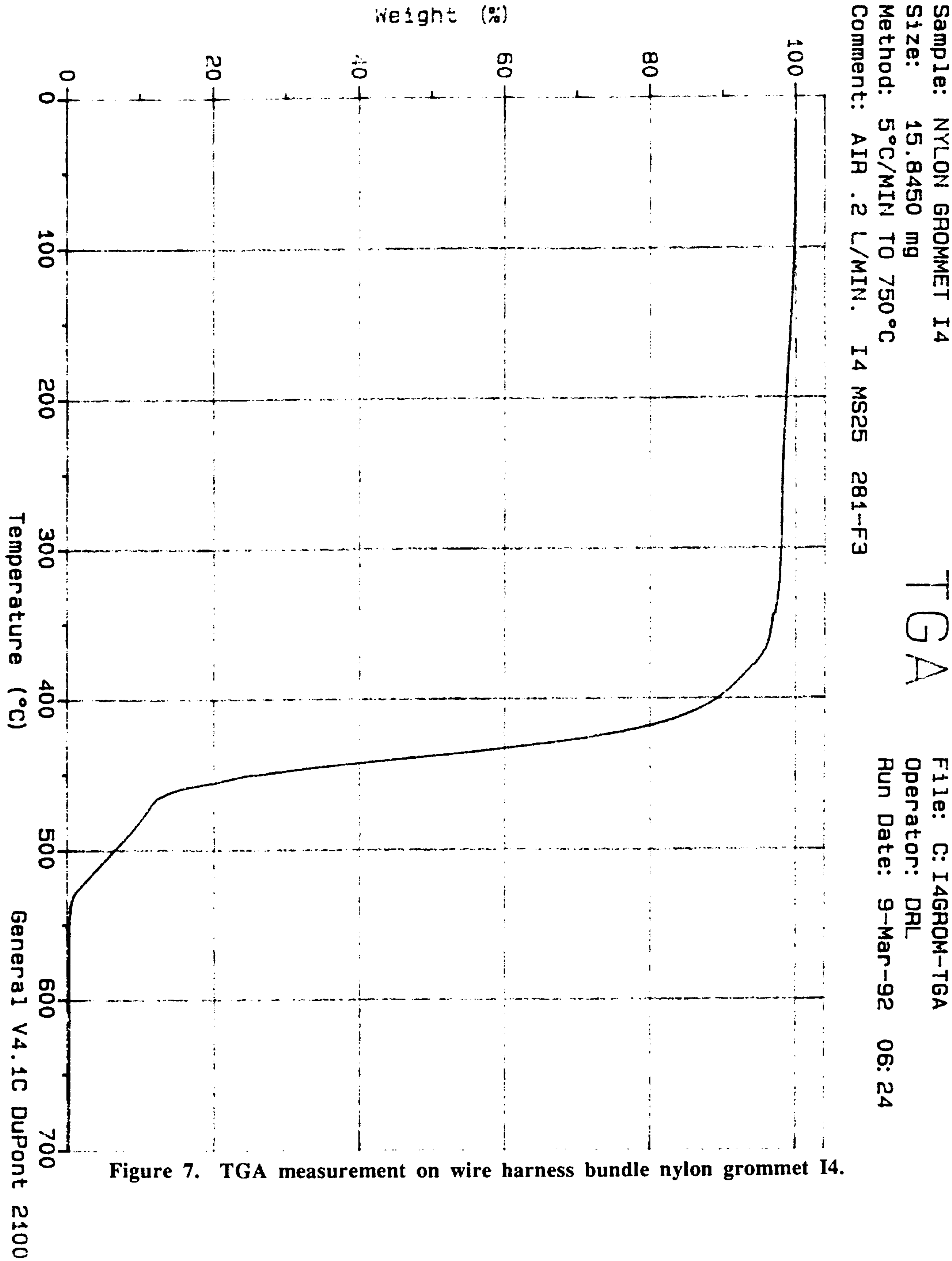

Figure 7. TGA measurement on wire harness bundle nylon grommet I4.

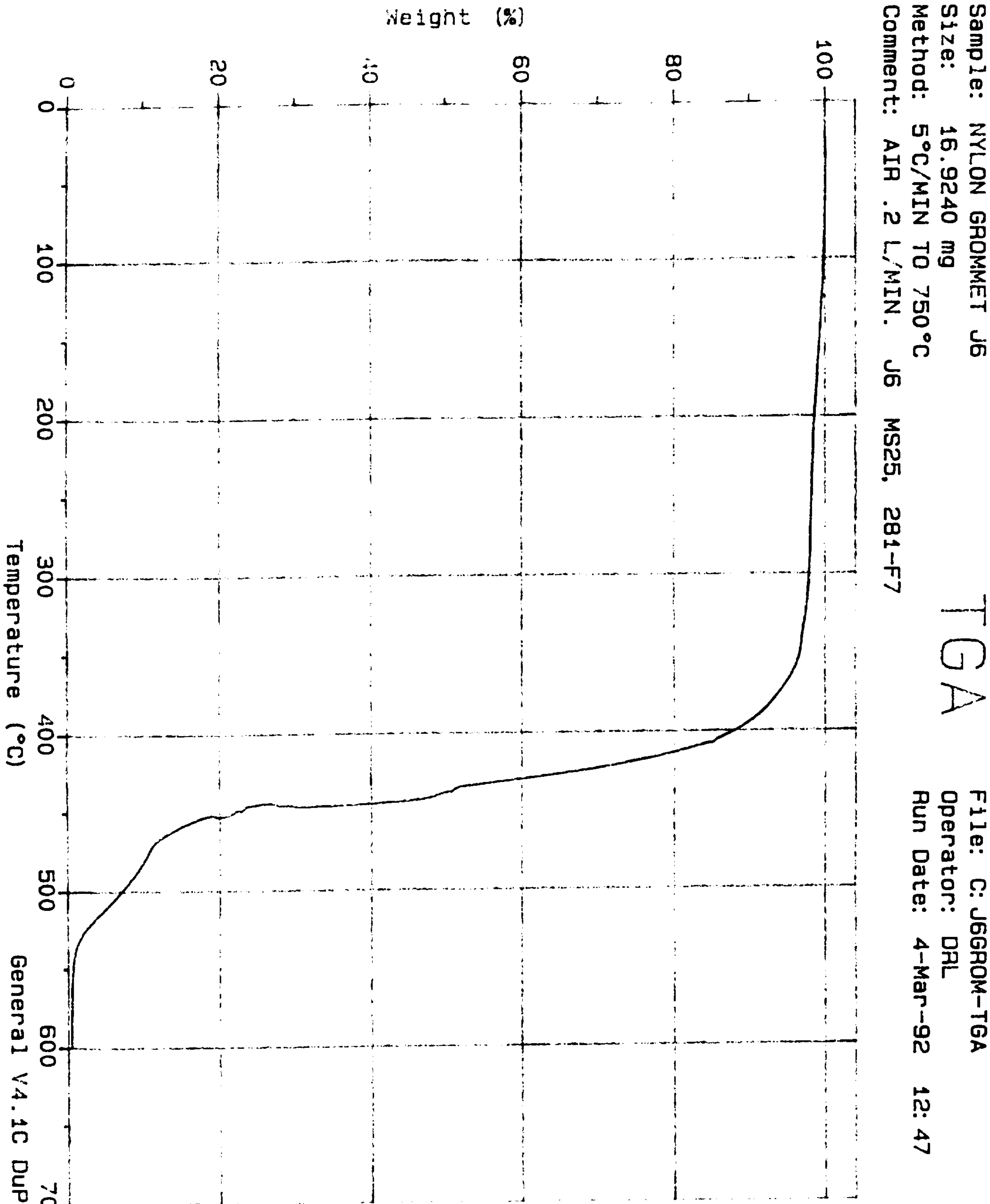

Figure 8. TGA measurement on wire harness bundle nylon grommet J6.

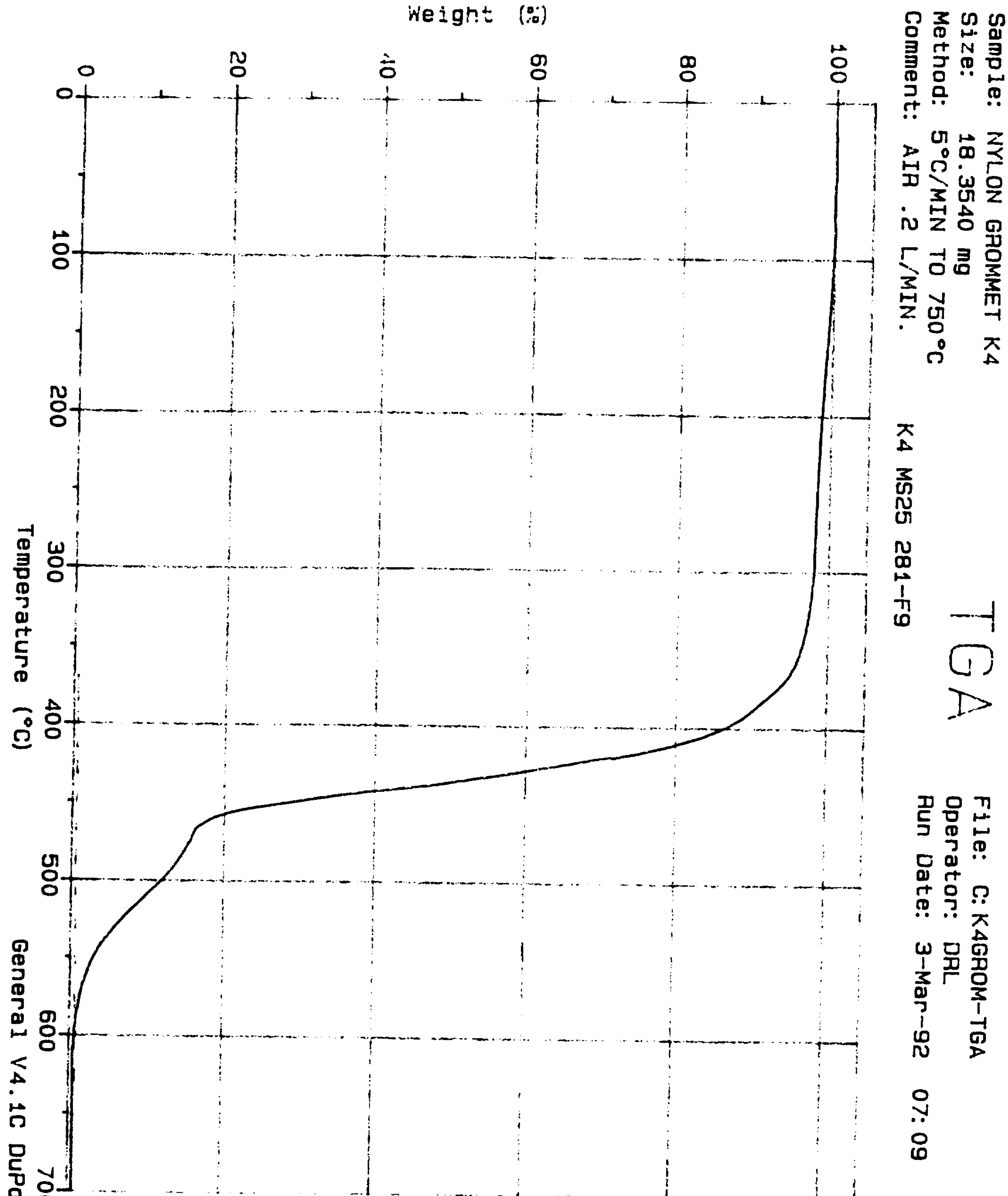

Figure 9. TGA measurement on wire harness bundle nylon grommet K4.

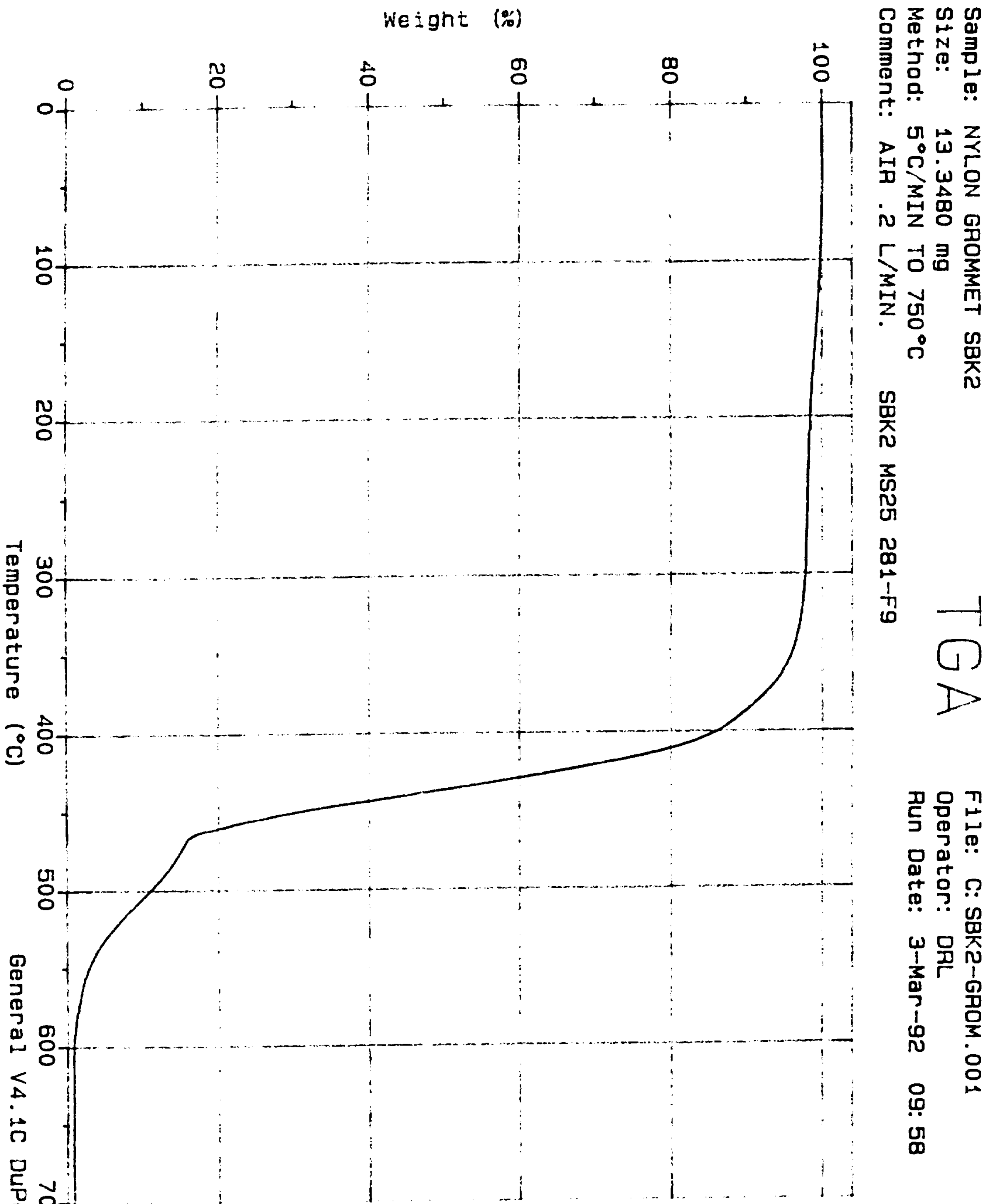

Figure 10. TGA measurement on wire harness bundle nylon grommet SBK2.

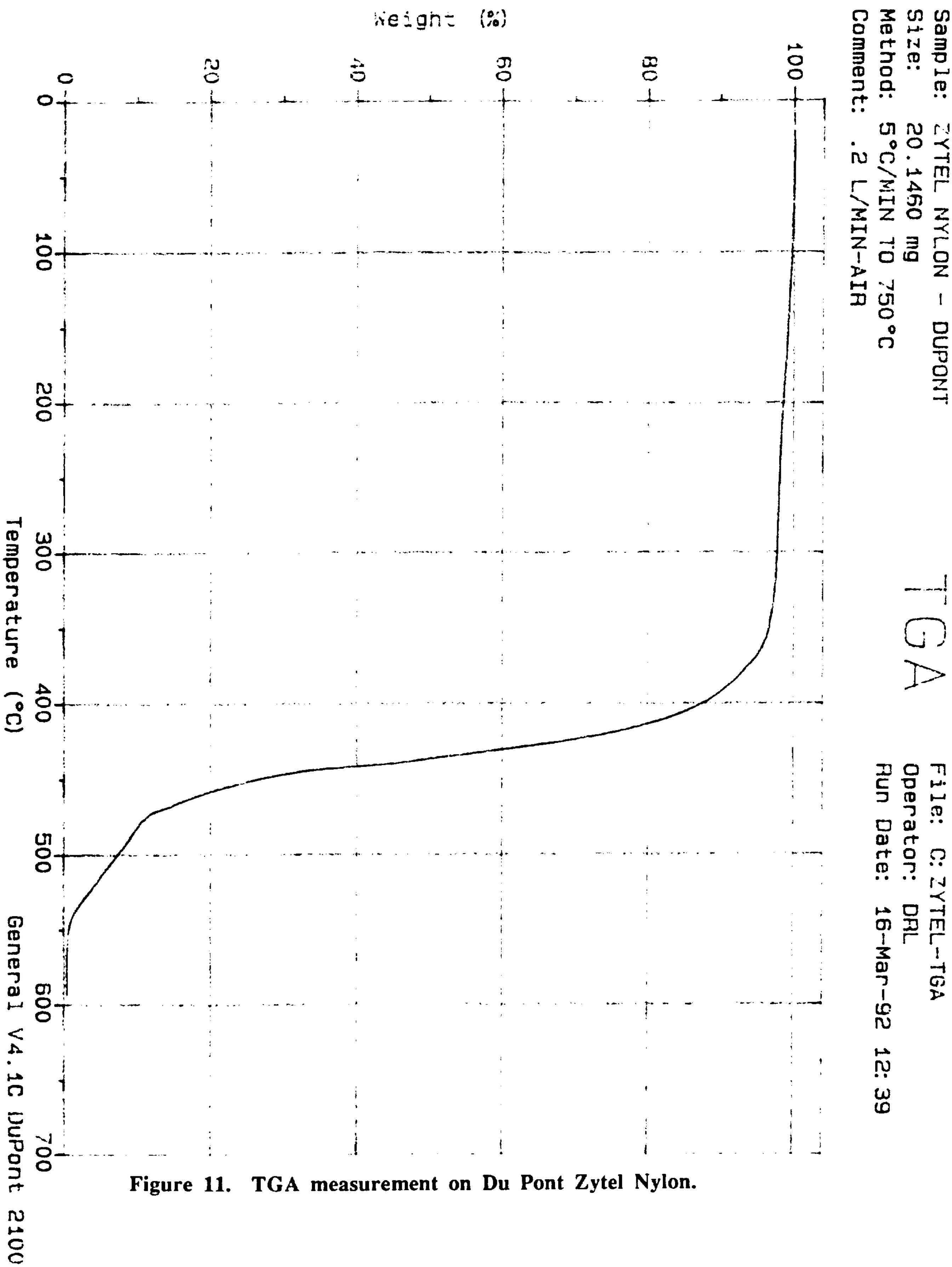

Figure 11. TGA measurement on Du Pont Zytel Nylon.

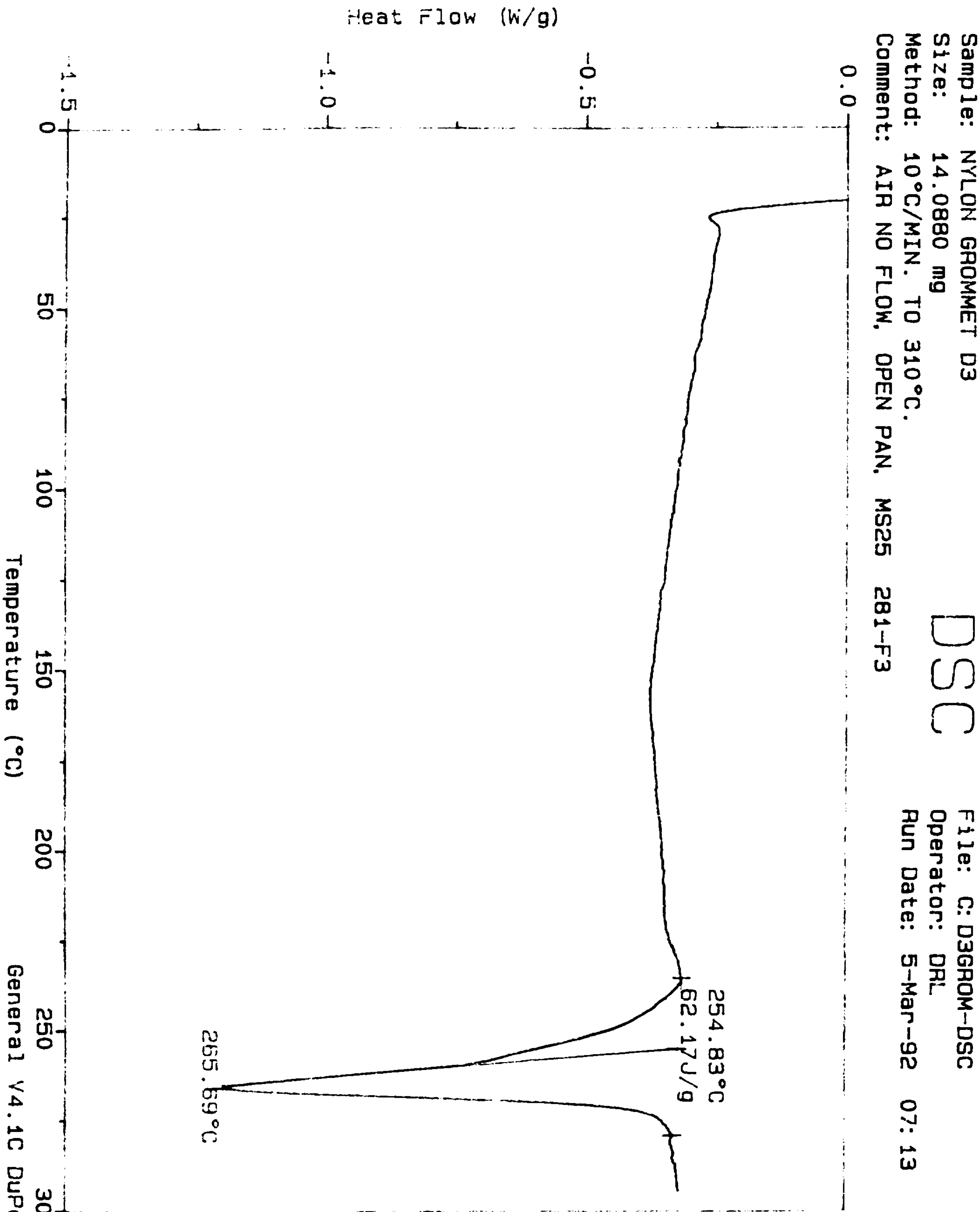

Figure 12. DSC measurement on wire harness bundle nylon grommet D3.

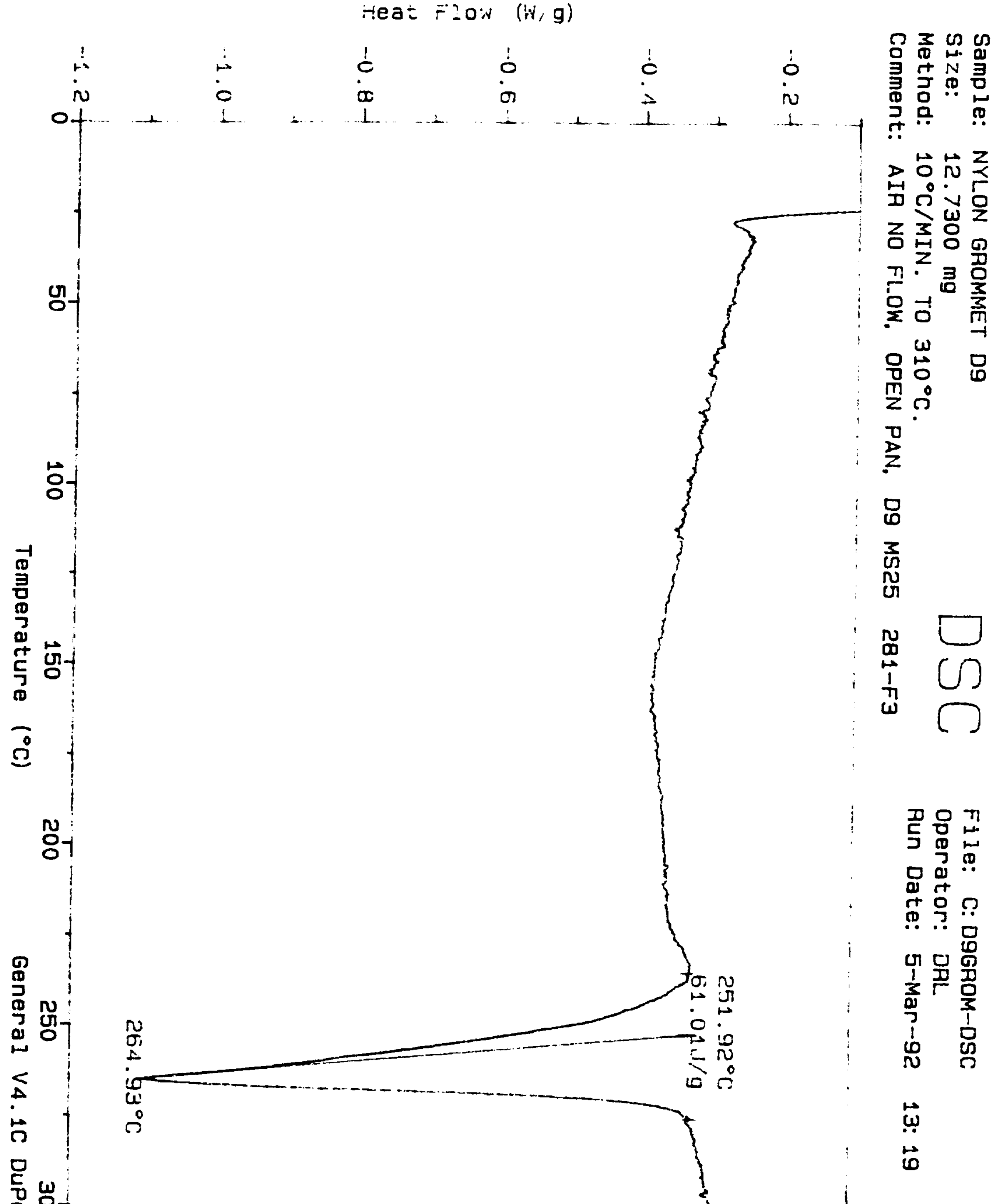

Figure 13. DSC measurement on wire harness bundle nylon grommet D9.

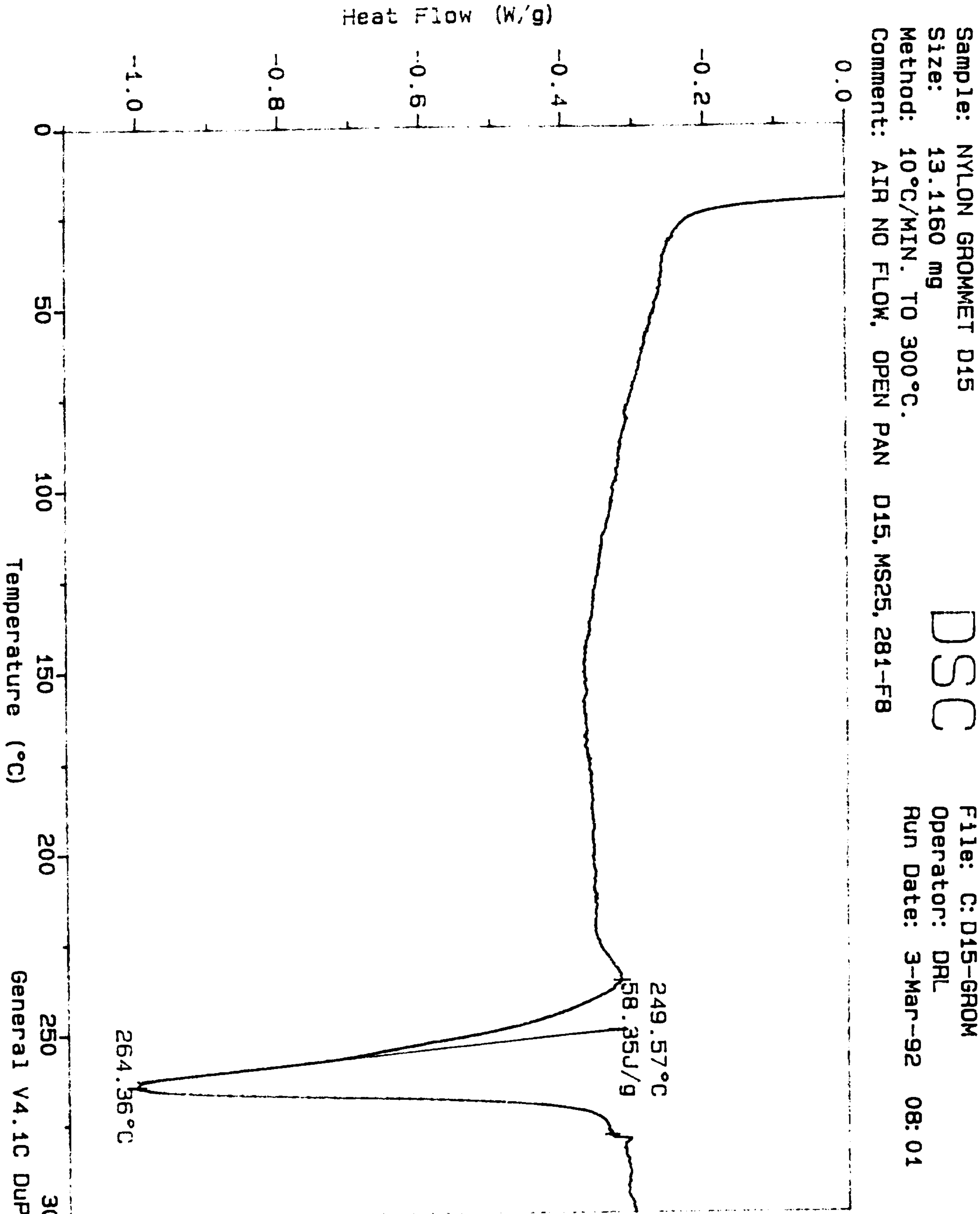

Figure 14. DSC measurement on wire harness bundle nylon grommet D15.

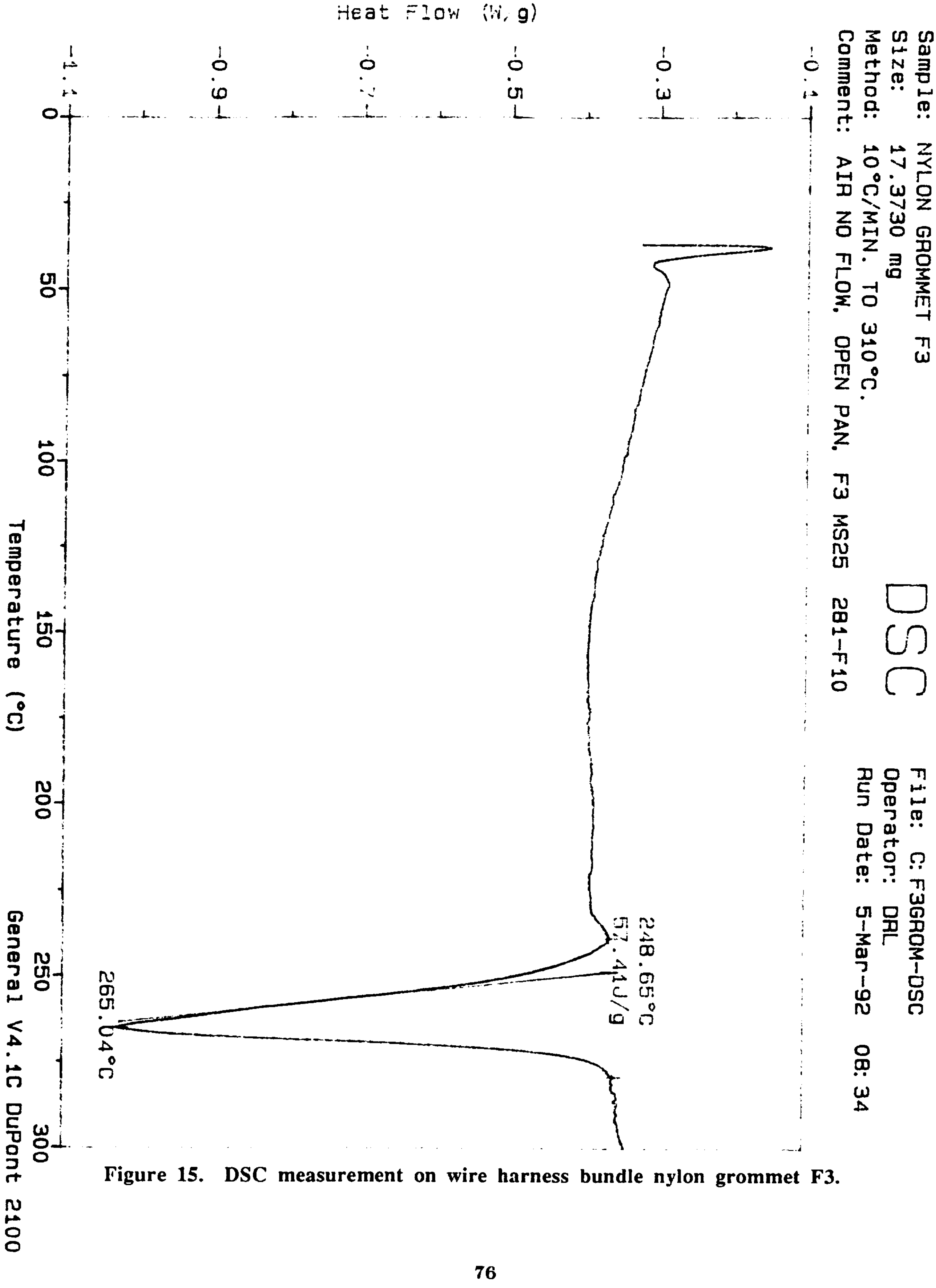

Figure 15. DSC measurement on wire harness bundle nylon grommet F3.

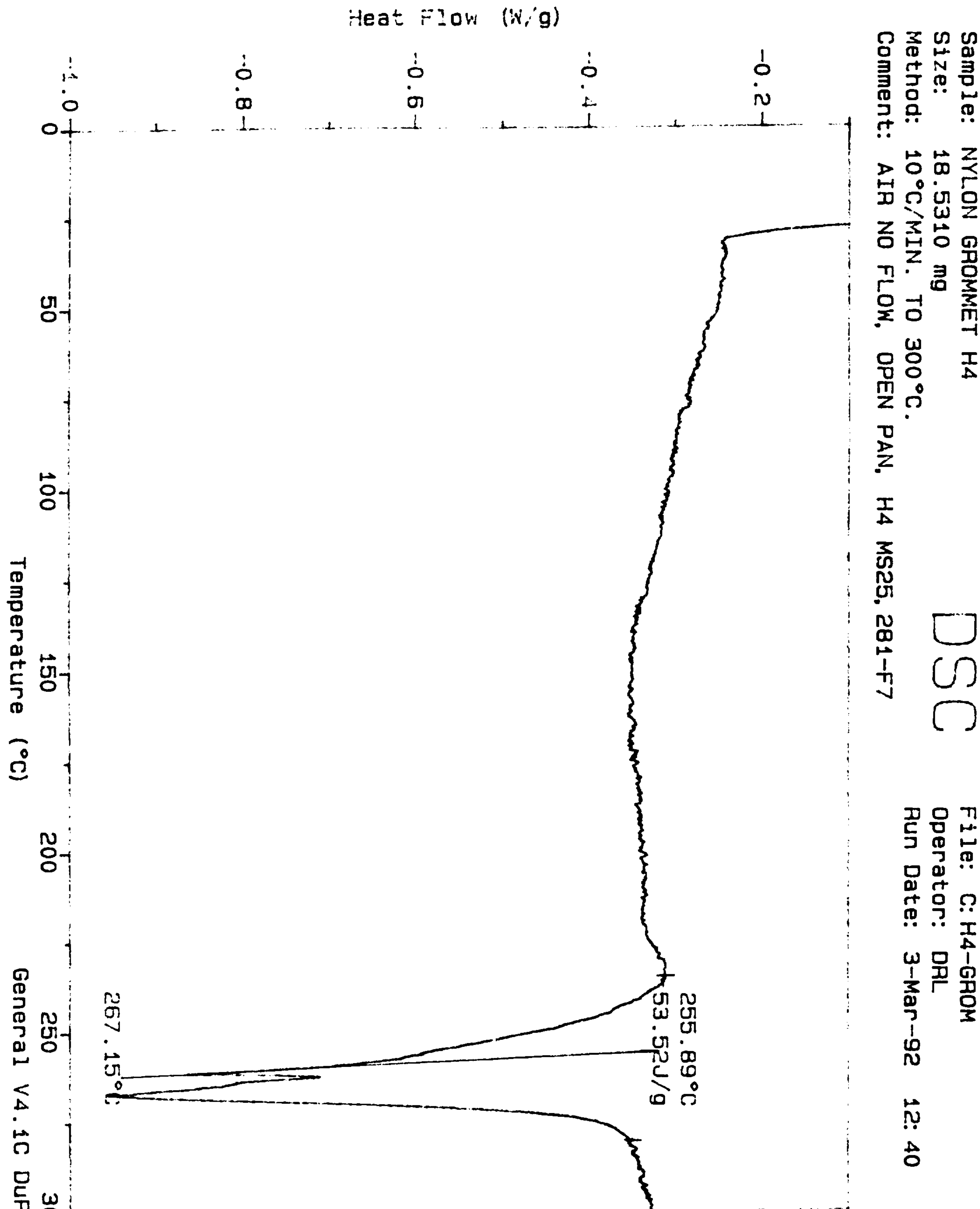

Figure 16. DSC measurement on wire harness bundle nylon grommet H4.

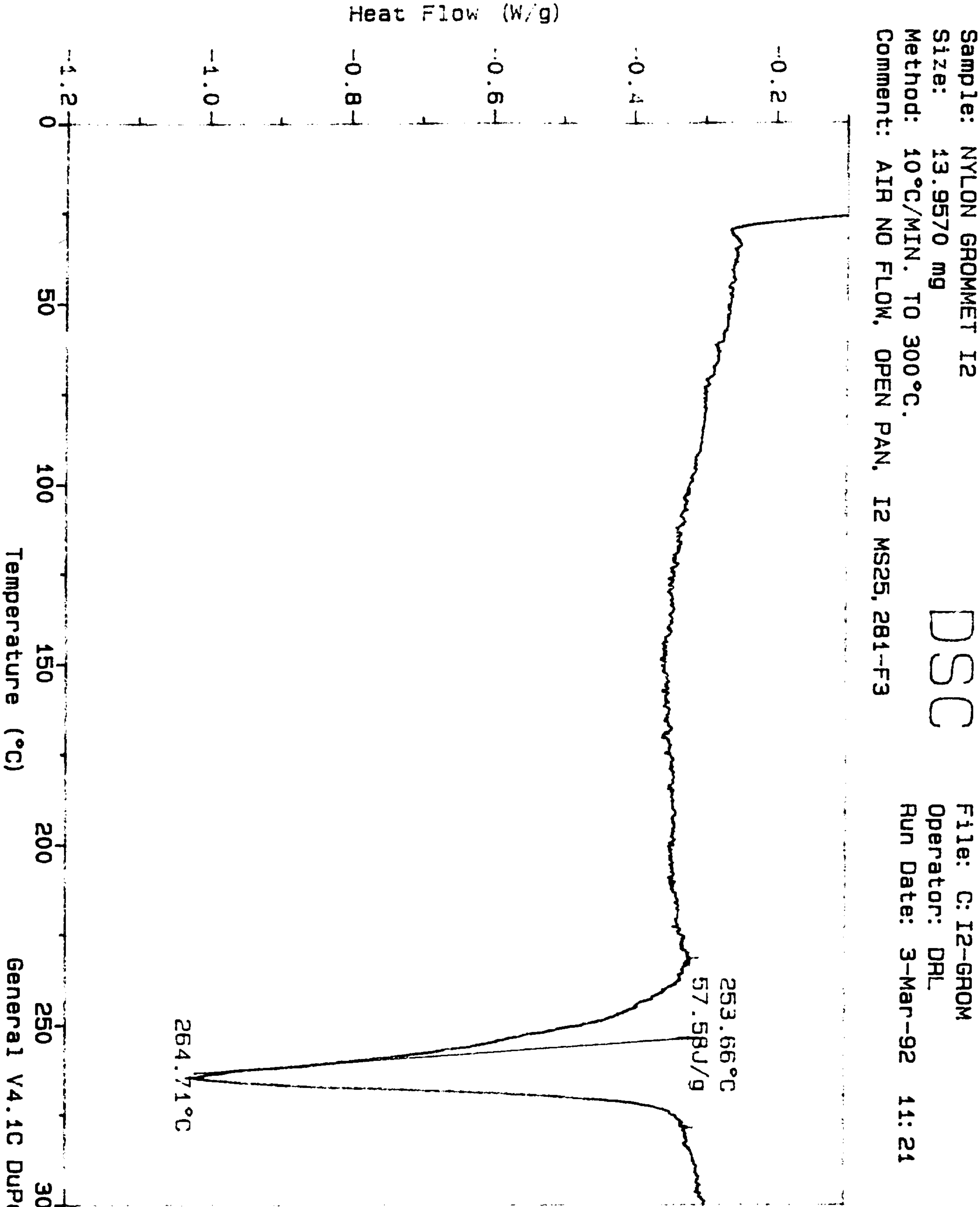

Figure 17. DSC measurement on wire harness bundle nylon grommet I2.

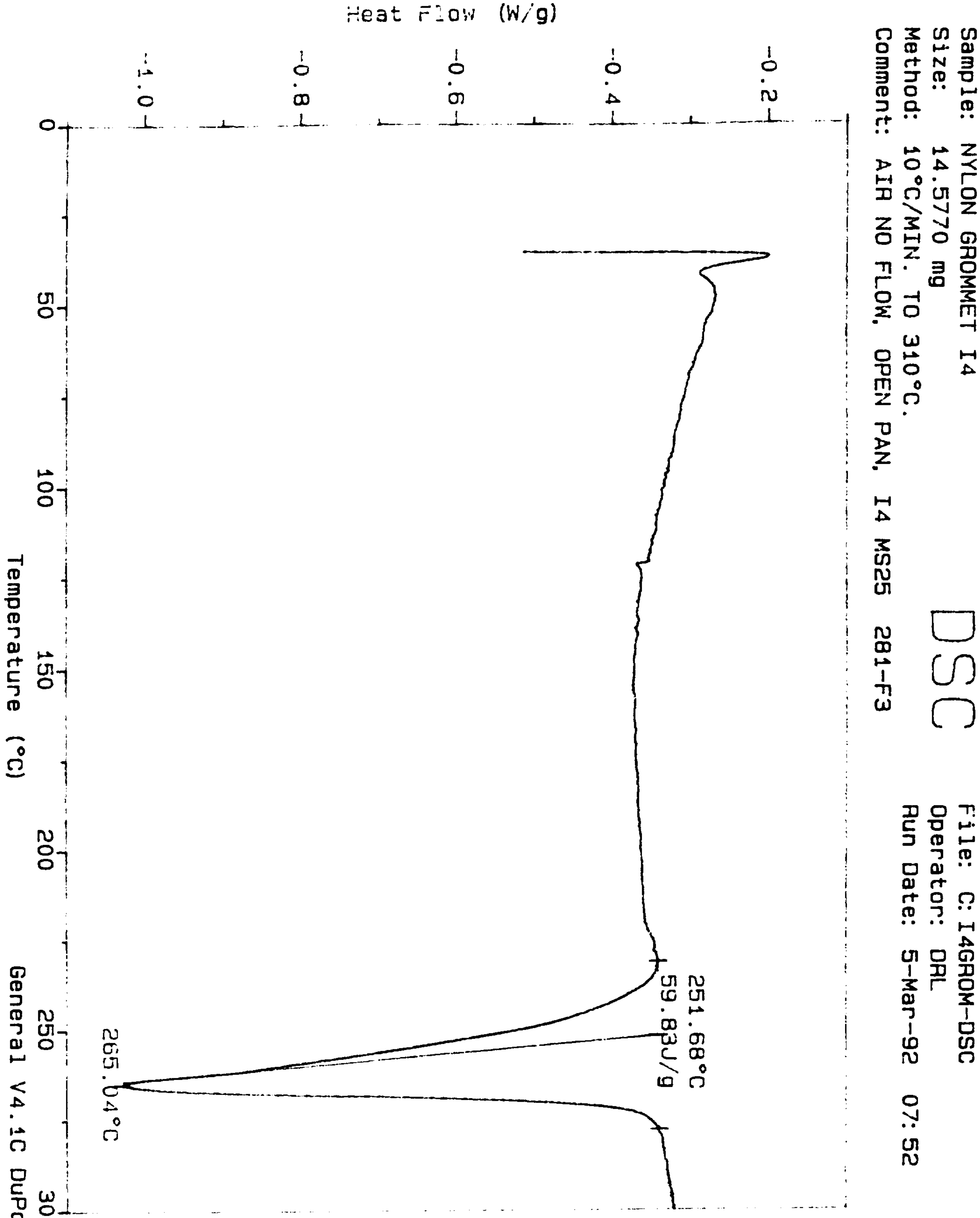

Figure 18. DSC measurement on wire harness bundle nylon grommet I4.

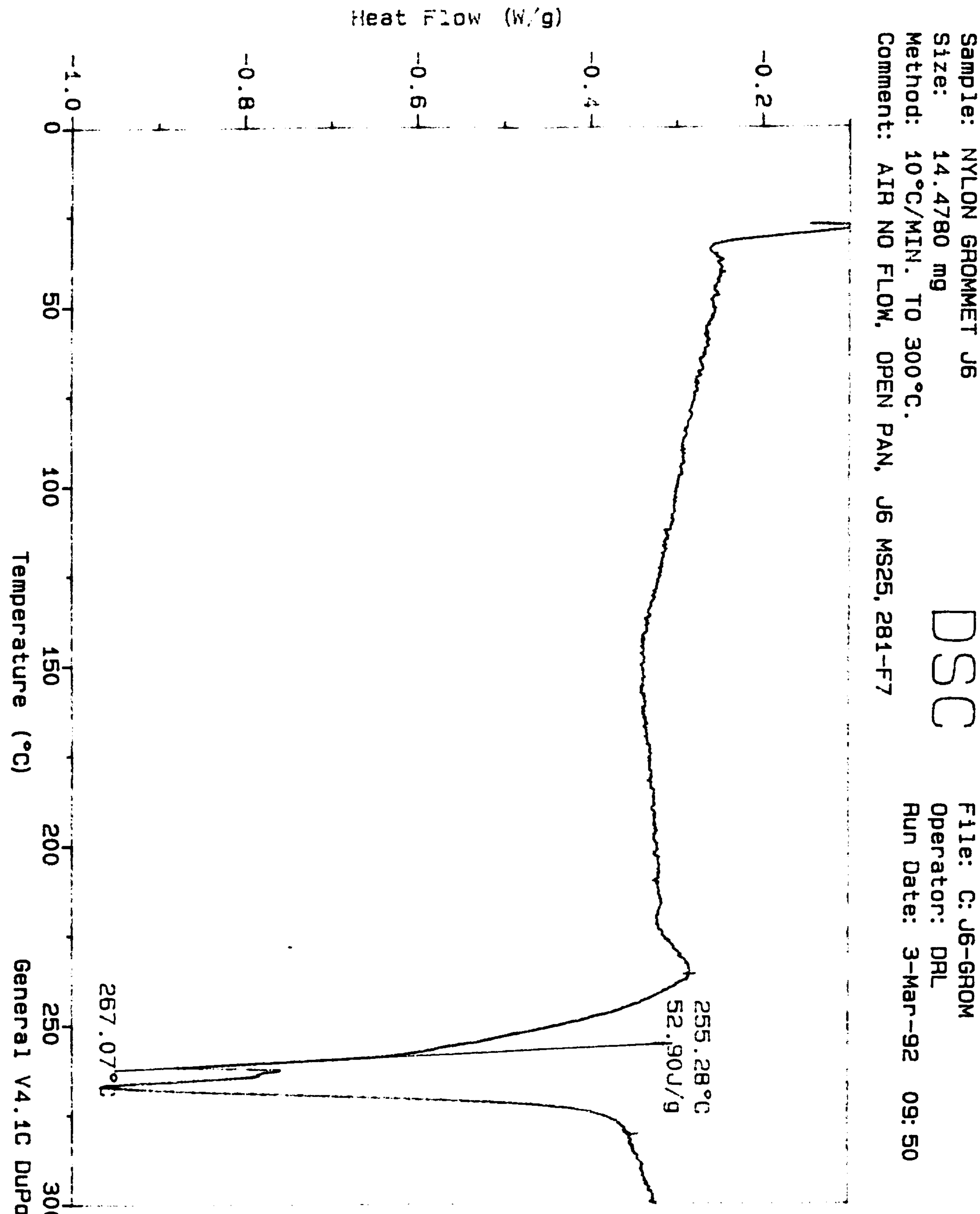

Figure 19. DSC measurement on wire harness bundle nylon grommet J6.

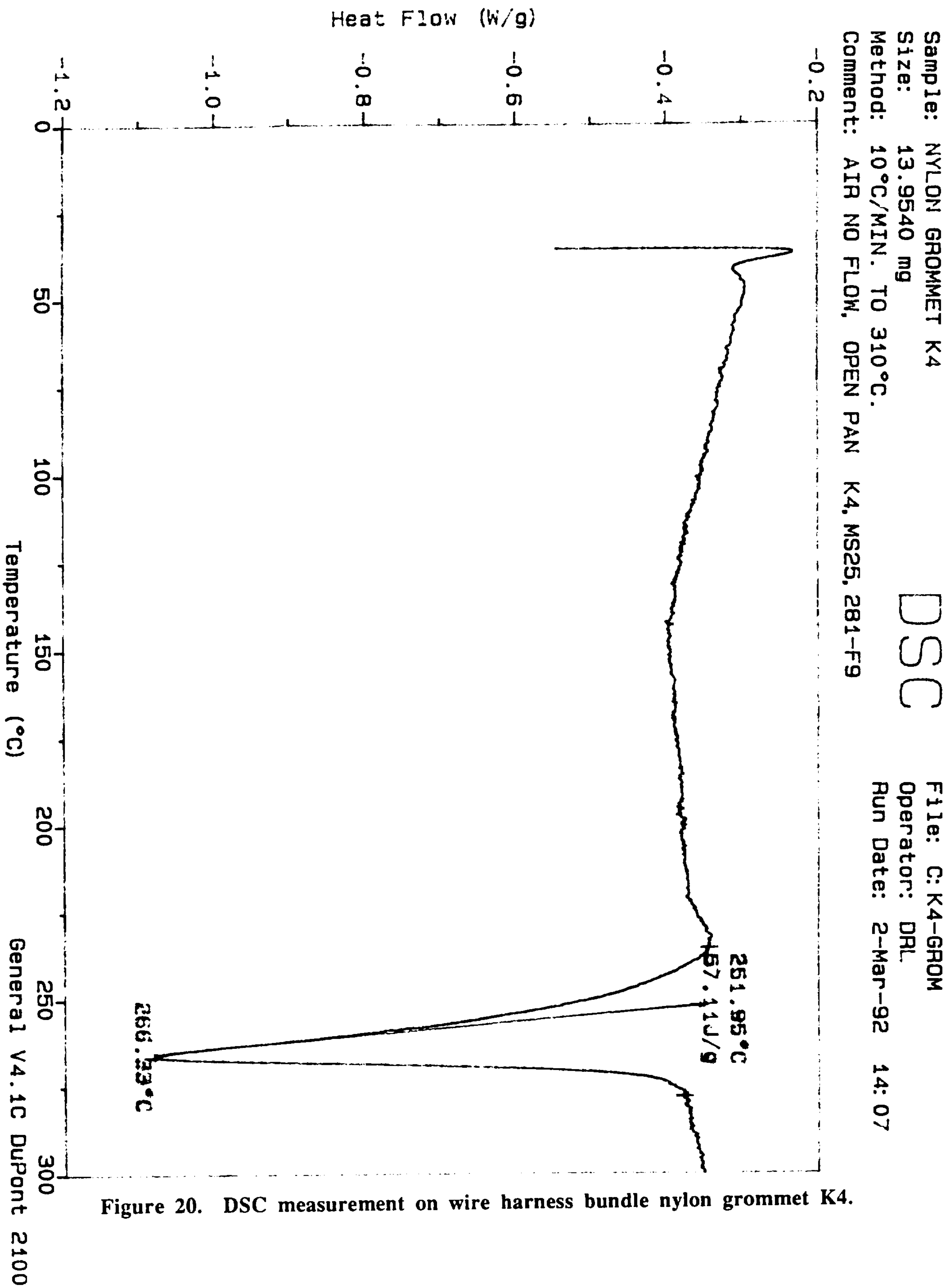

Figure 20. DSC measurement on wire harness bundle nylon grommet K4.

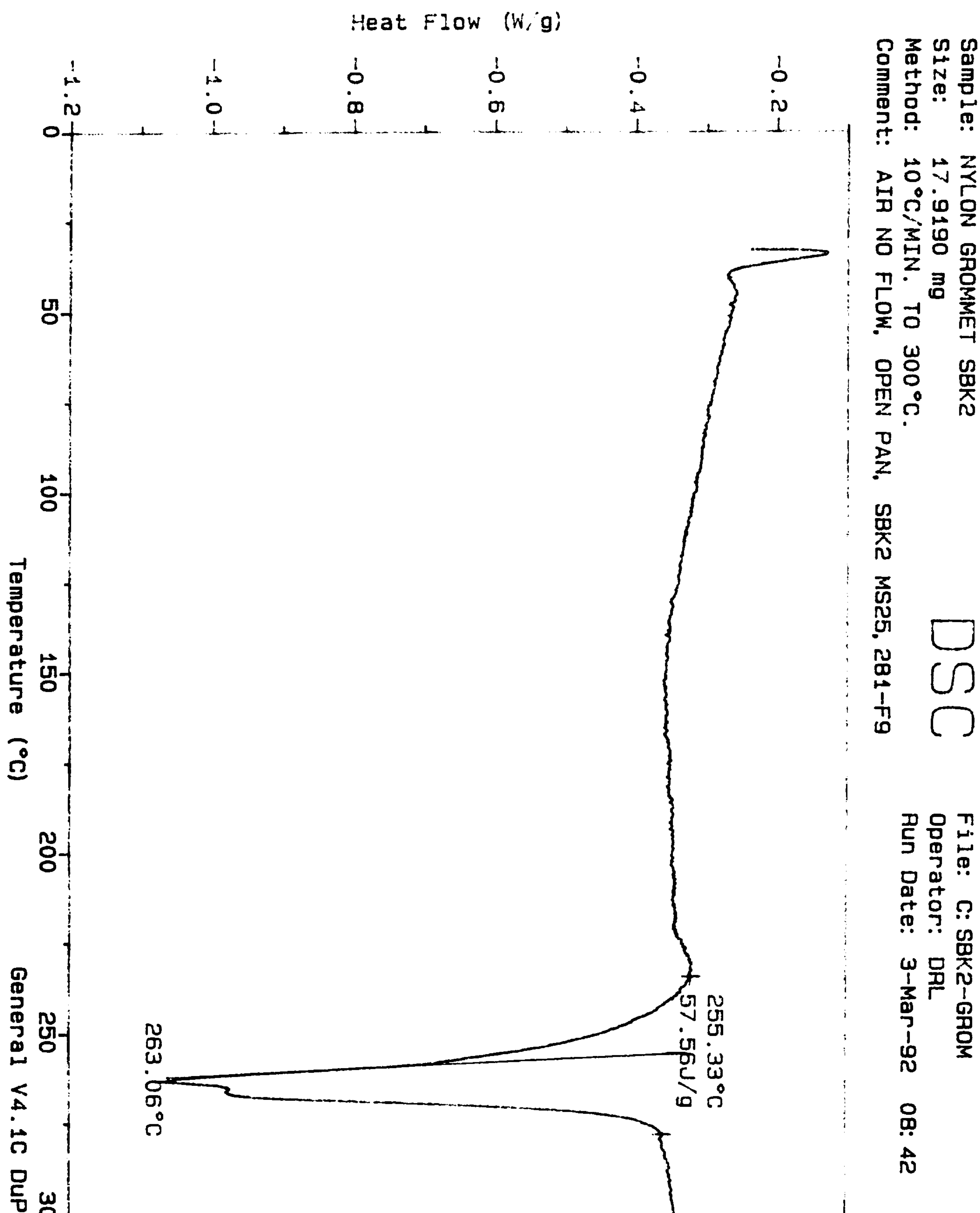

Figure 21. DSC measurement on wire harness bundle nylon grommet SBK2.

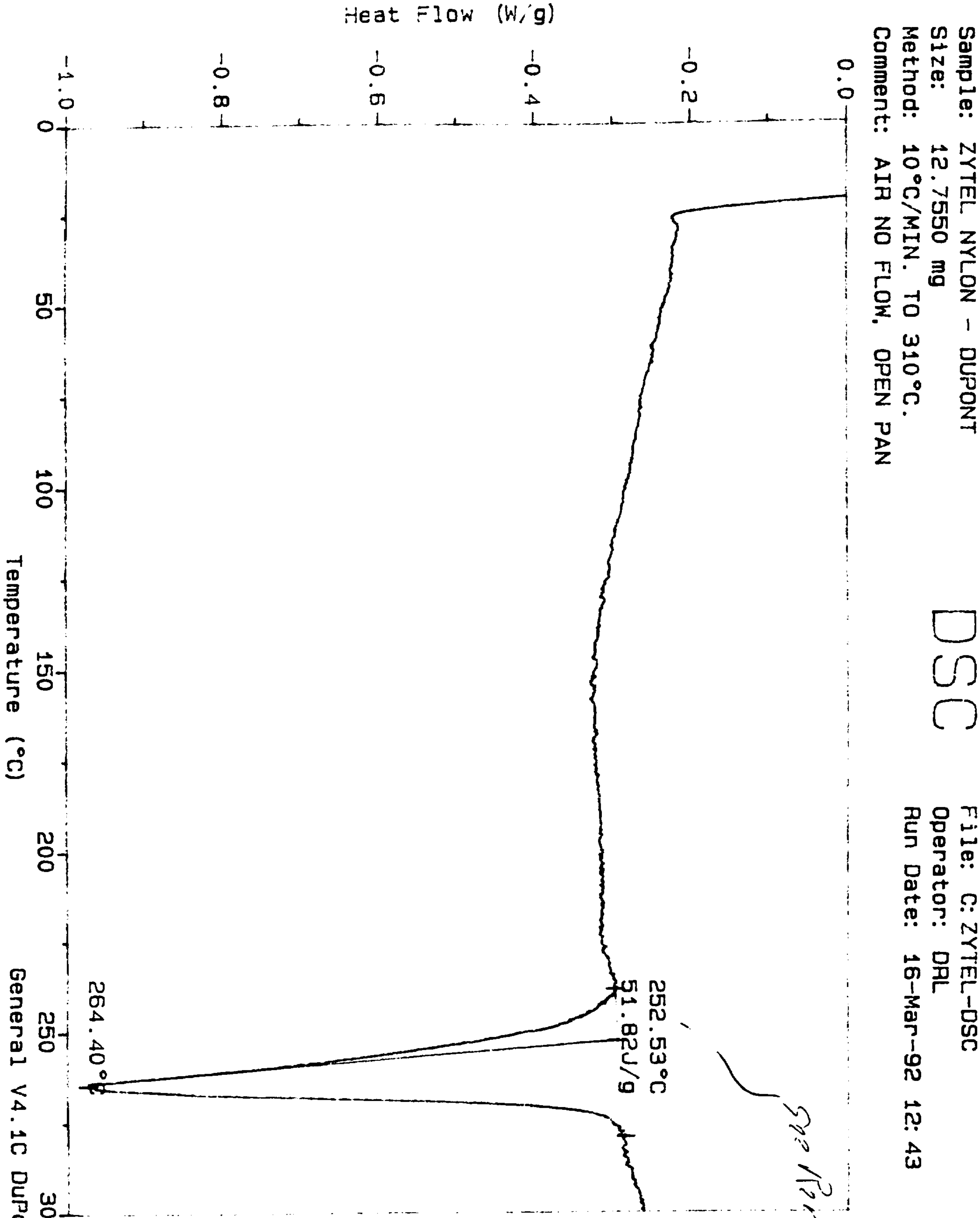

Figure 22. DSC measurement on Du Pont Zytel Nylon.

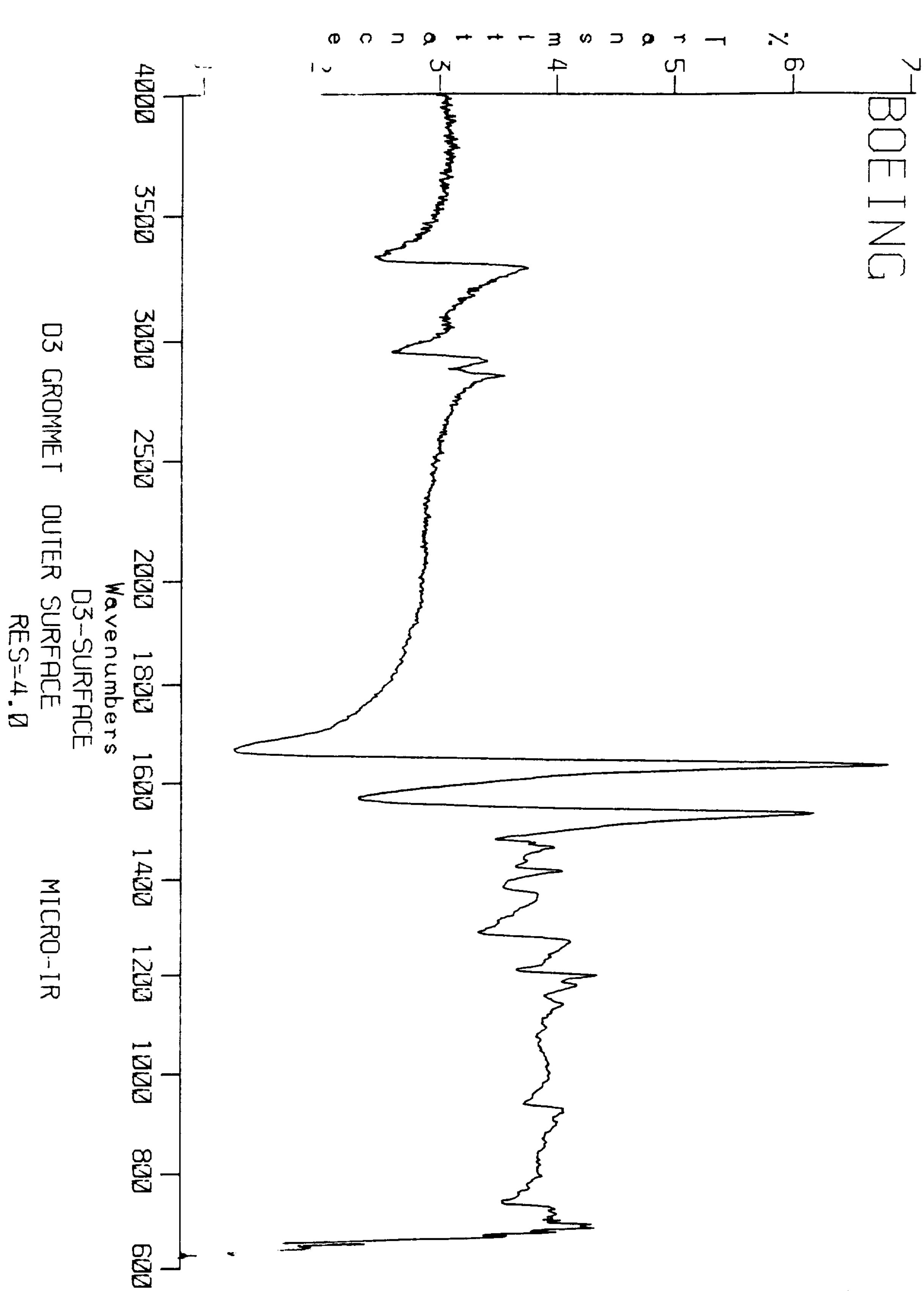

Figure 23. IR transmission spectrum of surface of wire harness bundle nylon grommet D3.

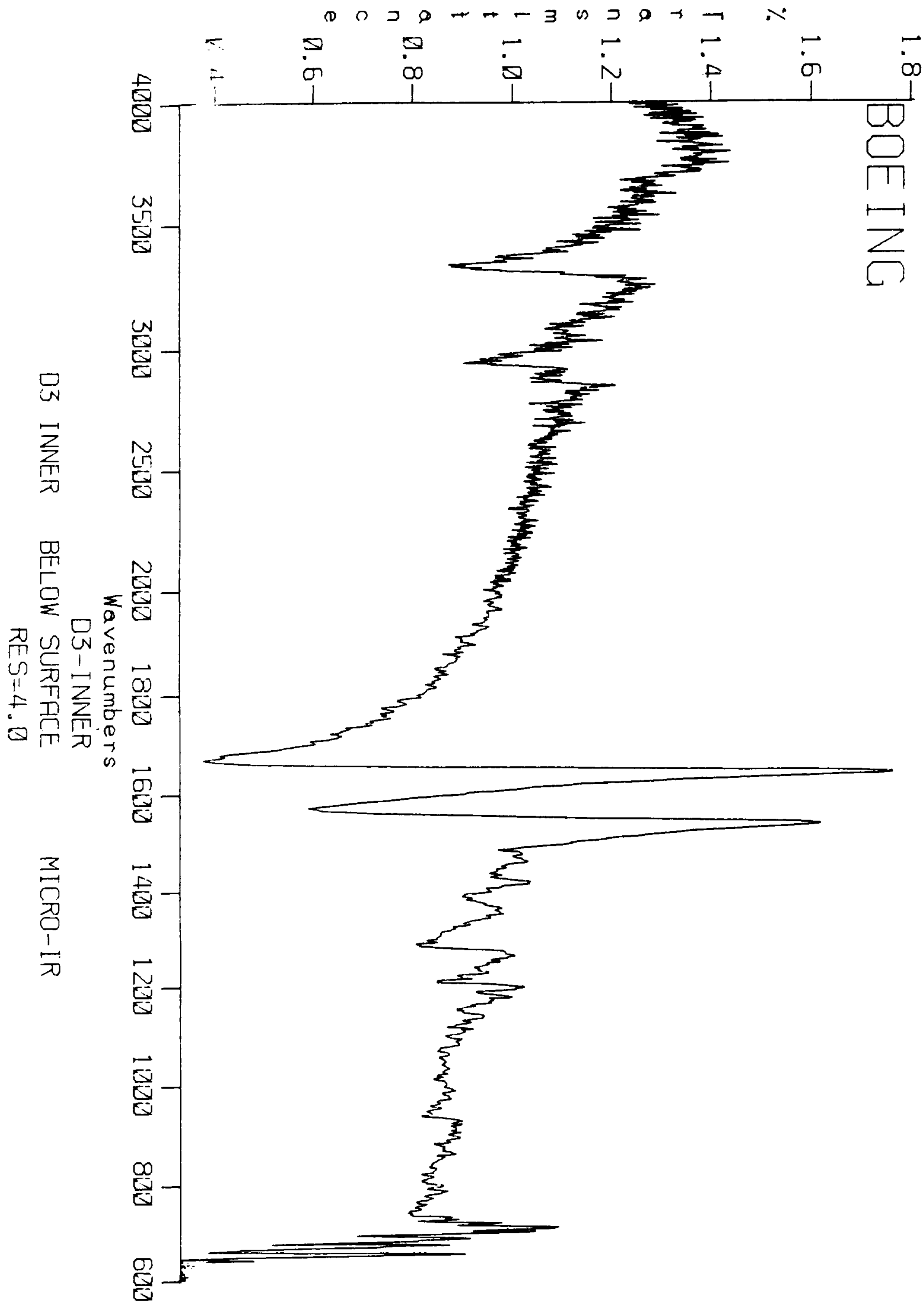

Figure 24. IR transmission spectrum of bulk material from wire harness bundle nylon grommet D3.

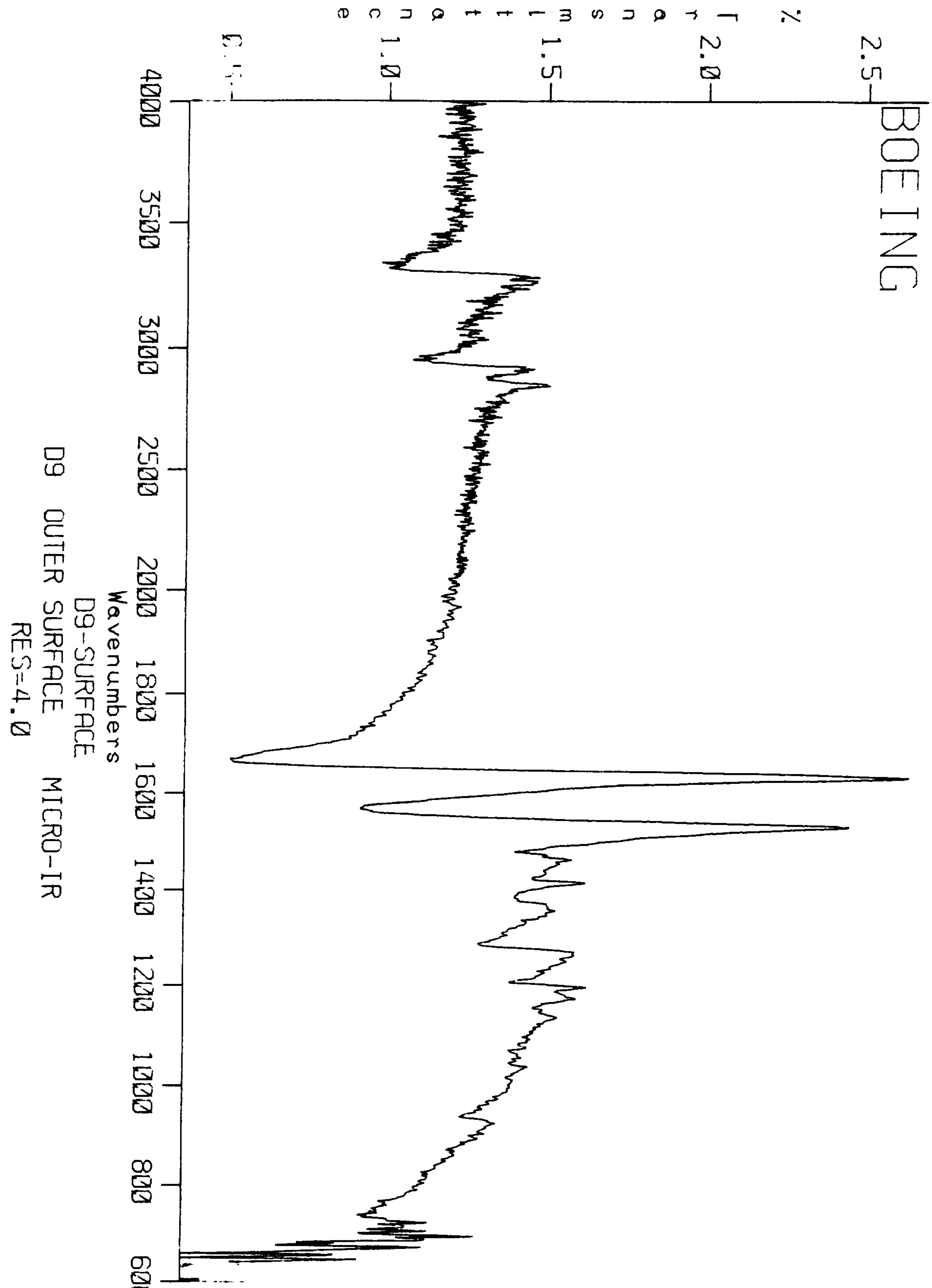

Figure 25. IR transmission spectrum of surface of wire harness bundle nylon grommet D9.

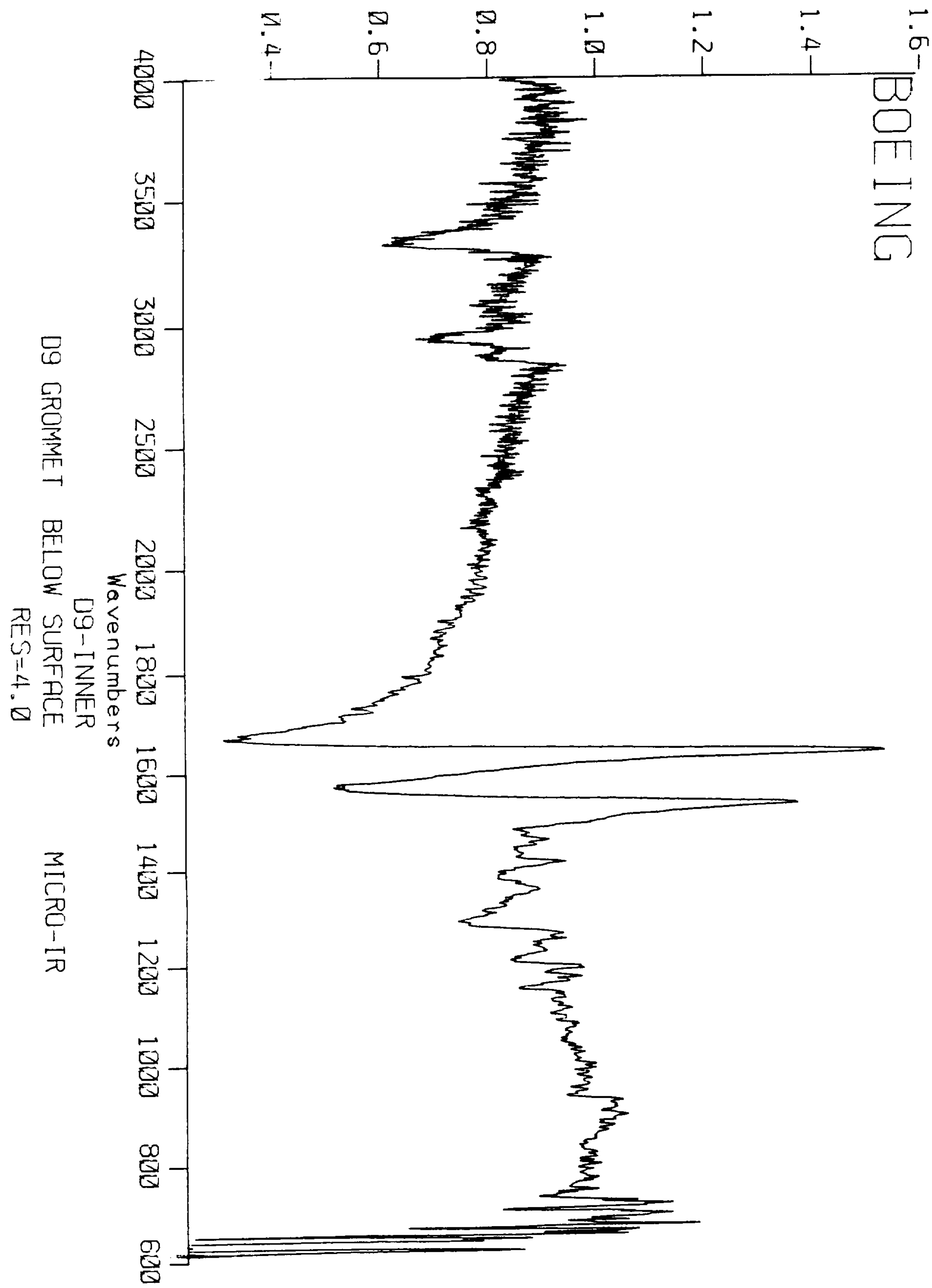

Figure 26. IR transmission spectrum of bulk material from wire harness bundle nylon grommet D9.

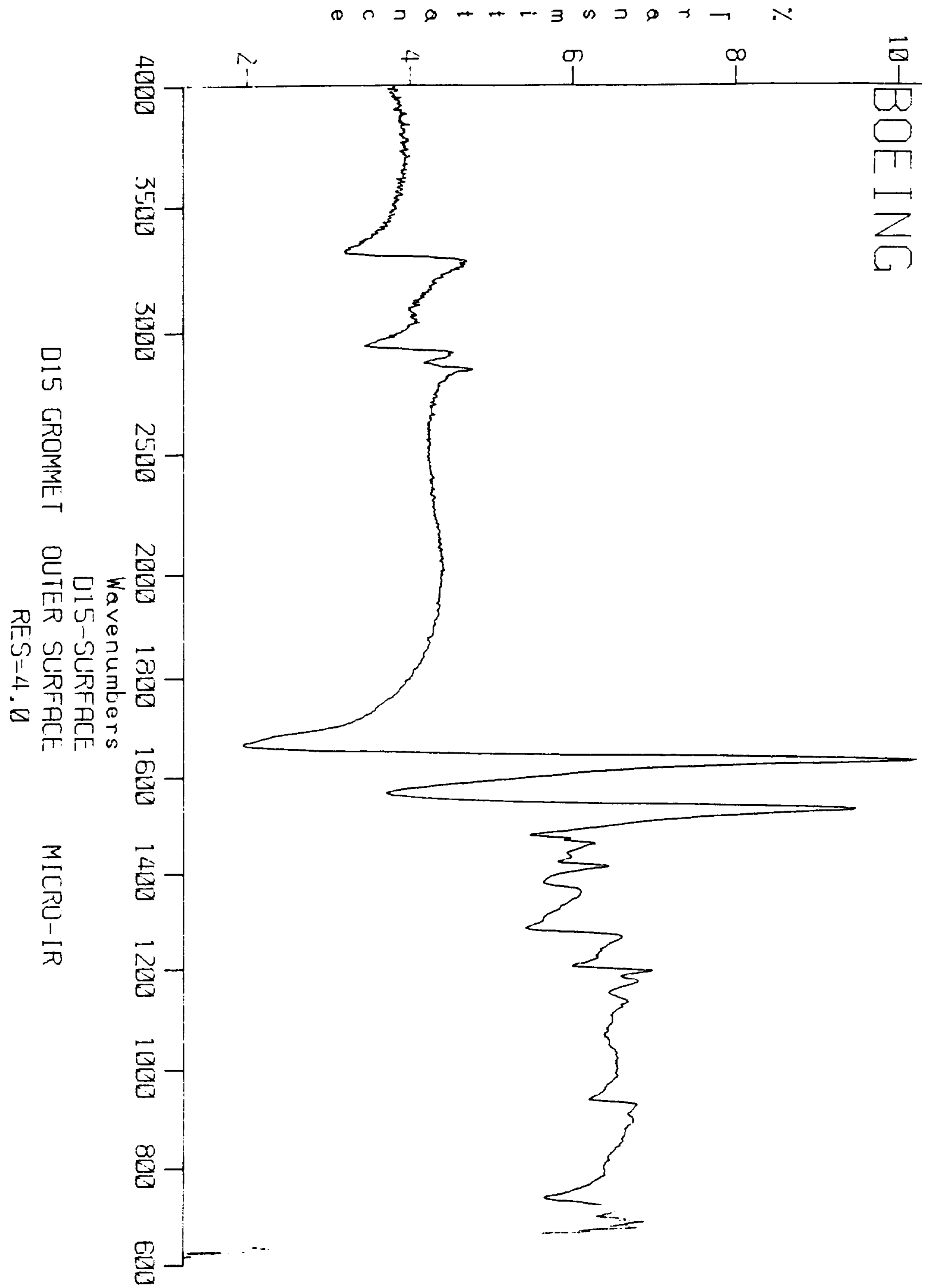

Figure 27. IR transmission spectrum of surface of wire harness bundle nylon grommet D15.

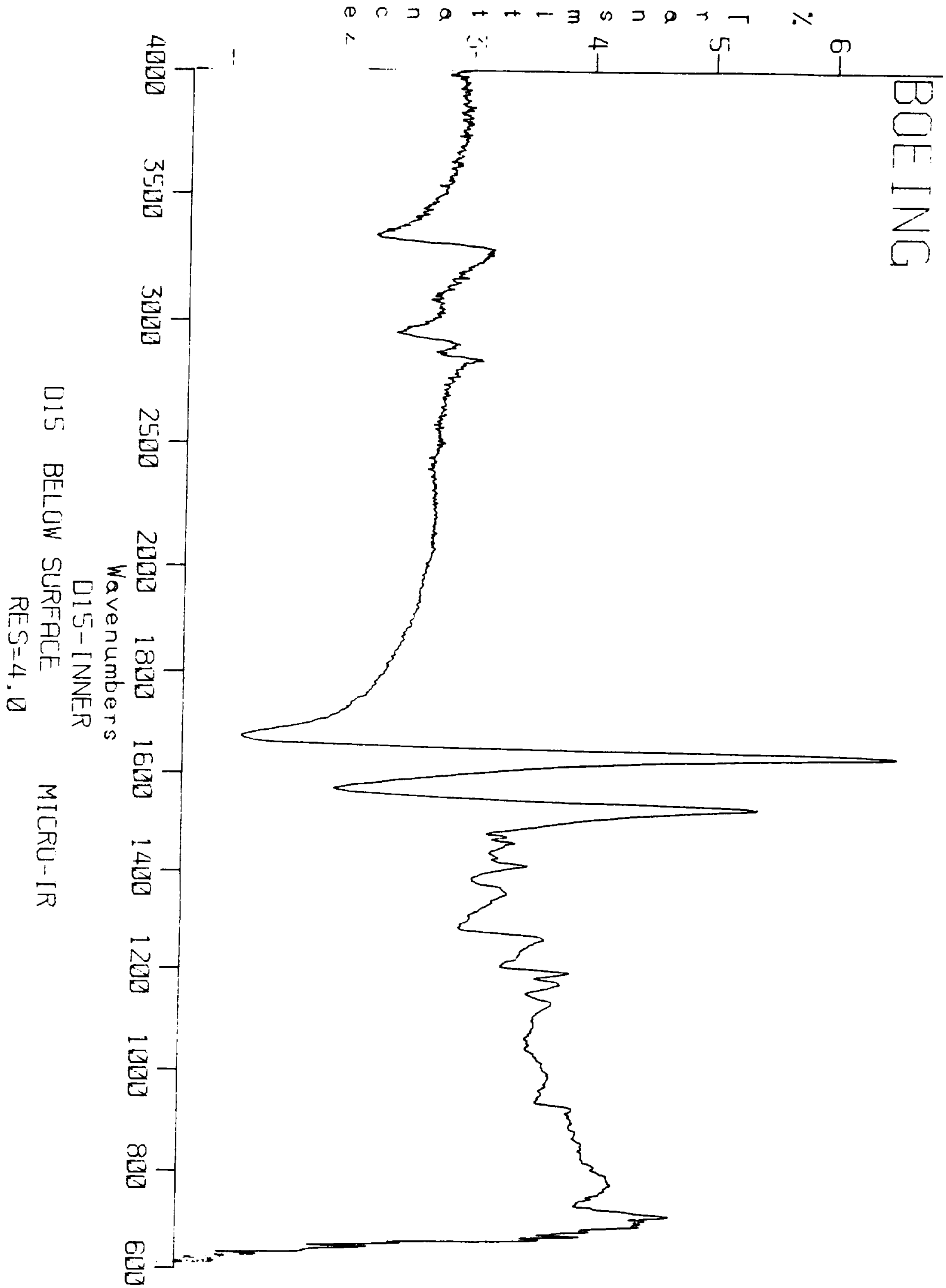

Figure 28. IR transmission spectrum of bulk material from wire harness bundle nylon grommet D15.

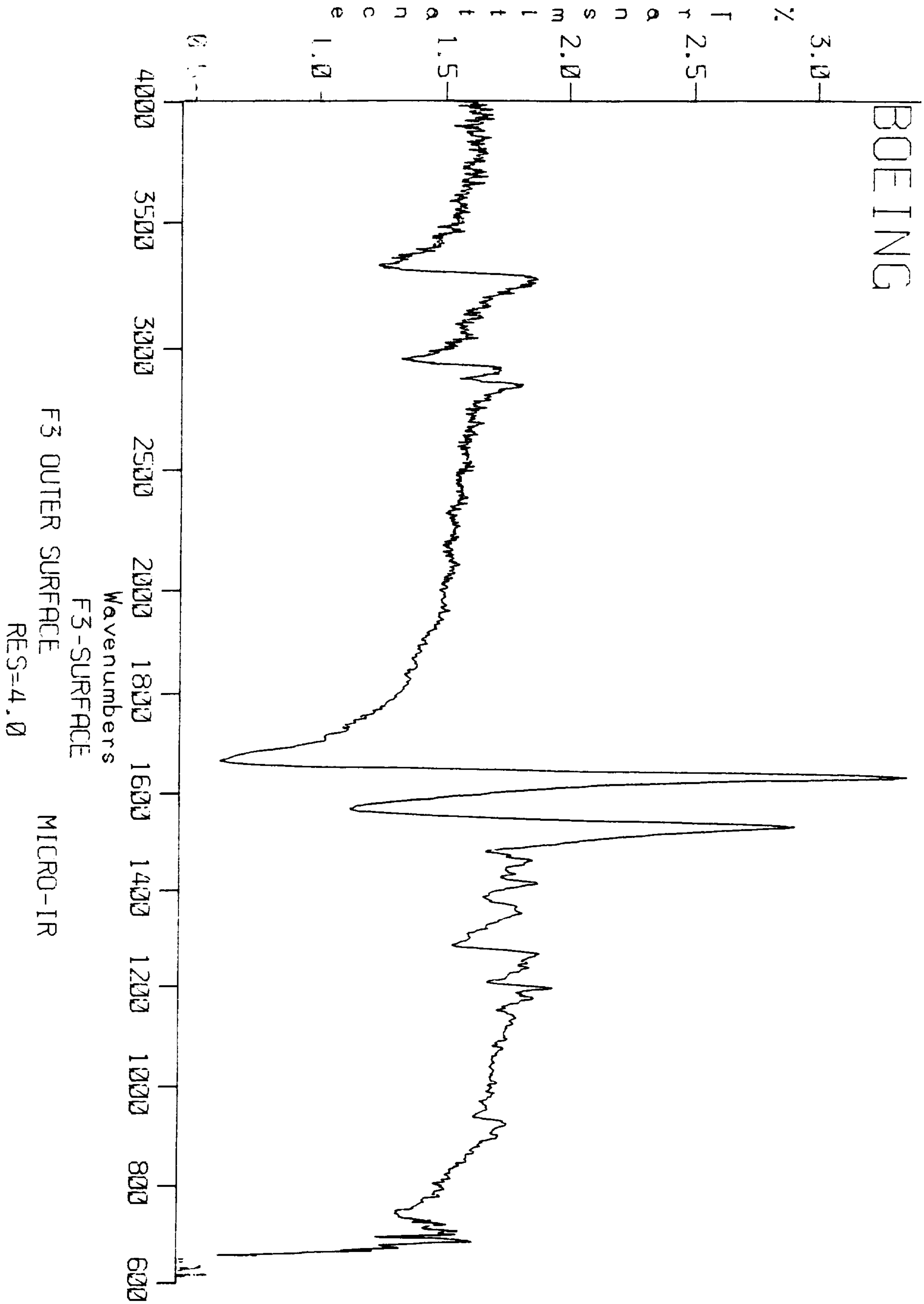

Figure 29. IR transmission spectrum of surface of wire harness bundle nylon grommet F3.

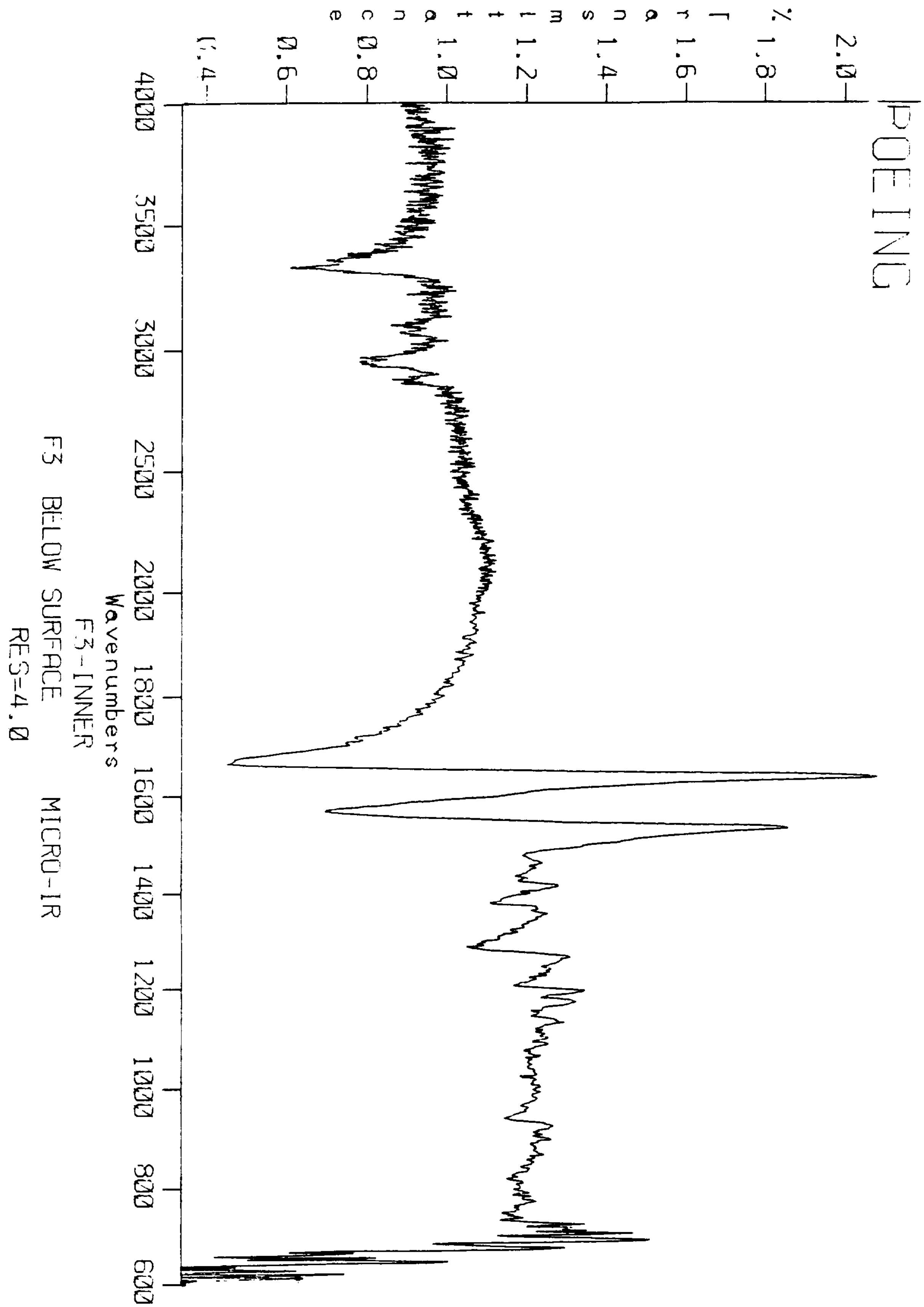

Figure 30. IR transmission spectrum of bulk material from wire harness bundle nylon grommet F3.

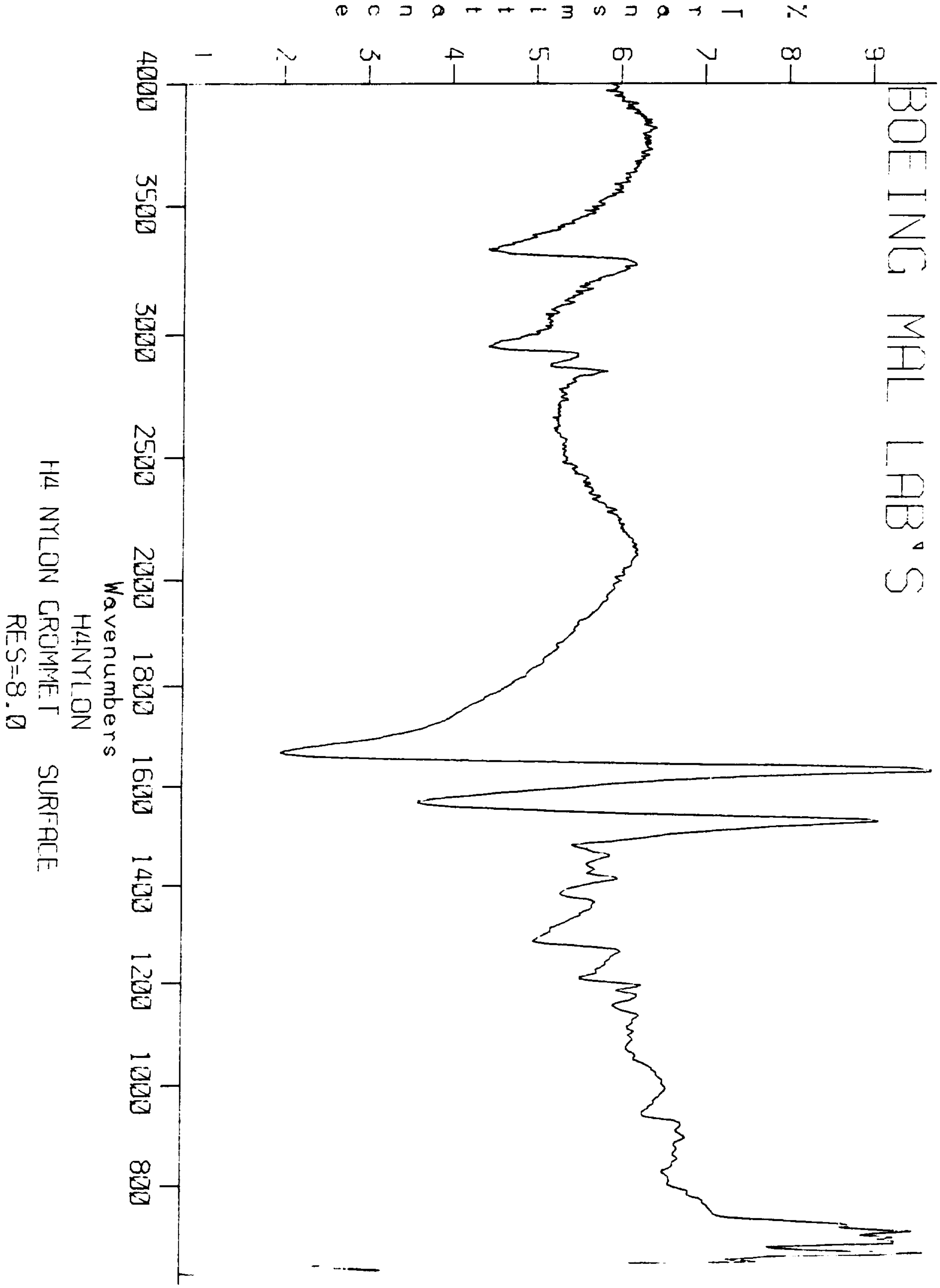

Figure 31. IR transmission spectrum of surface of wire harness bundle nylon grommet H4.

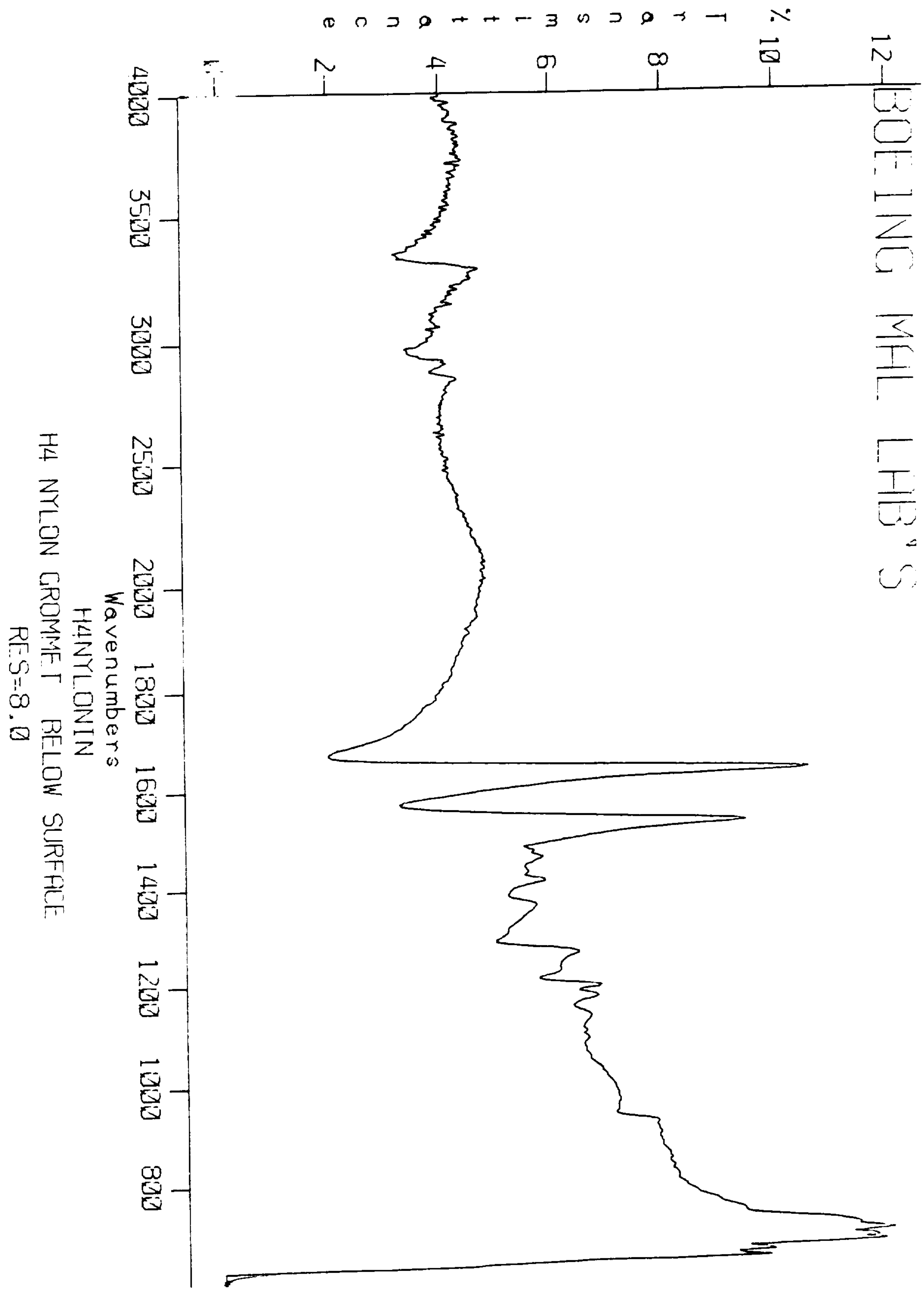

Figure 32. IR transmission spectrum of bulk material from wire harness bundle nylon grommet H4.

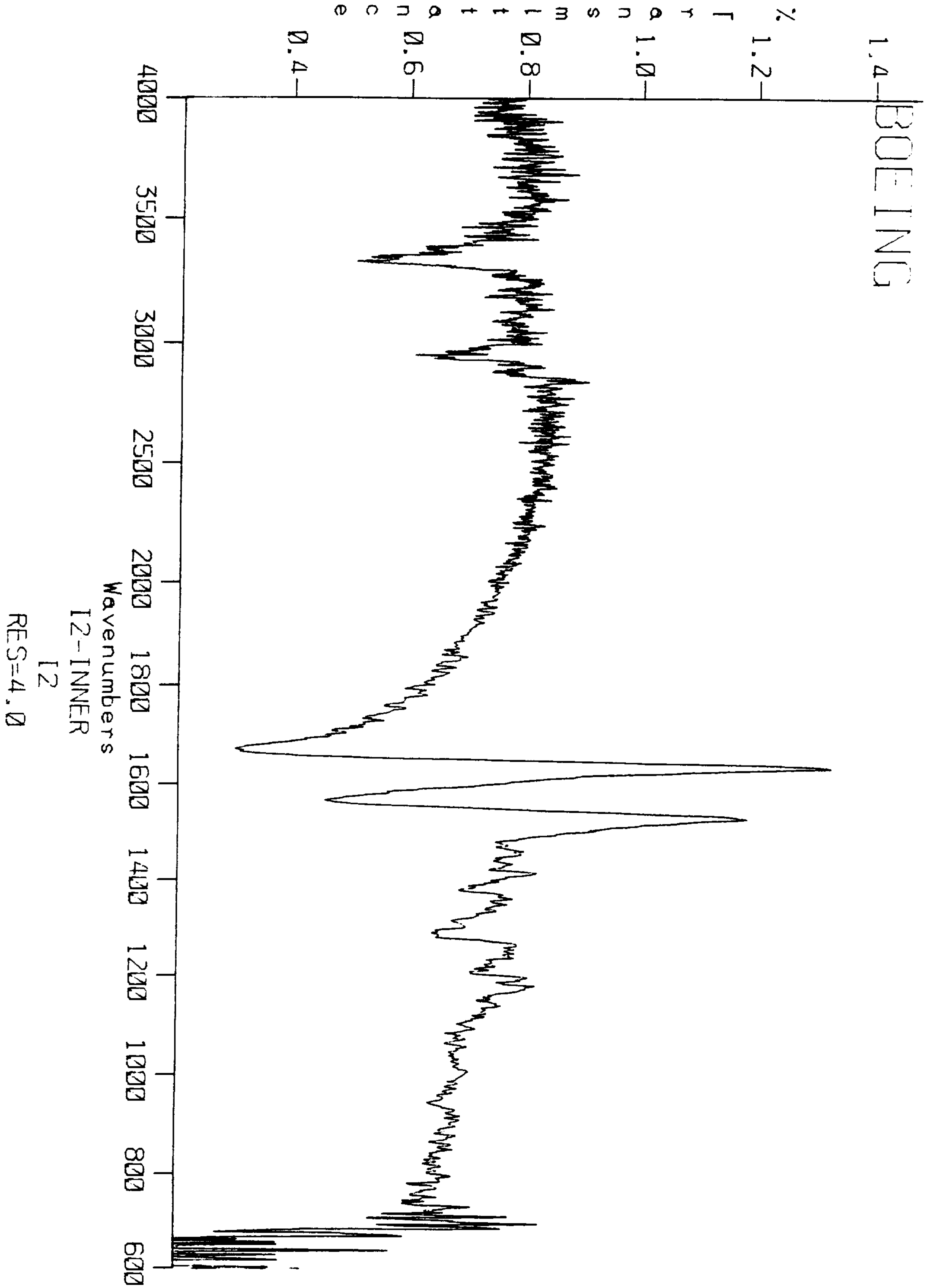

Figure 33. IR transmission spectrum of surface of wire harness bundle nylon grommet I2.

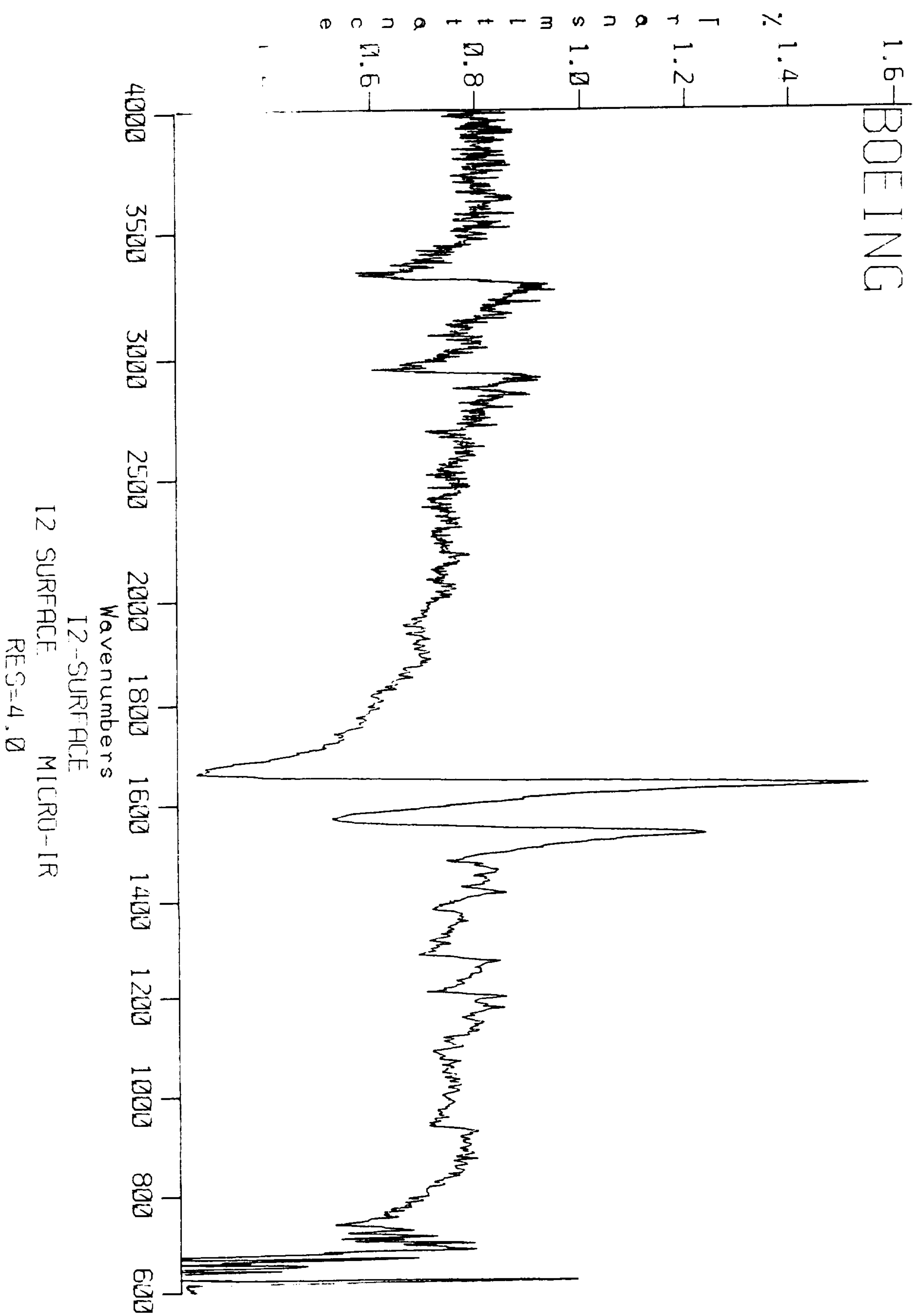

Figure 34. IR transmission spectrum of bulk material from wire harness bundle nylon grommet I2.

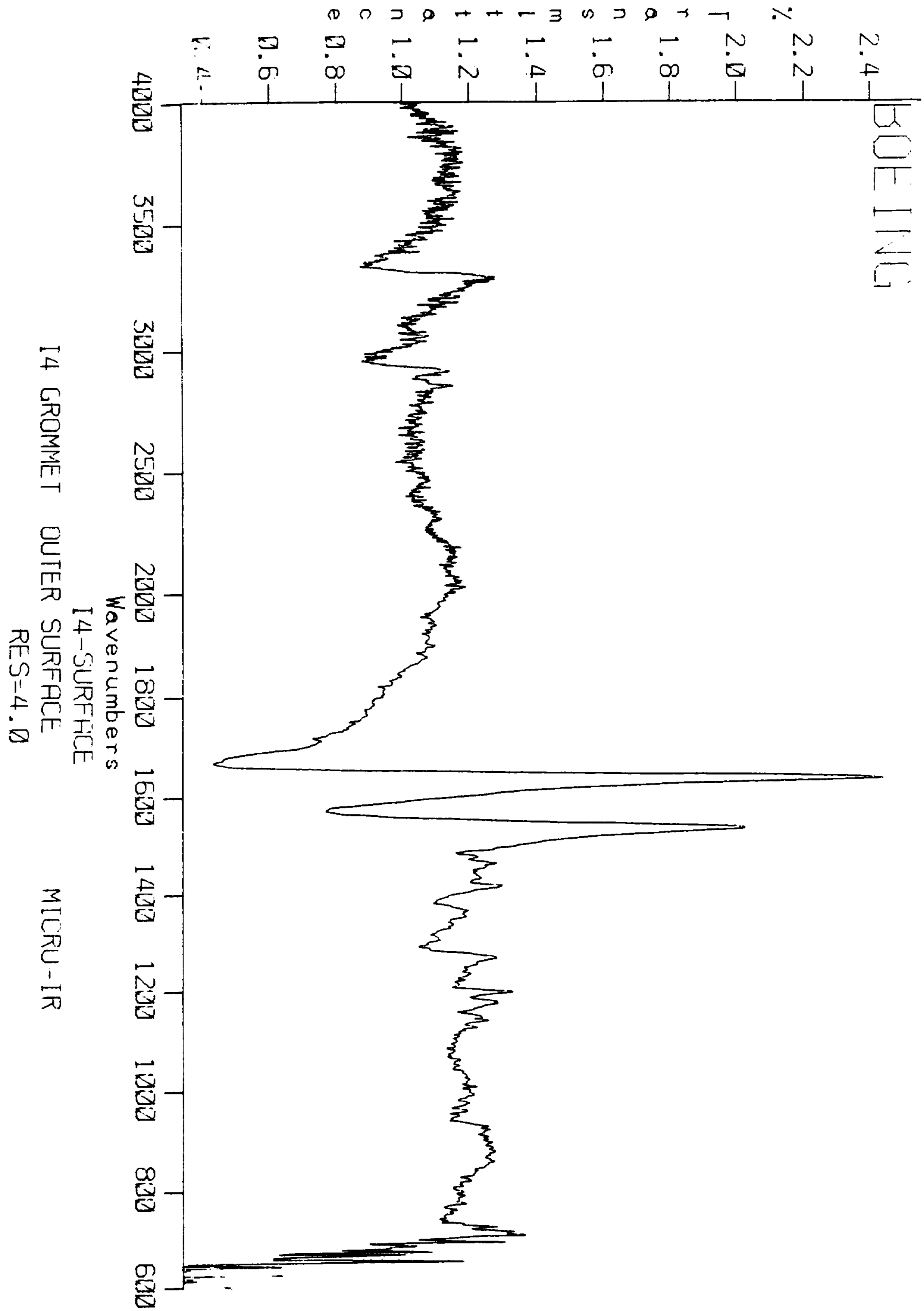

Figure 35. IR transmission spectrum of surface of wire harness bundle nylon grommet I4.

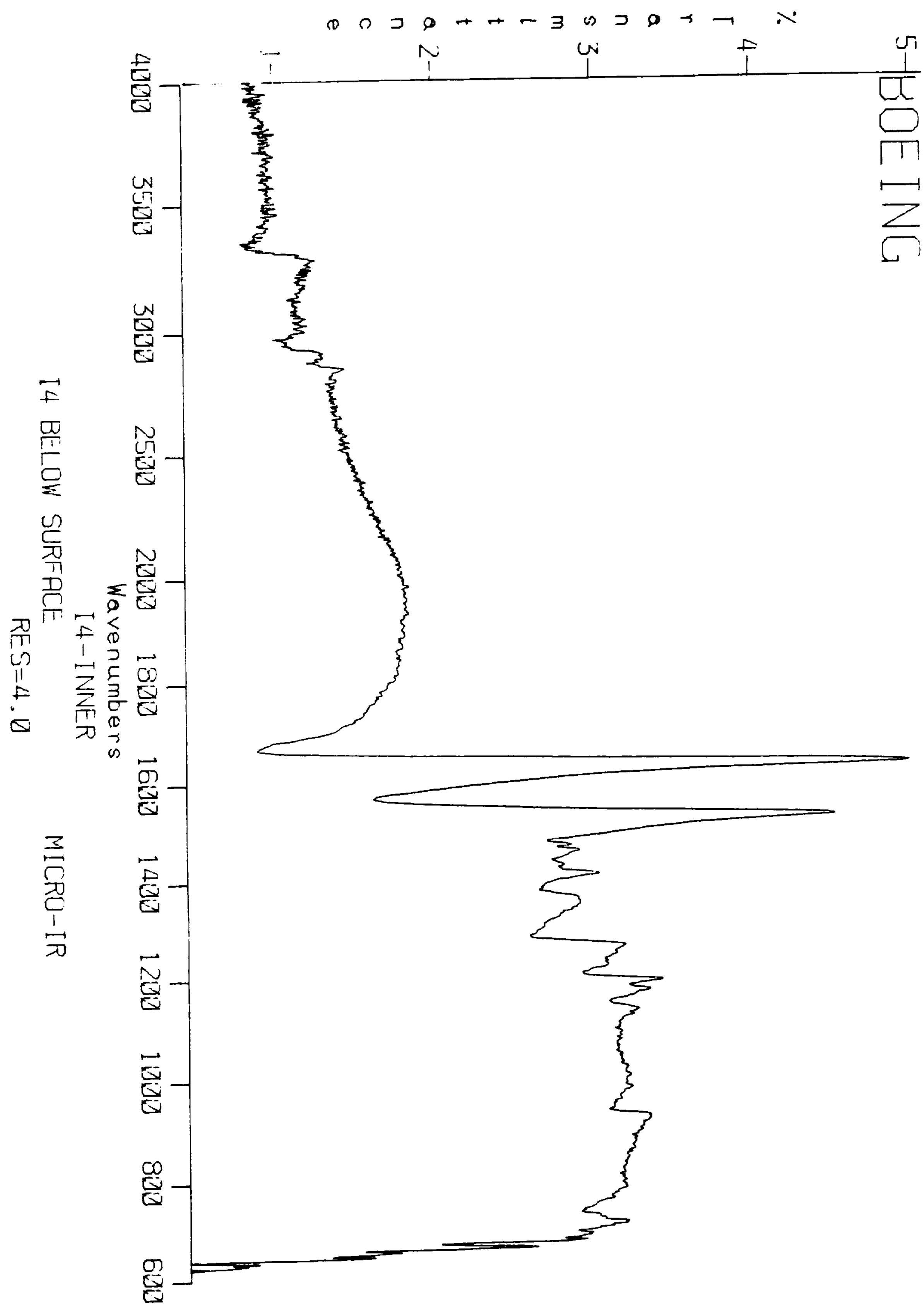

Figure 36. IR transmission spectrum of bulk material from wire harness bundle nylon grommet I4.

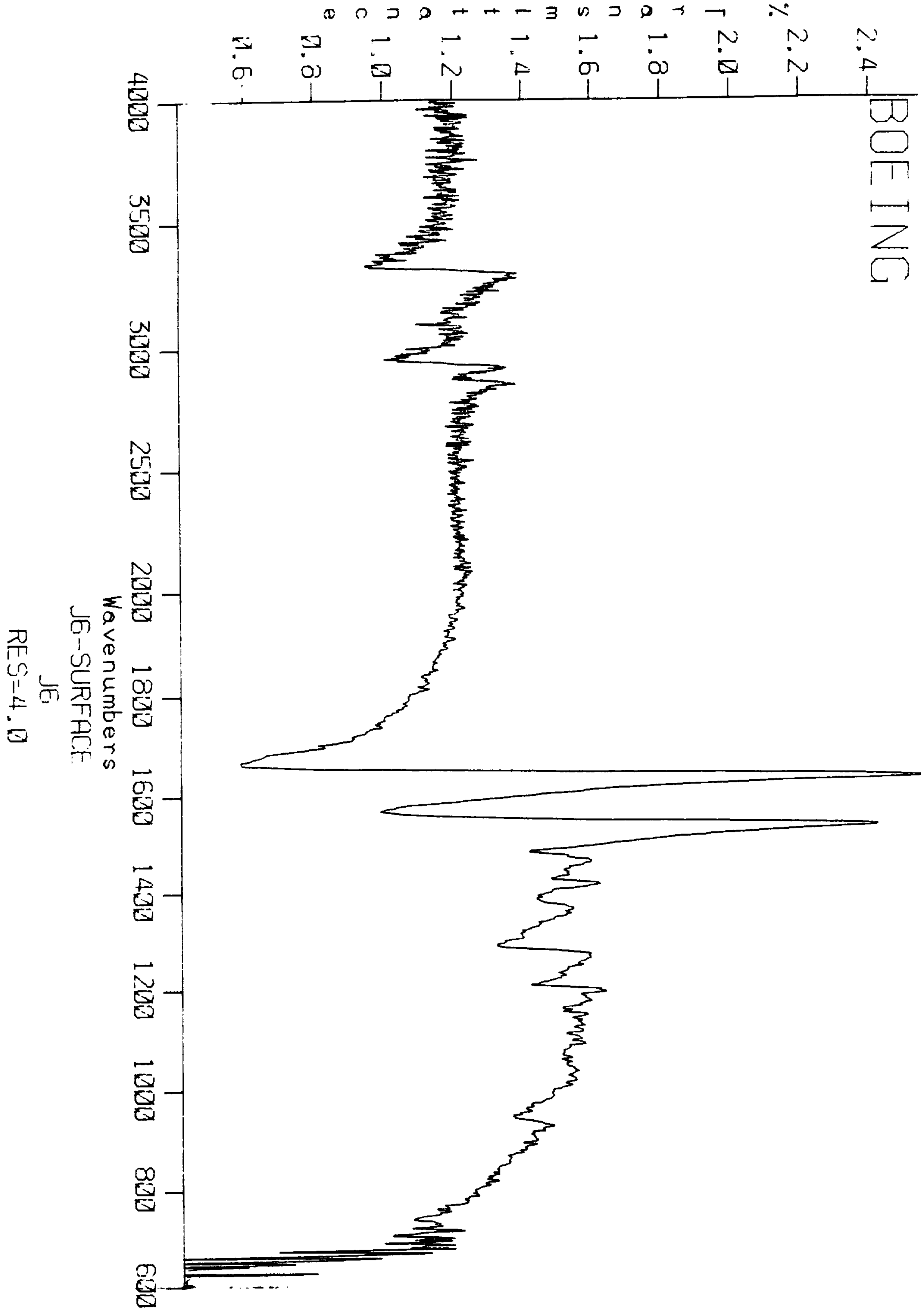

Figure 37. IR transmission spectrum of surface of wire harness bundle nylon grommet J6.

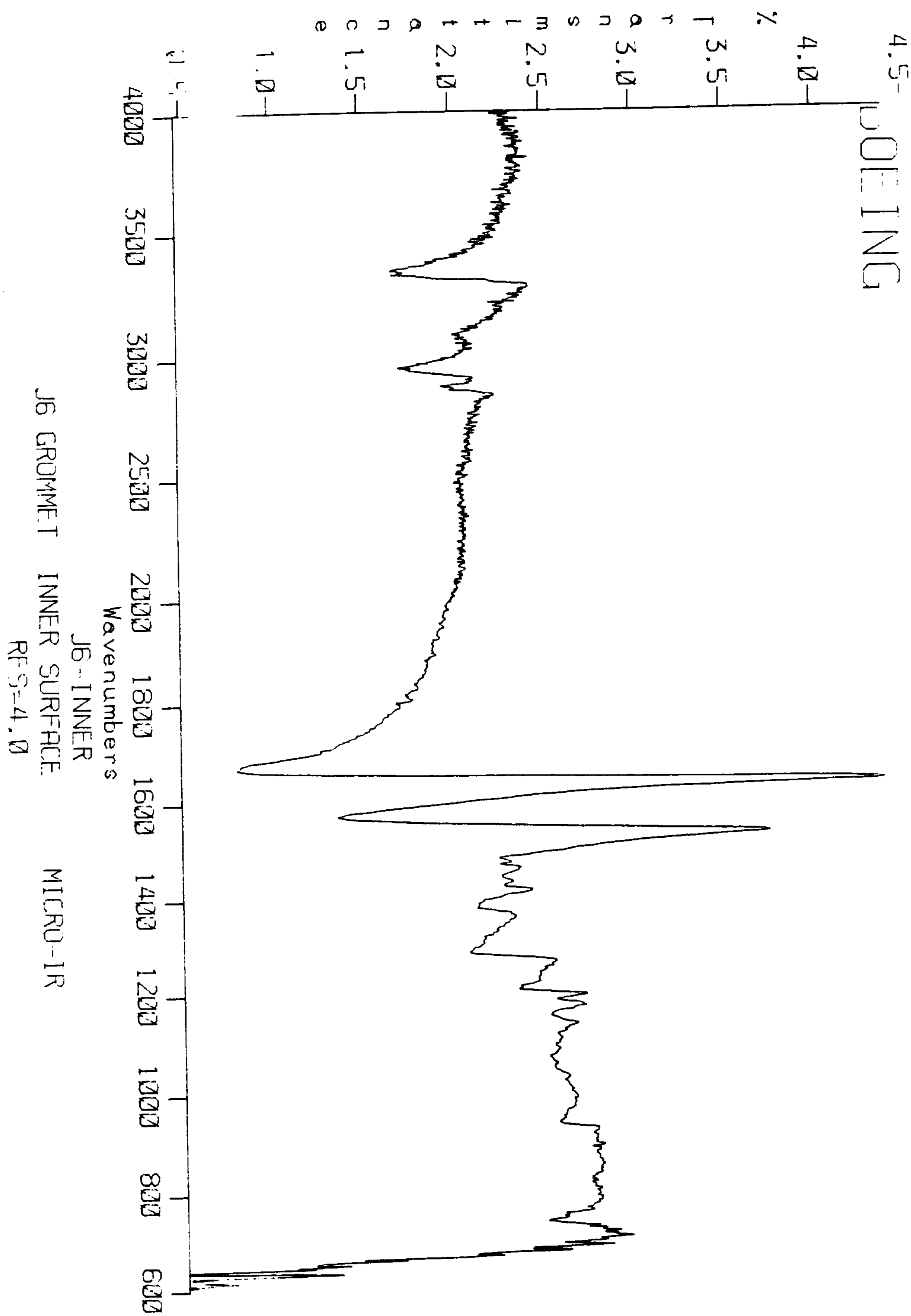

Figure 38. IR transmission spectrum of bulk material from wire harness bundle nylon grommet J6.

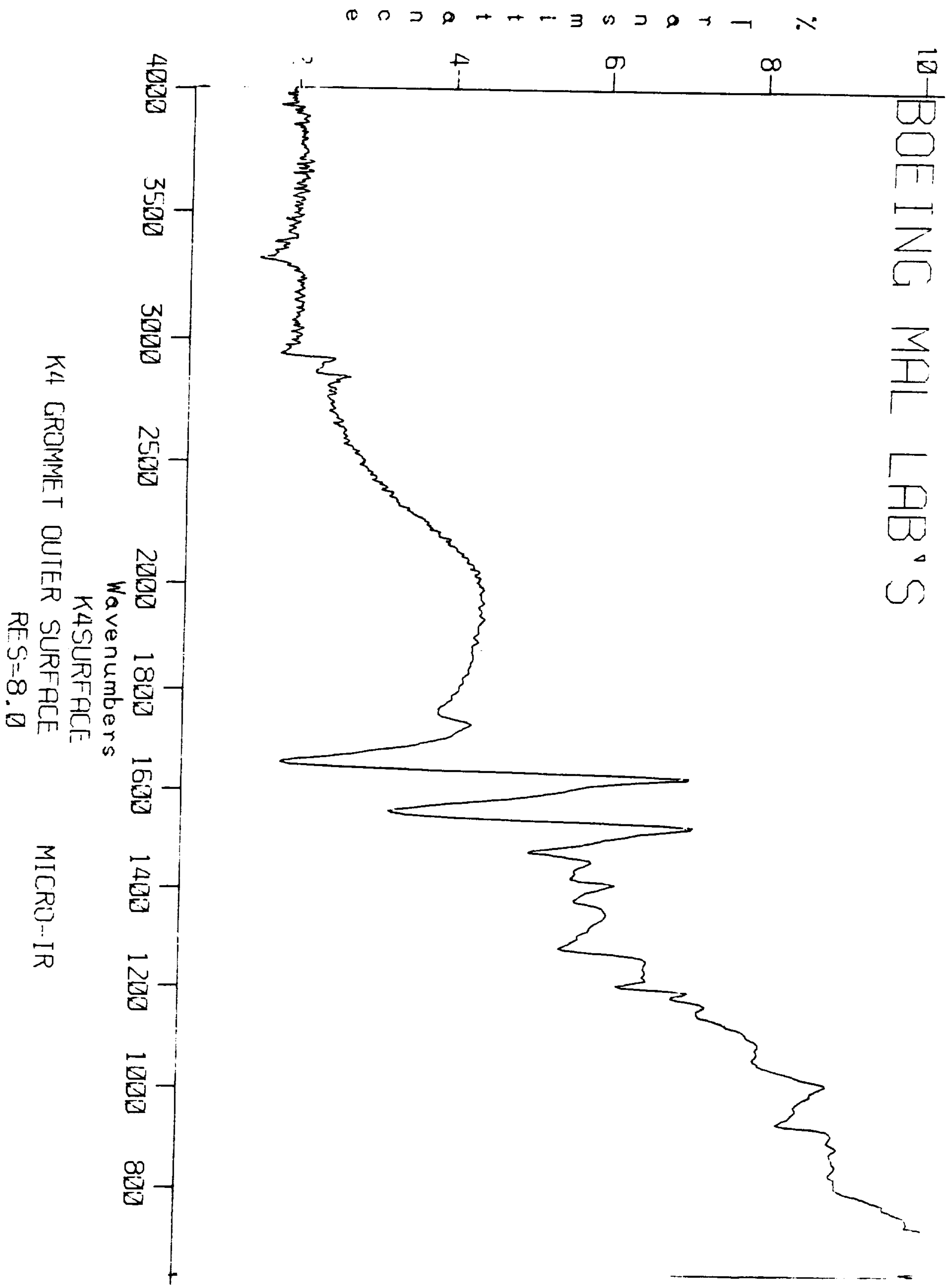

Figure 39. IR transmission spectrum of surface of wire harness bundle nylon grommet K4.

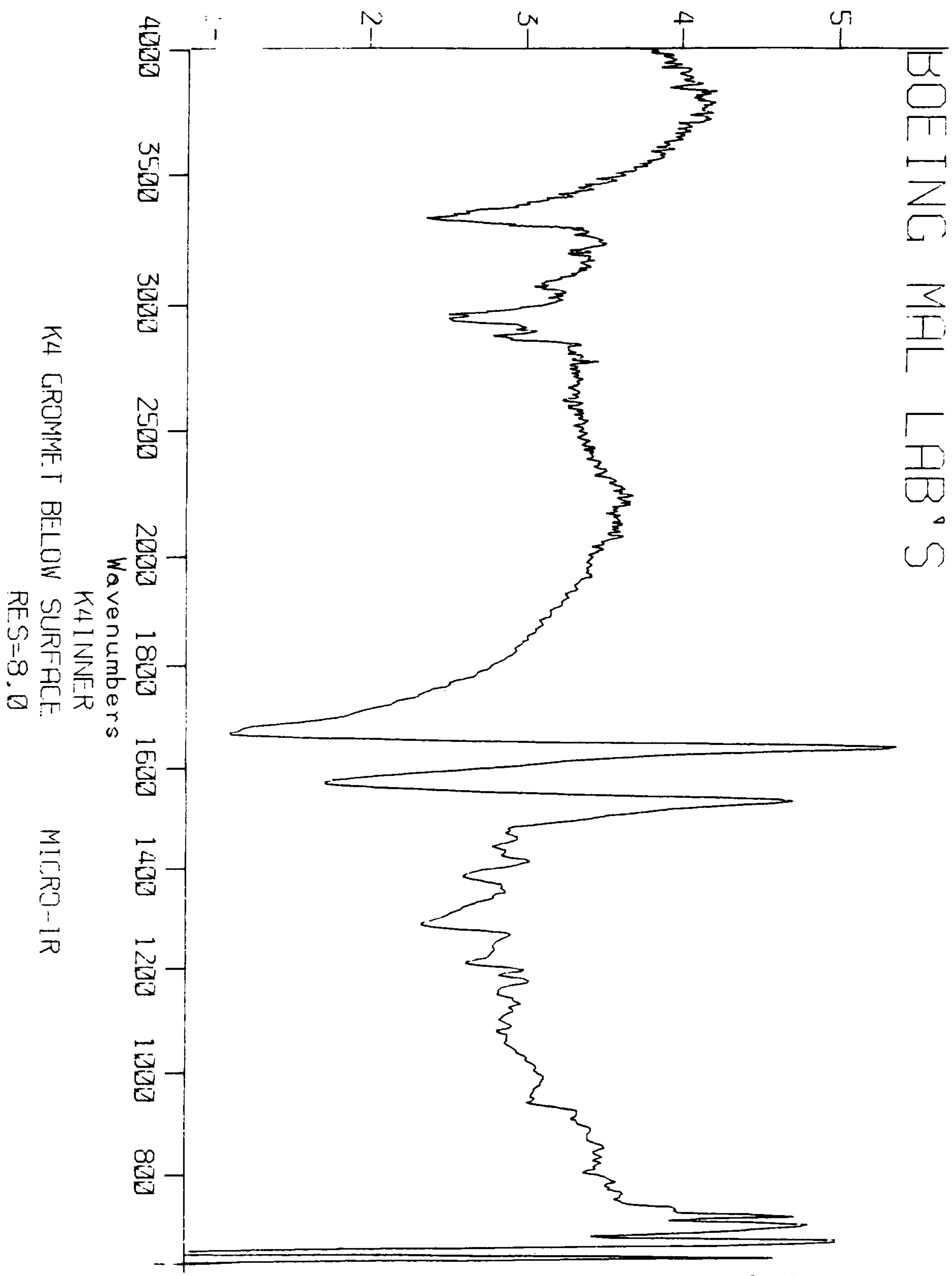

Figure 40. IR transmission spectrum of bulk material from wire harness bundle nylon grommet K4.

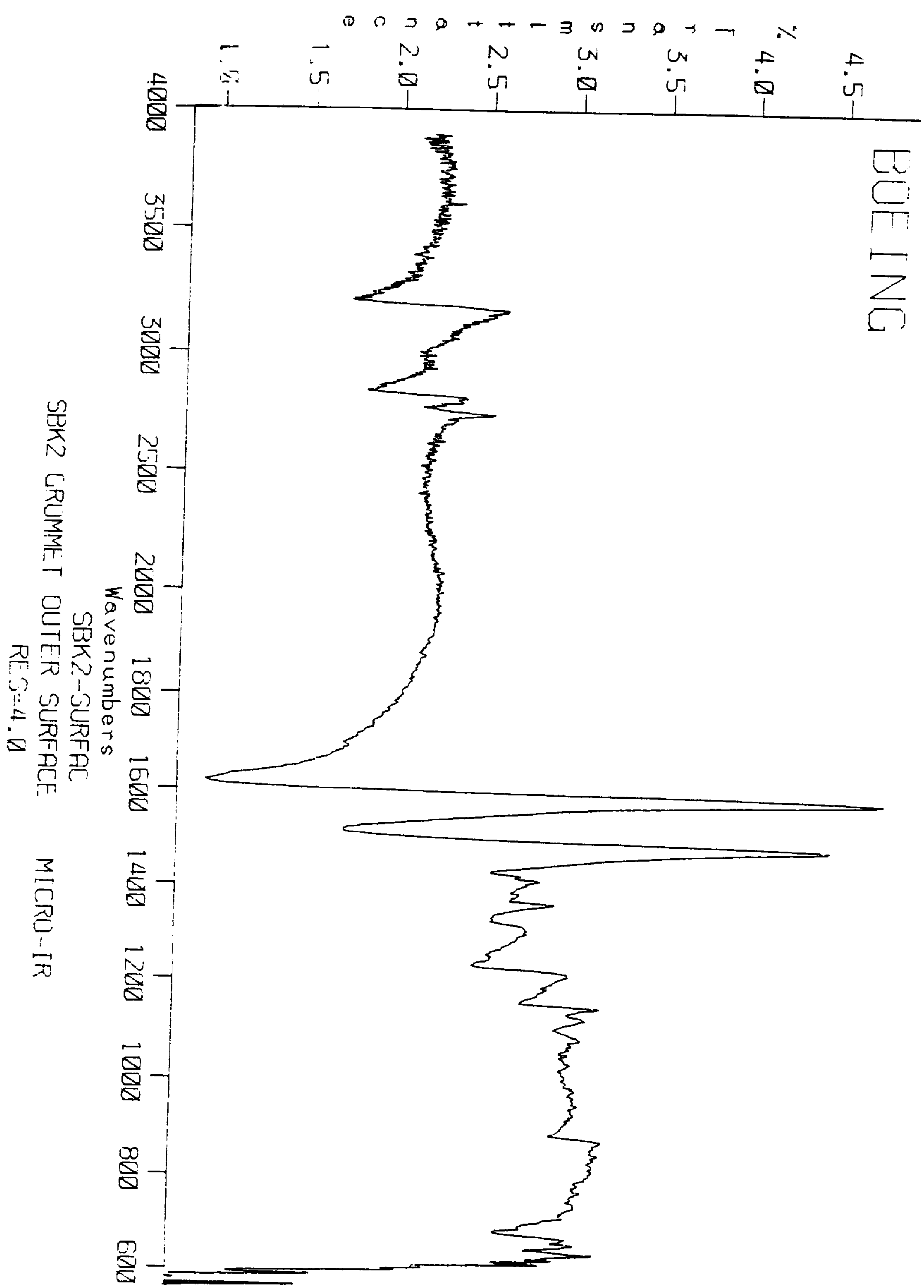

Figure 41. IR transmission spectrum of surface of wire harness bundle nylon grommet SBK2.

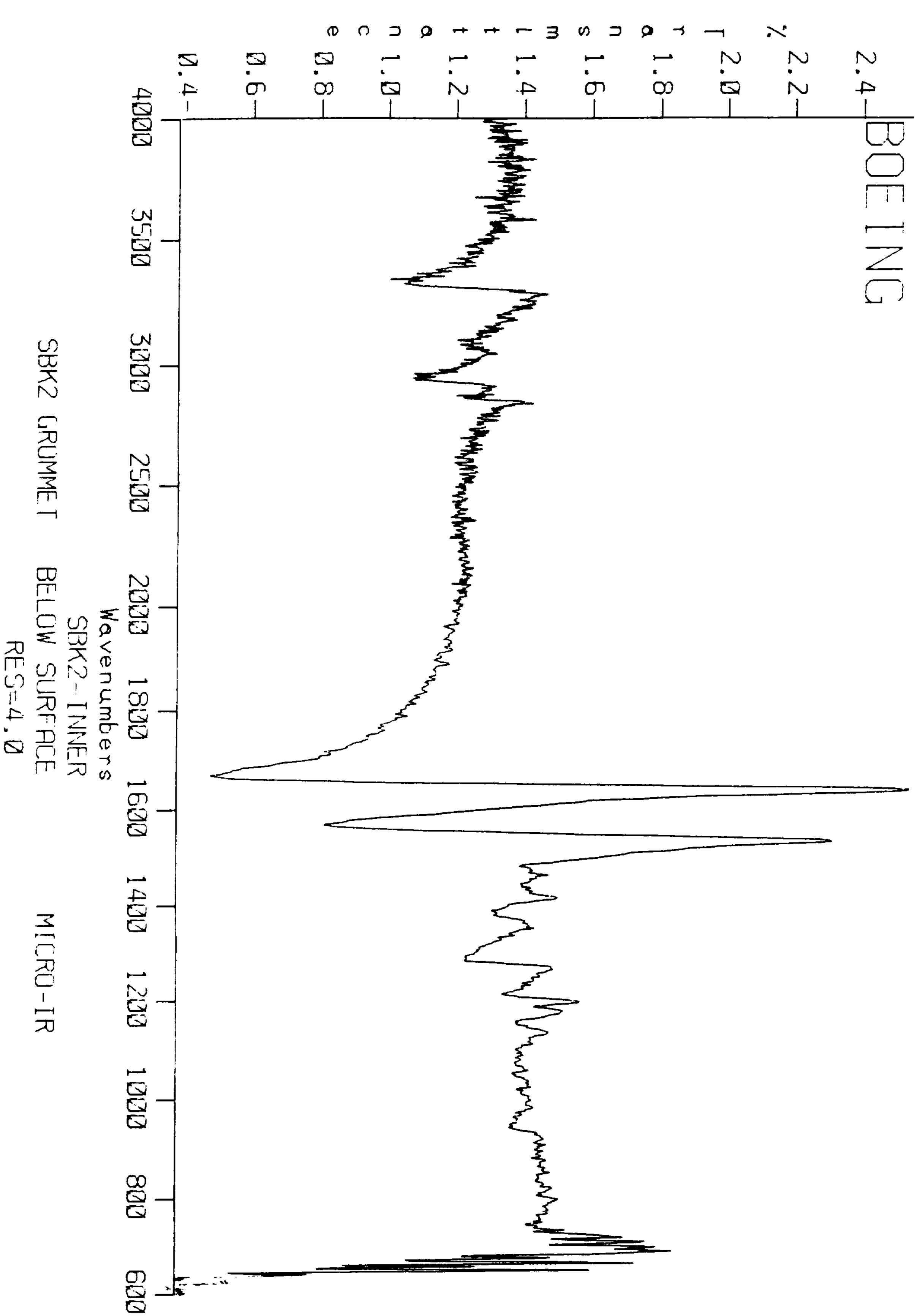

Figure 42. IR transmission spectrum of bulk material from wire harness bundle nylon grommet SBK2.

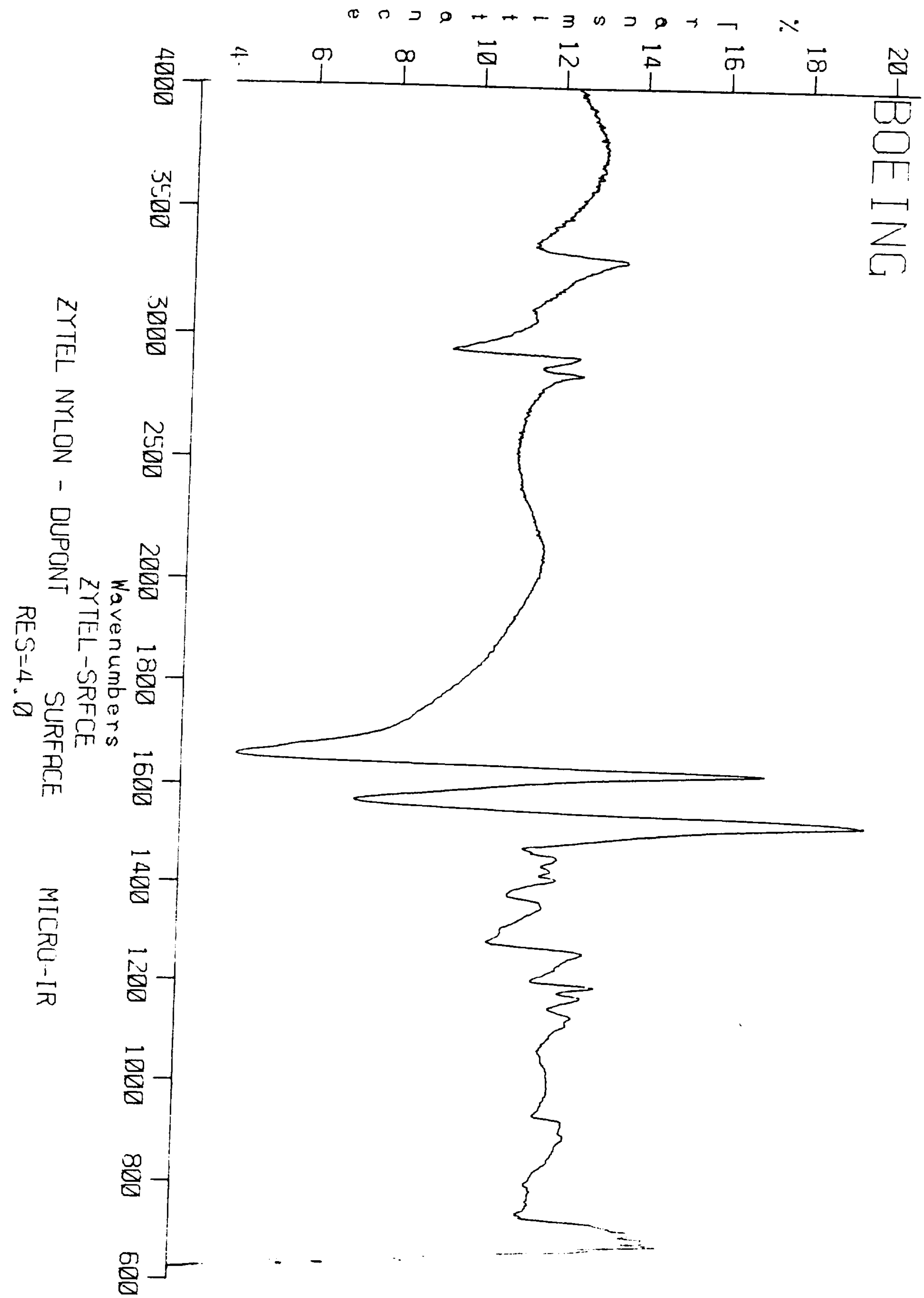

Figure 43. IR transmission spectrum of surface of Du Pont Zytel Nylon.

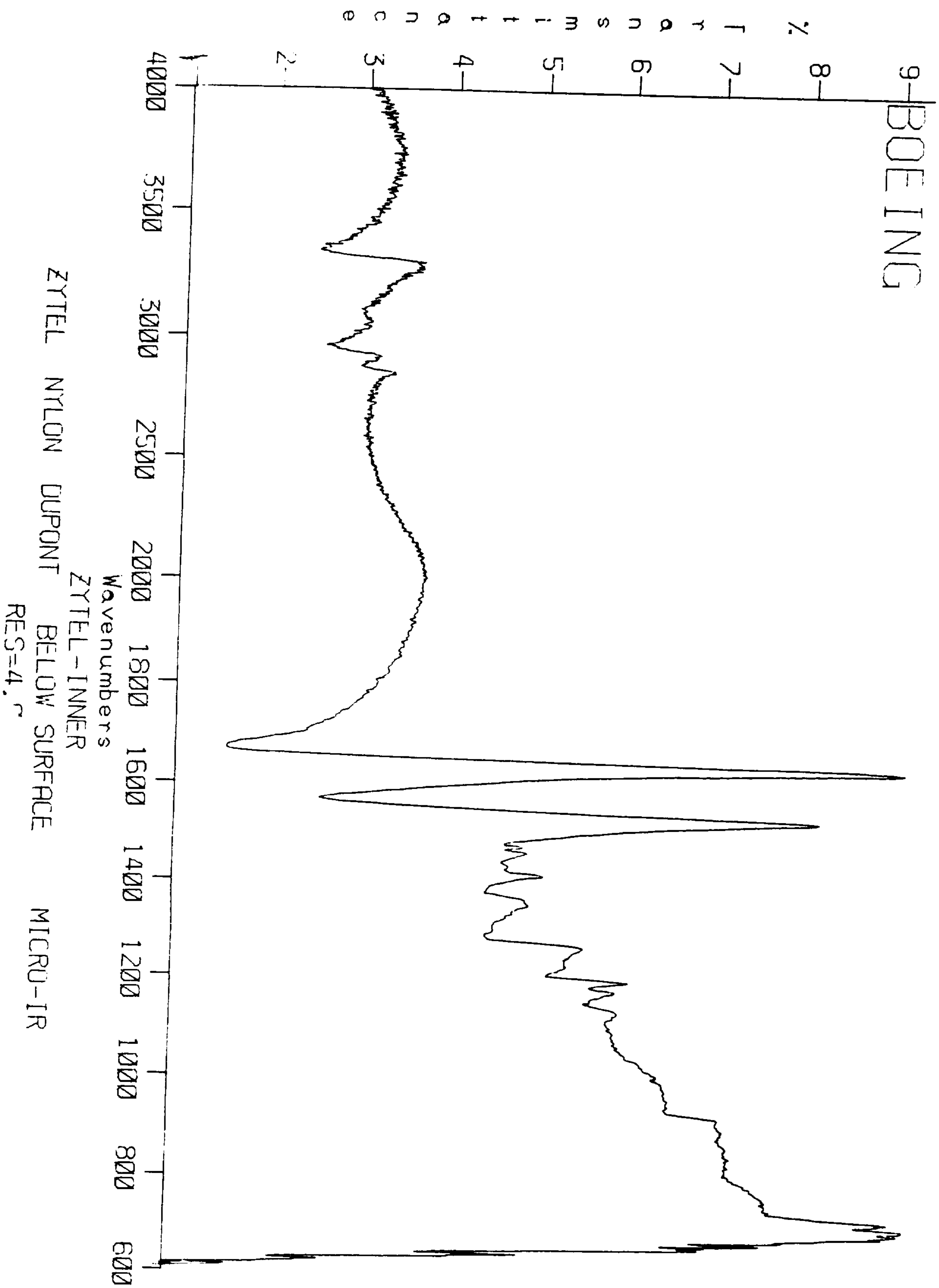

Figure 44. IR transmission spectrum of bulk material from Du Pont Zytel Nylon.

REPORT DOCUMENTATION PAGE

Form Approved
OMB No. 0704-0188

1. AGENCY USE ONLY *(Leave blank)*	2. REPORT DATE	3. REPORT TYPE AND DATES COVERED
	April 1994	Contractor Report (Oct. 1989-Dec. 1993)

4. TITLE AND SUBTITLE
Analysis of Selected Materials Flown on Interior Locations of the Long Duration Exposure Facility

5. FUNDING NUMBERS
NAS1-18224
NAS1-19247
506-43-61-02
233-03-02-04

6. AUTHOR(S)
H. A. Smith, K. M. Nelson, D. Eash, and H. G. Pippin

7. PERFORMING ORGANIZATION NAME(S) AND ADDRESS(ES)
Boeing Defense & Space Group
P.O. Box 3999
Seattle, WA 98124-2499

8. PERFORMING ORGANIZATION REPORT NUMBER

9. SPONSORING/MONITORING AGENCY NAME(S) AND ADDRESS(ES)
National Aeronautics and Space Administration
Langley Research Center
Hampton, VA 23681-0001

10. SPONSORING/MONITORING AGENCY REPORT NUMBER
NASA CR-4586

11. SUPPLEMENTARY NOTES
Langley Technical Monitor: Joan G. Funk

12a. DISTRIBUTION/AVAILABILITY STATEMENT
Unclassified-Unlimited
Subject Category 23

12b. DISTRIBUTION CODE

13. ABSTRACT *(Maximum 200 words)*
This report documents the post-flight condition of selected hardware taken from interior locations on the Long Duration Exposure Facility (LDEF). This hardware was generally in excellent condition. Outgassing data is presented for heat shrink tubing and fiberglass composite shims. Variation in total mass loss (TML) values for heat shrink tubing were correlated with location. Nylon grommets were evaluated for mechanical integrity; slight embrittlement was observed for flight specimens. Multi-layer insulation blankets, wire bundles, and paints in non-exposed interior locations were all in visibly good condition. Silicon-containing contaminant films wre observed on silver-coated hex nuts at the space- and Earth-end interior locations.

14. SUBJECT TERMS
Heat Shrink Tubing, Nylon Grommets, LDEF, Low Earth Orbit

15. NUMBER OF PAGES
116

16. PRICE CODE
A06

17. SECURITY CLASSIFICATION OF REPORT	18. SECURITY CLASSIFICATION OF THIS PAGE	19. SECURITY CLASSIFICATION OF ABSTRACT	20. LIMITATION OF ABSTRACT
Unclassified	Unclassified	Unclassified	UL

National Aeronautics and
Space Administration
Langley Research Center
Mail Code 180
Hampton, VA 23681-00001